

**METHOD DEVELOPMENT AND VALIDATION FOR THE ANALYSIS OF
SILICON, PHOSPHORUS, SULPHUR, CHROMIUM AND METAL OXIDES
IN CHARGE CHROME FERRO-ALLOY BY X-RAY FLUORESCENCE
SPECTROSCOPY.**

**By
Ferdinand van Niekerk**

**Dissertation submitted to the
School of Chemistry, University of the Witwatersrand,
in fulfilment of the requirements of the degree
Master of Science**

JUNE 2010

DECLARATION

I declare that this dissertation is my own, unaided work. It is being submitted for the degree Master of Science in the University of the Witwatersrand, Johannesburg. It has not been submitted before for any degree or examination in any other University.

Ferdinand van Niekerk

__ day of _____ 2010

ABSTRACT

High-carbon ferrochrome, also known as charge chrome can be used in the production of stainless steel of various grades. For charge chrome to be used as a raw material for stainless steel production, it is essential to know the chemical composition of the alloy.

Charge chrome is currently analysed by X-ray fluorescence spectroscopy (XRF) in the form of a button sample and the slags (oxides forming during the reduction process in charge chrome production) are analysed in the form of a briquette. The main aim during this study was to develop an XRF method for the analysis of charge chrome as a powder briquette and to develop a method for the analysis of the oxides.

During XRF analysis interference effects such as spectral overlaps and matrix effects (mainly in the form of absorption) must be compensated for to ensure accurate analysis. The general composition of the sample matrices, especially with regard to the oxides, is known. The possibility of matrix matching between calibration standards and samples was investigated to see if the necessity of corrections in terms of overlaps and interferences can be eliminated. After setting up calibration lines using production samples analysed by an alternative validated analytical technique (Inductively Coupled Plasma – Optical Emission Spectroscopy) for the elements and oxides (indirectly as elements), no corrections on the calibration lines were made using relevant mathematical correction algorithms.

The method development phase was followed by a complete validation of all the necessary parameters to ensure an accurate XRF analytical technique. The validation of the technique showed that the method is capable of yielding accurate and trustworthy results. This confirmed the theory that matrix matching between calibration standards and samples can compensate for the necessity to make any corrections for spectral overlaps and spectral interferences.

The preparation of samples as powder briquettes was also investigated to determine the optimum conditions for sample preparation. The main parameter studied was the influence of particle size on analysis. The optimum sample preparation conditions were determined and confirmed by validating the analytical results obtained when the powder briquette was analysed using the validated XRF method.

After research, the conclusions were made that charge chrome can be analysed in briquette form and that matrix matching between calibration standards and samples eliminates the need for any correction with regard to spectral overlaps and matrix effects.

The newly developed and validated methods for the analysis of Si, P, S and Cr in charge chrome metal and the oxide content in charge chrome slag will be implemented to assist in the daily routine analysis of charge chrome production samples.

Acknowledgements

I would like to use this opportunity to acknowledge and thank the following people and institutions who made this research project and the writing of this dissertation possible:

Firstly, Columbus Stainless (Pty) Ltd for giving me the opportunity to do the project using their laboratory facilities and instrumentation. Also a big thank you for their financial assistance in terms of a study grant.

Professor Ewa Cukrowska from the School of Chemistry, University of the Witwatersrand, for her mentorship and guidance.

My colleagues, especially Mrs Gloria Mokoena and Mr Thulani Mdluli at the Columbus Stainless Spectrochemical Laboratory for their willingness to help and assist especially with regard to sample preparation and analysis.

Mrs Faith Motau and her colleagues from the Columbus Stainless Chemistry Laboratory for the ICP-OES analysis of production samples.

Mrs Thandekile Zwane from Middelburg Ferrochrome for organising and supplying additional production samples that were used during the course of this project.

Sincere thanks to Mr Oswald Davies for his assistance with the proof-reading of this dissertation.

Mr Jaco Lombard and Miss Michelle van der Westhuizen for their help and guidance with regard to the technical content and the layout of the dissertation.

Professor James Willis and Mrs Maggi Loubser for sharing their vast amount of knowledge and experience when it was mostly needed.

Mr Lourens Campher for all his moral support and motivation.

And all the thanks to my Heavenly Farther for giving me so many opportunities in life and for His unconditional grace and love.

LIST OF FIGURES

Figure 3.1:	Schematic diagram of an analysing crystal, illustrating Bragg's Law.....	18
Figure 3.2:	Si wavelength scan.....	23
Figure 3.3:	P and S wavelength scan.....	25
Figure 3.4:	Cr, Mn and Fe wavelength scan.....	27
Figure 4.1:	SiK α calibration line without corrections.....	38
Figure 4.2:	PK α calibration line without corrections.....	41
Figure 4.3:	SK α calibration line without corrections.....	43
Figure 4.4:	CrK α calibration line without corrections.....	45
Figure 6.1:	Ti, Cr, Mn and Fe wavelength scan.....	77
Figure 7.1:	MgK α (for MgO) calibration line without corrections.....	83
Figure 7.2:	AlK α (for Al ₂ O ₃) calibration line without corrections.....	84
Figure 7.3:	SiK α (for SiO ₂) calibration line without corrections.....	85
Figure 7.4:	CaK α (for CaO) calibration line without corrections.....	86
Figure 7.5:	TiK α (for TiO ₂) calibration line without corrections.....	87
Figure 7.6:	CrK α (for Cr ₂ O ₃) calibration line without corrections.....	88
Figure 7.7:	MnK α (for MnO) calibration line without corrections.....	89
Figure 7.8:	FeK α (for FeO) calibration line without corrections.....	90
Figure 9.1:	The effect of particle size on the analysis of Si.....	111
Figure 9.2:	The effect of particle size on the analysis of P.....	112
Figure 9.3:	The effect of particle size on the analysis of S.....	112
Figure 9.4:	The effect of particle size on the analysis of Cr.....	113

LIST OF TABLES

Table 1.1:	Chemical composition of charge chrome.....	1
Table 2.1:	Excitation potential of elements in the X-ray tube and elements in charge chrome.....	14
Table 2.2:	Photon energies of the K X-ray spectral lines for the relevant elements.....	14
Table 3.1:	Analytical parameters to be used during wavelength scans for Si, P, S, Cr, Mn and Fe.....	21
Table 3.2:	Theoretical 2θ angles for Si, P, S, Cr, Mn and Fe Ka and $K\beta$ lines calculated using Bragg's Law.....	22
Table 3.3:	Summary of the Si wavelength scan.....	24
Table 3.4:	Summary of the P and S wavelength scan.....	25
Table 3.5:	Summary of the Cr, Mn and Fe wavelength scan.....	27
Table 3.6:	Summary of the Si, P, S and Cr energy profile runs.....	29
Table 4.1:	Standards used during the setting up of calibration lines.....	36
Table 4.2:	Standards and statistical values for the SiK α calibration line.....	38
Table 4.3:	Standards and statistical values for the PK α calibration line.....	41
Table 4.4:	Standards and statistical values for the SK α calibration line.....	42
Table 4.5:	Standards and statistical values for the CrK α calibration line.....	44
Table 5.1:	Results (% concentration) obtained during the elemental analysis of CRMs for accuracy.....	52
Table 5.2:	Summary of the statistical values obtained after the elemental analysis of CRMs for accuracy validation.....	52
Table 5.3:	Summary of the five analytical results (% concentration) and the precision indicators for Si, P, S and Cr.....	54
Table 5.4:	Dixon Q-test results for possible Si outliers.....	55

Table 5.5:	Regression statistics for the Si calibration line.....	58
Table 5.6:	Functions for the calculation of statistical parameters for validation of the Si calibration line.....	58
Table 5.7:	Summary of the validation parameters and values for the Si analytical method.....	66
Table 5.8:	Validation parameters and values for the P analytical method.....	68
Table 5.9:	Validation parameters and values for the S analytical method.....	69
Table 5.10:	Validation parameters and values for the Cr analytical method.....	70
Table 6.1:	Chemical composition of charge chrome slag.....	74
Table 6.2:	Analytical parameters to be used during wavelength scans for Mg, Al, Si, Ca, Ti, Cr, Mn and Fe.....	75
Table 6.3:	Theoretical 2θ angles for Mg, Al, Si, Ca, Ti, Cr Mn and Fe.....	75
Table 6.4:	Comparison between theoretical 2θ angles and experimental 2θ angles.....	76
Table 7.1:	Wavelength of the K-absorption edges for the slag matrix elements.....	80
Table 7.2:	Standards and statistical values for the MgK α calibration line.....	83
Table 7.3:	Standards and statistical values for the AlK α calibration line.....	84
Table 7.4:	Standards and statistical values for the SiK α calibration line.....	85
Table 7.5:	Standards and statistical values for the CaK α calibration line.....	86
Table 7.6:	Standards and statistical values for the TiK α calibration line.....	87
Table 7.7:	Standards and statistical values for the CrK α calibration line.....	88

Table 7.8:	Standards and statistical values for the MnK α calibration line.....	89
Table 7.9:	Standards and statistical values for the FeK α calibration line.....	90
Table 7.10:	SEE values and concentration ranges for the oxide calibration lines.....	91
Table 8.1:	Expected oxide content and possible concentration variations.....	93
Table 8.2:	Results (% concentration) obtained during the oxide analysis of CRMs for accuracy validation.....	95
Table 8.3:	Summary of the statistical values obtained after the oxide analysis of CRMs for accuracy.....	95
Table 8.4:	Summary of the five analytical results (% concentration) and the precision indicators for the oxides.....	96
Table 8.5:	Results and summary of the validation parameters for MgO.....	98
Table 8.6:	Results and summary of the validation parameters for Al ₂ O ₃	99
Table 8.7:	Results and summary of the validation parameters for SiO ₂	100
Table 8.8:	Results and summary of the validation parameters for CaO.....	101
Table 8.9:	Results and summary of the validation parameters for TiO ₂	102
Table 8.10:	Results and summary of the validation parameters for Cr ₂ O ₃	103
Table 8.11:	Results and summary of the validation parameters for MnO.....	104
Table 8.12:	Results and summary of the validation parameters for FeO.....	105
Table 9.1:	The effect of milling time on particle size.....	109
Table 9.2:	The effect of particle size on XRF analysis.....	111

Table 9.3: Results indicating the homogeneity of the sample preparation technique.....116

Table 9.4: Results (% concentration) obtained during the elemental analysis of charge chrome buttons and briquettes..... 118

Table 9.5: Summary of the statistical values obtained after the elemental analysis of charge chrome buttons and briquettes..... 118

ABBREVIATIONS AND SYMBOLS

ANOVA	Analysis of variance (Excel function)
CRM	Certified Reference Material
DF	Degrees of freedom
FPC	Flow Proportional Counter
ICP-OES	Inductively Coupled Plasma - Optical Emission Spectroscopy
LOD	Limit of detection
LOQ	Limit of quantitation
MAC	Mass absorption coefficient
PET	penta-erythritol
PHD	Pulse height distribution
SEE	Standard error of estimate
sec	Second(s)
WDXRF	Wavelength-dispersive X-ray fluorescence spectroscopy
XRF	X-ray fluorescence
XRFS	X-ray fluorescence spectroscopy
Å	Wavelength unit (1 Å = 10 ⁻¹⁰ m)
A ₀	Linear function intercept
A ₁	Linear function slope
a	Calibration line intercept
b	Calibration line slope
c	Speed of light (2.99 x 10 ⁸ m/s)
C	Concentration (expressed as %)
C _i	Weight fraction of element 'i'
°C	Degrees Celsius
d	Interplanar crystal spacing
E	Energy
g	Grams
h	Planck's constant (4.135 x 10 ⁻¹⁸ keV.sec)
H ₀	Null hypothesis
H ₁	Alternative hypothesis
I	Spectral line intensity
K, L, M, N	Spectral lines or energy levels
K _α	K-alpha photons or spectral lines
K _β	K-beta photons or spectral lines
kcps	Kilo counts per second
keV	Kilo electron volt
kV	Kilo volt
LiF	Lithium Fluoride
M _i	Matrix correction term for element 'i'
m	Number of samples analysed (for the calculation of U(r))
mA	milli ampere
mm	millimetre
m/s	Meters per second
n	Number of measurements made or order of diffraction
nm	Nano meter (10 ⁻⁹ m)
Q _{calc} / Q _{crit}	Calculated Q-value and critical Q-value (Dixon Q-test)

R	Range (population) of results
%RSD	Percentage relative standard deviation
r	Linear regression value
S	Sample preparation term (S_s / S_{STD})
$s_a; s_b$	Uncertainty in intercept; uncertainty in slope
$s_{x0} / U(r)$	Regression uncertainty
$s_{y/x}$	Random calibration uncertainty
STD	Standard
$t_{calc}; t_{crit}$	Calculated t-value and critical t-value (t-test)
\bar{x}_{avg}	Average of a set of analytical results
\bar{y}_{avg}	Average of a set of measured intensities
$x_{LOD}; y_{LOD}$	Limit of detection with regard to concentration / line intensity
$x_{LOQ}; y_{LOQ}$	Limit of quantitation with regard to concentration / line intensity
$y; \hat{y}$	Intensity calculated with regard to x
Z_{abs}	Absorption edge of element Z
Δ	Absolute difference
θ	Bragg angle (expressed as $\sin\theta$)
λ	Wavelength
μ	True concentration value
μm	micro metre
$\mu_{Y,ZKa}$	absorption coefficient of element Y with regard to the Ka line intensity of element Z
Σ	Summation
σ	Standard deviation of n measurements

TABLE OF CONTENTS

DECLARATION.....	ii
ABSTRACT.....	iii
ACKNOWLEDGEMENTS.....	v
LIST OF FIGURES.....	vii
LIST OF TABLES.....	viii
ABBREVIATIONS AND SYMBOLS.....	xii

CHAPTER 1 – INTRODUCTION AND AIMS

1.1 Charge chrome manufacturing process.....	1
1.2 Aims of research.....	3
1.2.1 Sample preparation.....	4
1.2.2 Equipment and instrumentation.....	5
1.2.3 XRF method development.....	6
1.2.4 Analytical method validation.....	6
1.3 XRF and the analysis of charge chrome.....	7

CHAPTER 2 – PRINCIPLES OF XRF SPECTROSCOPY

2.1 Principles of XRF spectroscopy.....	9
---	---

CHAPTER 3 – QUALITATIVE WAVELENGTH SCANS – ELEMENTS

3.1 Qualitative wavelength scans for Si, P, S and Cr.....	17
3.1.1 Derivation of the Bragg Law.....	17
3.2 Qualitative wavelength scans.....	20
3.3 Energy profiles.....	28

CHAPTER 4 – CALIBRATION LINES – ELEMENTS

4.1 Setting up of calibration lines for the analysis of Si, P, S and Cr.....	30
4.2 Matrix effects.....	31
4.3 Setting up a calibration line for the analysis of Si.....	36
4.4 Setting up a calibration line for the analysis of P.....	41
4.5 Setting up a calibration line for the analysis of S.....	42
4.6 Setting up a calibration line for the analysis of Cr.....	44

CHAPTER 5 – METHOD VALIDATION – ANALYSIS OF ELEMENTS

5.1	Method validation for the analysis of Si, P, S and Cr.....	47
5.2	Validating accuracy for the analysis of Si, P, S and Cr.....	49
5.3	Validating precision for the analysis of Si, P, S and Cr.....	53
5.4	The analytical range and the detection and quantitation limits.....	56
5.5	Statistical results and interpretation for the Si calibration.....	57
5.5.1	The regression value.....	59
5.5.2	Random calibration uncertainty.....	59
5.5.3	Uncertainty in the intercept and slope.....	60
5.6	Determining the analytical range and the detection and quantitation limits for Si.....	61
5.7	Regression and the calculation of uncertainty in the analytical concentration of Si.....	63
5.8	Statistical results and analysis for the P calibration line.....	67
5.9	Statistical results and analysis for the S calibration line.....	68
5.10	Statistical results and analysis for the Cr calibration line.....	69
5.11	Conclusions.....	70

CHAPTER 6 – QUALITATIVE WAVELENGTH SCANS – OXIDES

6.1	Qualitative wavelength scans for oxides.....	73
-----	--	----

CHAPTER 7 – CALIBRATION LINES – OXIDES

7.1	Setting up calibration lines for the analysis of oxides.....	78
7.2	Matrix matching.....	79
7.3	Spectral overlaps expected in the oxide samples.....	79
7.4	Spectral interferences expected in the oxide samples.....	80
7.5	Setting up a calibration line for the analysis of MgO.....	83
7.6	Setting up a calibration line for the analysis of Al ₂ O ₃	84
7.7	Setting up a calibration line for the analysis of SiO ₂	85
7.8	Setting up a calibration line for the analysis of CaO.....	86
7.9	Setting up a calibration line for the analysis of TiO ₂	87
7.10	Setting up a calibration line for the analysis of Cr ₂ O ₃	88
7.11	Setting up a calibration line for the analysis of MnO.....	89
7.12	Setting up a calibration line for the analysis of FeO.....	90
7.13	Interpretation of the calibration line data.....	91

CHAPTER 8 – METHOD VALIDATION – ANALYSIS OF OXIDES

8.1	Method validation for the analysis of the oxides.....	93
8.2	Validating accuracy for the analysis of the oxides.....	94
8.3	Validating precision for the analysis of the oxides.....	96
8.4	Validation of the remaining parameters for oxide analysis.....	97
8.5	Conclusions.....	106

CHAPTER 9 – SAMPLE PREPARATION

9.1	Sampling.....	107
9.2	Effect of milling time on particle size.....	108
9.3	Influence of particle size on XRF analysis.....	110
9.4	Homogeneity.....	114
9.5	Comparison of analysis between button and briquette samples.....	116

CHAPTER 10 – SUMMARY AND CONCLUSIONS

10.1	Qualitative wavelength scans.....	121
10.2	Setting up calibration lines.....	122
10.3	Method validation.....	124
10.4	Areas of improvement.....	125

11 APPENDICES

APPENDIX A	SiK α Energy Profile.....	127
APPENDIX B	PK α Energy Profile.....	128
APPENDIX C	SK α Energy Profile.....	129
APPENDIX D	CrK α Energy Profile.....	130
APPENDIX E.1	Regression statistics for the P-calibration line.....	131
APPENDIX E.2	Data obtained from P-calibration line.....	132
APPENDIX E.3	Regression statistics for the S-calibration line.....	133
APPENDIX E.4	Data obtained from S-calibration line.....	134
APPENDIX E.5	Regression statistics for the Cr-calibration line.....	135
APPENDIX E.6	Data obtained from Cr-calibration line.....	136
APPENDIX F	Mg wavelength scan.....	137
APPENDIX G	Al wavelength scan.....	138
APPENDIX H	Si wavelength scan.....	139
APPENDIX I	Ca wavelength scan.....	140
APPENDIX J	MgK α Energy Profile.....	141
APPENDIX K	AlK α Energy Profile.....	142
APPENDIX L	CaK α Energy Profile.....	143
APPENDIX M	TiK α Energy Profile.....	144

APPENDIX N	MnK α Energy Profile.....	145
APPENDIX O	FeK α Energy Profile.....	146
12	REFERENCES.....	147

CHAPTER 1 INTRODUCTION AND AIMS

1.1 Charge chrome manufacturing process

Chromite ore ($\text{FeO}\cdot\text{Cr}_2\text{O}_3$) is a chromium-bearing ore used in the manufacture of ferro-alloys known as ferrochrome. Chromium is the main agent in ferrochrome that forms a protective layer on the surface of stainless steel mainly protecting it from corrosion (Liptrot,1992).

The main types of ferrochrome alloy include Low Carbon Ferrochrome, Medium Carbon Ferrochrome and High Carbon Ferrochrome (referred to as charge chrome). Table 1.1 summarises the basic chemical composition of charge chrome.

Table 1.1: Chemical composition of charge chrome.

Element	Concentration (%)
Cr	50 – 54
Fe	33 - 37
C	8.0 – 8.5
Si	< 1
Mn	< 1
P	< 0.02
S	< 0.04

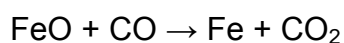
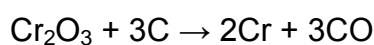
The manufacturing process of charge chrome includes the first stage where pre-reduction of the ore is done in a kiln (heating furnace), followed by the second stage where the now pre-reduced ore is smelted in a plasma furnace.

The ore is reduced in the kiln by adding coal and quartz sand which results in a metallised ore embedded in sintered slag. The use of coal ensures a high degree of metallisation, with the result that less power is needed during the smelting stage. When fed into the kiln the charge is pre-heated to 800 °C. As the charge passes through the kiln-length, the temperature is raised to approximately 1000 °C where the main iron reduction and coal gasification starts. Silica reduction starts at 1200 °C, and at this stage the silica is dissolved in the metallic phase and accelerates the reduction of the chromite.

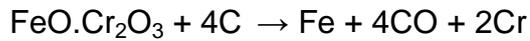
Complete reduction of the ore is done by feeding the metallised ore into the direct-current plasma arc furnace in which the arc is sustained by a single hollow graphite electrode (cathode). The reduction of the chromium oxide starts at a temperature above 1400 °C. The aim of the smelting process is to yield chromium and iron metals via the reduction of their respective oxides, as well as to remove unwanted minerals in the form of slag.

The slag mostly consists of a variety of oxides from different sources. Due to its lower density and immiscibility the slag phase separates from the metallic phase. The reduction process in the plasma furnace yields charge chrome with a chromium content of 50 – 54%.

The reductant used in the plasma furnace is anthracite with a fixed carbon content. The carbon is used in the reduction process to produce charge chrome. This reduction process is endothermic and requires high temperatures for complete reduction to take place. The total carbothermal reduction process of the chromite ore to yield charge chrome takes place according to the following simplified chemical equations:



The overall reduction reaction of the chromite ore can therefore be summarised as follows:



The main goal of this production process is to be cost effective, yielding a quality product in large quantities.

The chemical composition of the charge chrome alloy must be known since Columbus Stainless will use the alloy as a raw material for the manufacturing of stainless steel of various grades. The main elements that will be analysed include Si, P, S and Cr. Certain oxides (in the form of slag) will be a component in the analysis. One of the main purposes of this study was to develop a suitable analytical method that will enable a quick and effective analysis of charge chrome and the slag giving accurate and trustworthy results.

1.2 Aims of research

This dissertation will focus on the manufacturing process and method development for the chemical analysis of charge chrome, which is a silvery grey metal alloy with a melting point of >1550 °C and a boiling point of 2700 – 3000 °C. The specific gravity of the material is 6.8 – 7.0. The aims and main focus points of this dissertation included:

- optimisation of the sample preparation process
- investigation of the available equipment and instrumentation for sample preparation and analysis
- development of a suitable analytical method
- validation of the analytical method according to international quality standards where available, otherwise by using secondary standards

- implementation of a quality control system to monitor the effectiveness of the new analytical method.

Wavelength-Dispersive X-ray Fluorescence Spectroscopy (WDXRF) was researched as an analytical technique.

1.2.1 Sample preparation

The current technique involves the preparation of a button sample by melting the charge chrome at a high temperature (<1500 °C). After melting and cooling the sample, the surface is polished to ensure a sample surface that is suitable for XRF analysis. The main disadvantages of this method are that it is time consuming, and contamination of the sample may occur (especially Si contamination directly from the crucible used during the melting process). The use of platinum crucibles which will avoid Si contamination was not considered due to cost implications.

An alternative technique involves the preparation of the sample as a powder briquette where a lesser amount of the sample is crushed and milled, resulting in a powder sample with a very small particle size. A cellulose binder is added to the milled sample which is compressed to form a briquette that is suitable for analysis. Briquettes are prepared with automated crushing, milling and pressing equipment, which makes sample preparation quick and easy and this largely excludes the possibility of sample contamination.

These two different sample preparation techniques were investigated and compared. The most suitable technique was identified with due regard to the simplicity of the technique, preparation time and the homogeneity of the final sample. Mass aliquots of the same sample were analysed and relevant statistical calculations were used to determine the homogeneity of the sample. The particle size obtained by the automated preparation

technique after milling was investigated as well given that very small particle sizes of samples in briquette form give more accurate results when XRF is used as an analytical technique. At this stage it was expected that the briquette method will be much more convenient and less time consuming compared to the button method.

1.2.2 Equipment and instrumentation

The equipment used during the sample preparation stage included a button machine for the melting and preparation of the sample in button form, as well as crushers, milling and pressing equipment for the preparation of the sample as a briquette. The crushers, milling and pressing equipment are available either as manual equipment or as automated machines. Parameters such as adequate milling time to give the desired particle size for the sample were investigated and compared using equipment and machines as indicated.

Analytical method development was done on a Thermo ARL 9800 XRF spectrometer. This instrument is able to analyse all the elements simultaneously during a single analysis. The same is true for the analysis of the oxides. The fact that analysis of all the elements and oxides (separate programs were developed for the analysis of the elements and the oxides respectively) can be done simultaneously as well as simpler and quicker sample preparation makes the use of XRF as an analytical method more advantageous than other techniques such as ICP-OES, for example. XRF analysis is also very quick. On average up to 12 elements can be analysed in less than 2 minutes. Further advantages of XRF analysis are that the method is non-destructive and the concentration range that can be analysed is very broad (Al-Merey, Karajou and Issa, 2004). The expectation was that this method will yield accurate and repeatable results. This was determined and confirmed during the validation stage of the study.

1.2.3 XRF method development

Method development for the accurate analysis of the mentioned elements and oxides with the aid of XRF spectroscopy was investigated during this part of the study. The aim was to develop a method which will enable the simultaneous analysis of all the elements and simultaneous analysis of all oxides using separate programs. Method development started with a qualitative analysis (using wavelength scans) of production samples and was expanded to eventually implement and use a fully quantitative method of analysis. All possible complications, such as line overlaps, matrix effects such as spectral interferences, and the setting up of linear calibration lines for each element and oxide were researched, implemented and validated.

Line overlaps and/or matrix effects that may influence the analytical results can be compensated and corrected for by using available instrumental software and suitable mathematical models if necessary.

1.2.4 Analytical method validation

A complete validation of the method was done after setting up the calibration lines that would be used during analysis of the analytes. The method was validated according to the requirements of the ISO 17025-2005 quality control management system. Validation criteria stipulated in this system and applicable to the analytical method were investigated and validated. Relevant statistical methods were used to prove that the method adheres to all the necessary quality requirements. Where applicable, the statistical techniques were fairly adjusted to compensate for any deviations that occurred when compared to other standard techniques.

The aim during this part of the study was to validate the linear calibration lines (response curves) used for the analysis of all elements and oxides.

The statistical variation of critical validation parameters can be determined with the aid of these linear functions. The relevant parameters include the homogeneity of the sample preparation technique, accuracy, precision and repeatability, detection and quantitation levels, as well as regression values used to determine the linear fit of the response curve in terms of spectral line intensity vs. concentration. The uncertainty range with regard to each concentration result obtained after analysis also played a fundamental role during these calculations.

1.3 XRF and the analysis of charge chrome

Analysis of the elements Si, P, S, Cr and oxides in charge chrome was investigated in the study under review. The basic composition of charge chrome is known but the aim was to use a validated XRF method to analyse samples quantitatively. Recent developments in analytical techniques such as XRF allows the quantitative analysis of alloy and steel samples with elements on major, minor and trace levels, traditionally performed by wet chemical techniques or instrumental techniques such as atomic absorption spectroscopy (Abu El-Haija *et al.*, 1987 and Brown and Milton, 2005). The suitability of the technique used to analyse the above-mentioned elements and oxides was investigated by evaluating and discussing the theoretical concepts of the field of research. Some of these theories were practically tested during the method - development stage and included concepts such as the chemical and quantum physical properties of the elements and oxides under investigation. This included wavelength scans (qualitative analysis) that formed the basis for the complete development of a validated XRF analytical method.

Some limitations that may be encountered during the method-development stage may include line overlaps and matrix effects. It is possible though to compensate for this by using customised instrumental design and existing mathematical correction models if necessary. A further limitation is the

poor availability of certified reference standards needed to set up calibration lines for each element for quantitative analysis. This was overcome by the development of secondary standards with the analyte concentrations verified by using other validated analytical techniques. The method-development stage was followed by a complete validation of the method. Existing validation criteria and statistical calculations were used and adjusted where necessary to suit the requirements of the quality control system (ISO 17025-2005) implemented in the laboratory.

Literature that is mainly focused on the analysis of steel products by means of XRF is rare. The greater part of this dissertation was therefore devoted to developing methods and techniques that will satisfy the unique needs of Columbus Stainless and Middelburg FerroChrome for the analysis of charge chrome.

CHAPTER 2 PRINCIPLES OF XRF SPECTROSCOPY

2.1 Principles of XRF spectroscopy

X-rays are electromagnetic waves of a short wavelength (therefore highly energetic) found between the gamma and ultraviolet region of the electromagnetic spectrum. The wavelength range of X-rays is approximately 10^{-5} Å to about 100 Å. Conventional X-ray spectroscopy is confined to the measurement of X-rays in the region of ~0.1 - ~25 Å (or 0.01 – 2.5 nm on the nano scale). The measurement may include the emission, absorption, scatter, diffraction and fluorescence of radiation (Skoog, 1992). This dissertation will mainly focus on the aspect of X-ray fluorescence (XRF).

X-rays are produced during XRF analysis in an X-ray tube using a tungsten (W) filament (cathode, negative) which is heated to incandescence by an electron current passing through external filament terminals. The hot W filament produces a cloud of electrons which are accelerated along a focusing tube towards a target material (anode, positive) which is rhodium (Rh). The Rh anode consists of a thin film of Rh mounted on a copper block which serves to conduct heat away from the electron-beam focusing point. The high-energy electrons produced by the W filament are accelerated towards the Rh target material due to a potential difference between the W cathode and the Rh anode. During this study the tube voltage and current were kept at 50 kV and 50 mA, respectively for the analysis of all the elements and oxides.

When the high-energy filament electrons hit the Rh film, the inner electrons of the Rh atoms absorb this energy with the results that the electrons in the Rh atom are excited. When the filament electrons have sufficient energy to excite the inner electrons in a Rh atom, these electrons can be expelled from the inner orbitals of the atom. The atom is now in the

so-called excited state. Energy is released in the form of X-rays - known as primary X-rays (photons) because they originate from the Rh tube - during the process of relaxation (returning to the original energy state) of the inner electrons as a result of electron transitions from higher to lower energy levels in the atom to fill the created electron vacancies.

The sample is now bombarded with these primary X-ray photons. If the photons have a high enough excitation potential the photons may be absorbed by inner electrons in the sample atoms which will then expel electrons from their atomic orbitals and consequently leave the atoms in an excited state. This process closely resembles the way Rh atoms are excited in the X-ray tube. During the relaxation process of the electrons of the elements in the sample (after excitation by the primary X-rays), characteristic X-rays are produced from each element, now known as secondary X-ray photons due to their origin from the sample.

Therefore, an incident quantum of primary X-rays can remove an electron out of an atom. This will cause the emission of characteristic radiation (spectral lines). The incident photon is absorbed in this process. The ejected electron is known as a photoelectron, or secondary photon, and the emitted characteristic radiation is known as secondary or fluorescent radiation (Agarwal and MacAdam, 1979). This process is known as X-ray fluorescence. X-ray photons produced by the atoms of each sample element are unique in energy for each element because of the characteristic energy levels (also known as orbitals or shells) within different atoms. This whole procedure can be related back to the energy conservation equation from a quantum-theory viewpoint where:

$$h\nu_0 = \frac{1}{2}mv^2 + E_k \quad (2.1)$$

Where $h\nu_0$ = energy of the primary X-ray photon
 $\frac{1}{2}mv^2$ = kinetic energy of the ejected electron
 E_k = binding energy of the electron in a specific shell

This process gives rise to measurable (in terms of intensity) characteristic X-ray (spectral) lines. These lines are notated as K-lines, L-lines, M-lines and N-lines depending on which shell (energy level) the electron vacancy was filled from during the relaxation process. The K-shell is the shell closest to the atomic nucleus, followed by the L-shell, M-shell and N-shell. A K-vacancy filled with an electron from the L-shell will produce characteristic K-lines, an L-vacancy filled from the M-shell will produce L-lines, and so on. Because of the instrumental parameters and analytical conditions used, the focus point in this study will be on the measurement of K-lines produced during relaxation. Si, P and S produce only K-lines because they are elements with a low atomic number.

A further reason for only measuring the K-lines is that the relative intensity of the K-lines within a K, L, M and N series are significantly higher compared to the intensities of the other lines. If the relative intensity of a K-line is given a virtual value of 100 the approximate relative intensities of the L-lines will be in the range of 5 – 10, with a value in the range of 1 for the M-lines and much less for the N-lines. It therefore serves a useful purpose to measure the K-lines because their higher intensity leads to more effective detection than the lower intensity of the other lines.

The excitation potential of a particular electron in an atomic orbital is a direct function of the amount of protons in the atomic nucleus and the distance of the electrons from the nucleus. The more protons in the nucleus (heavier elements) and the closer the electrons are to the nucleus in terms of energy levels, the stronger the electrostatic attraction between the protons and electrons will be. The amount of electrostatic energy that attracts an electron towards the atomic nucleus is known as the electron binding energy which is different for each electron in the atom because of the variance in distance of the electrons from the nucleus and the variance in the amount of protons in the nuclei of different elements.

The probability of absorption of a primary X-ray photon by an inner electron in a sample atom and of the electron then being expelled from the

atom is at its highest when the photon energy of the primary X-ray equals or exceeds the binding energy of that specific electron. This energy is expressed by the Duane-Hunt Law (Skoog, 1992):

$$E = h \times c / \lambda \quad (2.2)$$

Where E = energy of the X-ray photon (keV units)
 h = Planck's constant (4.135×10^{-18} keV.sec)
 c = speed of light (3×10^8 m/s)
 λ = wavelength of photon (in Å)

Substitution of the constant values for h and c into the equation yields:

$$E = 12.4 / \lambda \quad (2.3)$$

This is a useful relationship for the conversion of energy to wavelength or *vice versa*.

The intensity of characteristic secondary X-ray photons (seen as spectral lines) produced during XRF analysis can be measured with relevant detectors, specifically the Flow Proportional Counter (FPC) for the study under review. This detector is effective for the analysis of elements ranging widely from Be to Zn, including the analyte elements Si, P, S and Cr. The detector's metal casing serves as a cathode while a filament inside it serves as the anode. A high voltage is applied across the two electrodes. The FPC is filled with Ar-gas mixed with methane as a quenching gas. An X-ray photon from an analyte element enters the detector and ionises the gas to form an electron pair. The number of electron pairs formed is a function of the energy of the incident photon. Therefore, the number of electron pairs formed inside the detector is a function of the energy of the incident photons. This process forms electric charges which are amplified to measure the intensity of the specific spectral line (K-lines noted earlier), thereby offering the means to determine which elements are present in the sample. Elements in the

sample can be analysed qualitatively and quantitatively by comparing the intensity of spectral lines produced by sample elements with the intensity of spectral lines produced by calibration standards (with known chemical composition and concentrations).

An example regarding the electron transitions and the attendant characteristic energy will be described with particular reference to Cr as an example.

In Cr, the excitation potential of electrons is 5.988 kV in the K-shell and 0.574 kV in a particular L-shell. This means that the energy needed to expel a K-electron, thus causing a vacancy in the K-shell of the Cr atom is 5.988 kV while 0.574 kV is needed for the same purpose in the L-shell. When a K-electron is removed from the Cr atom it follows that the atom is left with 5.988 kV excess (the energy needed to remove the K-electron). The atom is now in an excited state. When the K-shell vacancy is filled by the relaxation of the L-electron, the relaxation process will produce an X-ray photon with a characteristic energy of 5.414 kV. This energy is calculated by subtracting the excitation potential of the electron in the L-shell from that in the K-shell as the electron from the L-shell fills the vacancy formed in the K-shell:

$$5.988 \text{ kV} - 0.574 \text{ kV} = 5.414 \text{ kV}.$$

Therefore, a CrK α -photon with energy of 5.414 kV (energy of a CrK α line) is released. Note that all spectral lines within a series are excited and emitted simultaneously due to the fact that K-shell vacancies may be filled with electrons from the L-shell and M-shell, thus producing K α and K β lines, each with a characteristic energy. K β lines originate when the K-vacancy is filled with an electron from the M-shell instead of an electron from the L-shell. Similarly, vacancies created in the L-shell will result in corresponding L α and L β lines when vacancies are filled from the M-shell and N-shell respectively, with sub-series lines where applicable.

In this study the analyte element in charge chrome with the highest excitation potential is Cr (5.988 kV for the K-shell). It is therefore relevant to note that the photon energy of a RhK α 1 line (20.214 keV) emitted from the X-ray tube has sufficient energy to remove a K-electron from a Cr atom. The excitation potentials and photon energies of the elements that will be studied and analysed for are all summarised in Tables 2.1 and 2.2.

Table 2.1: Excitation potential of elements in the X-ray tube and elements in charge chrome.

X-ray line	Excitation Potential (kV)
Rh K-line (from X-ray tube)	23.224
Si K-line	1.838
P K-line	2.142
S K-line	2.470
Cr K-line	5.988
Mn K-line	6.537
Fe- K-line	7.111

Table 2.2: Photon energies of the K X-ray spectral lines for the relevant elements.

Element	K α 1 (keV)	K α 2 (keV)	K β 1 (keV)
Rh	20.214	20.072	22.721
Si	1.740	1.739	1.832
P	2.015	2.014	2.136
S	2.308	2.306	2.464
Cr	5.414	5.405	5.946
Mn	5.898	5.887	6.490
Fe	6.403	6.390	7.057

The reason for the slight differences in the energy values of the various K-lines for the same element is that there is a different set of quantum numbers for each electron inside the atom. According to the Pauli

Exclusion Principle no two electrons in the same atom can have the same set of quantum numbers, hence the different energy values.

The quantum numbers defining the characteristic energy value of each electron are dependent on and determined by four factors, namely:

- the principal quantum number (n) which indicates the energy level (shell) in which the electron is situated. For the K-shell $n = 1$, for the M-shell $n = 2$, etc.
- the angular quantum number (l) determines the shape of the orbital with values of 0, 1, 2... for s, p, d orbitals etc.
- the magnetic quantum number (m) defines the angular momentum associated with a specific orbital and defines the direction of the magnetic field for a specific orbital. This value is influenced by the angular quantum number and can take on values of +1, -1 or 0.
- the spin quantum number (s) indicates the direction of the electron spin inside an orbital and can take on values of $+\frac{1}{2}$ or $-\frac{1}{2}$.

It is clear from these factors that the characteristic energy values of electrons in a particular shell and orbital will differ, with the result that similar slight energy differences will characterise individual K-lines within the same atom.

Quantitative analysis of the sample is possible if the X-ray emission spectrum of a sample containing various elements can be obtained and compared with the spectra of the pure elements. The reason for this is that the inner shell energies are almost independent of the outer shell chemical properties and depend exclusively on the atomic number, which is unique for each element (Howarth, 1973). The fact that the transitions responsible for fluorescence involve the inner electrons that take no part in chemical bonding causes the position and intensities of the K-lines to be the same regardless of whether the target is in the pure elemental state or in the oxide form (Skoog, 1992).

To summarise: An atom is left in an excited state when a K-shell electron is removed from the atom by a primary X-ray. The atom regains stability by single or multiple electron transitions from outer shells in the atom. The energy associated with these transitions between shells (energy levels) in the atom decreases in the order $K^+ > L^+ > M^+ > N^+$ (Harada and Sakurai, 1999).

Each time an electron is transferred, the energy is emitted as a secondary X-ray photon with a wavelength corresponding to the difference in the energies between the initial and final states of the electron being transferred. This process continues until the energy of the atom approximates the energy value associated with the atom before excitation (Jenkins and De Vries, 1967). The excitation potential (expressed in kV) of an element is the minimum energy required to expel an electron from a certain orbital within the element. The relaxation of atoms to their original state with the subsequent release of energy is the source of characteristic and measurable X-ray lines for each specific element. The intensities of these X-ray lines are directly proportional to the concentration of the elements analysed (Misra and Mudher, 2002).

An XRF-spectrometer basically consists of the X-ray tube (generates primary X-rays to excite atoms in the sample), collimators (to focus X-rays on the crystal and detector) and the detector which generates photon energy from the sample which is transformed into measurable electrical signals.

CHAPTER 3 QUALITATIVE WAVELENGTH SCANS - ELEMENTS

3.1 Qualitative wavelength scans for Si, P, S and Cr

Doing qualitative wavelength scans on a production sample indicates the 2θ angles at which each element line of interest is diffracted by the crystal used for analysis. This will give an indication of spectral overlaps, if any, between the elements present in the sample. The sample is scanned over a predetermined wavelength range taking into account the element spectral lines of interest as well as the necessary instrumental parameters that will be used during the eventual analysis of the samples. Wavelength dispersive XRF is based on the Bragg Law which will now be discussed in detail.

3.1.1 Derivation of the Bragg Law

After the elements in the sample have been excited by the primary X-rays from the tube, each element emits secondary X-ray photons with a characteristic wavelength (fluorescence). These secondary X-ray photons from the sample are focused onto an analysing crystal using a collimator that intercepts the photons from the sample to ensure that a parallel photon beam is projected onto the crystal. The collimator, which is situated between the sample and crystal also ensures that only X-rays that arise from the sample are allowed to reach the crystal. The function of the analysing crystal is to separate all the characteristic secondary X-ray wavelengths emitted by the elements in the sample into distinct wavelengths by means of diffraction.

This process conforms to Bragg's Law which is explained using the following equation:

$$n\lambda = 2d \sin\theta \quad (3.1)$$

Where n = order of diffraction
 λ = wavelength of photon (Å)
 d = interplanar crystal spacing (Å)
 θ = Bragg angle, the angle between incident X-rays and diffracting planes

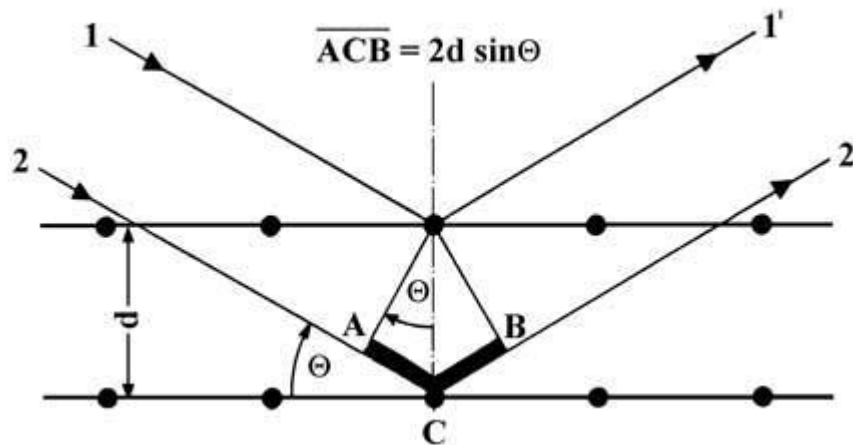


Figure 3.1: Schematic diagram of an analysing crystal, illustrating Bragg's Law

Analytical crystals consist of the periodic arrangement of atoms or molecules in numerous lattice planes, horizontally, vertically and diagonally. All these lattice planes are a set distance from each other and are known as the lattice plane distance, or interplanar crystal spacing (the value "d" in the Bragg equation). This crystal spacing is illustrated in Figure 3.1.

QUALITATIVE WAVELENGTH SCANS - ELEMENTS

When secondary X-ray waves from the sample fall on the parallel lattice planes, the incident waves are scattered by the atoms or molecules in the crystal below the angle θ . The scattered wavelengths are notated as waves 1' and 2' in Figure 3.1. The waves are amplified when coherent interference of the waves occurs (i.e. the reflected waves are precisely in phase). The phase difference between the incident waves 1 and 2 (scattered on the first plane and second plane respectively) is 'ACB'. According to the trigonometrical sine function:

$$'AC' / d = \sin\theta \text{ or } 'AC' = d \sin\theta \quad (3.2)$$

The phase difference between the two waves will be twice 'ACB' so that:

$$'ACB' = 2d \sin\theta \quad (3.3)$$

When coherent interference occurs (amplification of the waves) the phase difference of the waves will be a whole multiple of the wavelength λ , so that:

$$'ACB' = n\lambda, \text{ giving equation 3.1:}$$

$$n\lambda = 2d \sin\theta$$

The value 'n' indicates the order of reflection ($n = 1, 2, 3 \dots$). By using Bragg's Law the wavelength (λ) of a line can be calculated when measuring the angle (θ) using a crystal with known crystal spacing (d). This enables the identification of chemical elements since emitted wavelengths are unique in energy for each element. By measuring θ and keeping λ constant it is possible to calculate the value of d , thus enabling determination of the crystal structure. This forms the basis of X-ray diffraction spectroscopy (www.bruker-axs.de Accessed on 2009-06-24).

3.2 Qualitative wavelength scans

As mentioned earlier, doing wavelength scans for the elements to be determined in the sample will verify the 2θ angle at which each element line is diffracted by the crystal and to see if spectral overlaps occur between element lines, in which case corrections need to be made accordingly.

No spectral overlaps are really expected for the elements with low atomic numbers like Si, P and S because the line wavelengths for these elements are not as close together as those for elements with higher atomic numbers (Hollas, 1990). Wavelength scans for elements with higher atomic numbers (Cr, Mn and Fe) were thoroughly investigated for possible spectral overlaps.

The fact that the elemental composition of the samples as well as the expected concentrations of the different elements are known makes it easier to choose the analytical parameters to be used during the wavelength scans. Fe (as a major element, > 30%) and Mn (< 1%) also make up the composition of charge chrome and were therefore included in the wavelength scans to determine if these element lines might overlap with any of the analyte lines. The preselected analytical parameters that will be used at this stage include the type of analysing crystals, the collimators and detectors as well as the instrumental parameters (voltage and current). These parameters are summarised in Table 3.1.

QUALITATIVE WAVELENGTH SCANS - ELEMENTS

Table 3.1: Analytical parameters used during wavelength scans for Si, P, S, Cr, Mn and Fe

Element	Crystal	Collimator (mm)	Detector	Voltage (kV)/Current (mA)
Si	PET	Coarse (0.6)	FPC	50/50
P	PET	Medium (0.25)	FPC	50/50
S	PET	Medium (0.25)	FPC	50/50
Cr	LiF200	Coarse (0.6)	FPC	50/50
Mn	LiF200	Coarse (0.6)	FPC	50/50
Fe	LiF200	Coarse (0.6)	FPC	50/50

The PET (Penta-Erythritol) crystal was used for the light elements Si, P and S due to its high reflection efficiency. This will allow higher intensities from the reflected photons to reach the detector. The LiF200 crystal was used for the heavier elements (Cr, Mn and Fe) because it is known that this crystal is suitable for the analysis of a very wide range of elements and the reflection efficiency of this crystal is very high. A further advantage of using these crystals is that the possibility of crystal fluorescence is eliminated. Crystal fluorescence takes place when the elements of which the crystal itself is composed are excited by incident X-rays from the tube, or by X-rays generated by the sample itself (secondary X-rays). The crystal therefore emits its own characteristic X-ray lines which will cause background intensity during the scan. The absorption edges (the maximum wavelength needed to excite an electron at a specific energy level) of the elements comprising the two crystals (H, C and O for the PET crystal and Li and F for the LiF200 crystal) do not fall in the wavelength range of the element lines to be determined. The probability is extremely low that the elements of which the two crystals consist will be excited by X-rays and hence give rise to crystal fluorescence (Bonnelle, 1982). Hydrogen and lithium are extremely light elements and do not fall in the scope of XRF analysis.

QUALITATIVE WAVELENGTH SCANS - ELEMENTS

A medium collimator (0.25 mm) for the wavelength scans for P and S was used to filter out some background noise. The reason for this is the low line intensities of the lighter elements, and the low concentration of P and S in the sample contributes further to the lower intensities. There is a possibility that the intensities of the P and S lines may be close to the average intensity of the background. A medium collimator will remove some background noise, which will make the identification of the analyte lines easier. A coarse collimator was used for the remaining elements. A FPC detector was used for all the wavelength scans.

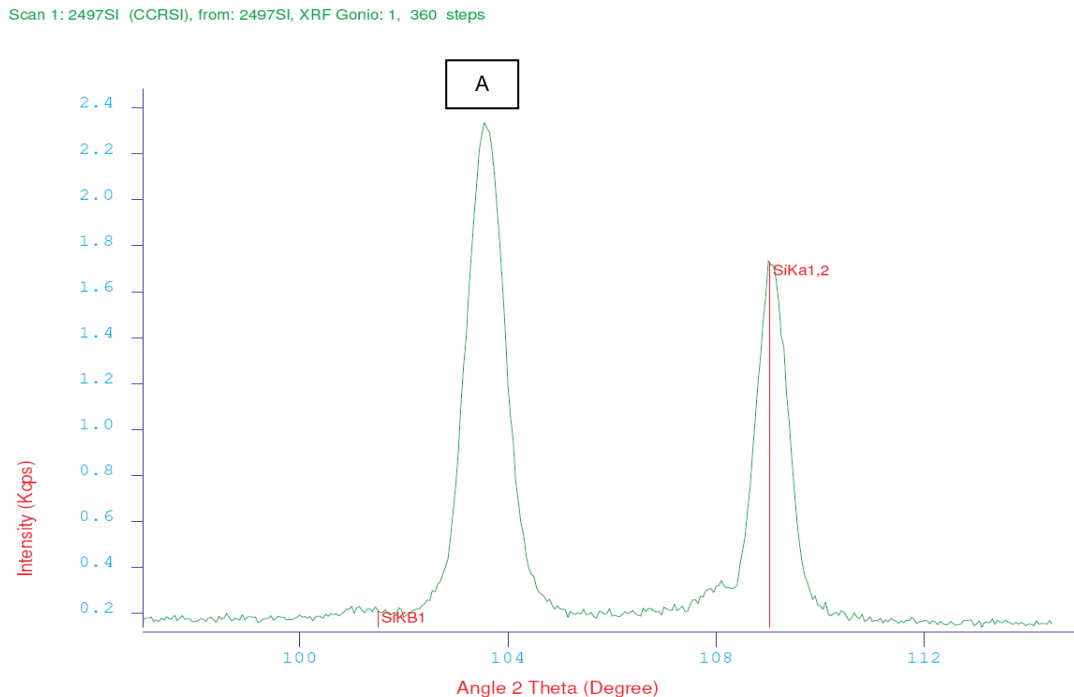
The theoretical 2θ angles of the $K\alpha$ and $K\beta$ lines for Si, P, S, Cr, Mn and Fe were calculated using the Bragg Law (equation 3.1). The calculations were done using first-order lines ($n = 1$), the wavelength of the principal $K\alpha$ -line (in Å units) and the crystal spacing of the PET and LiF200 crystals respectively. The results obtained during these calculations are summarised in Table 3.2.

Table 3.2: Theoretical 2θ angles for Si, P, S, Cr, Mn and Fe $K\alpha$ and $K\beta$ lines calculated using Bragg's Law

Spectral line	λ (Å)	$2d$ (Å)	2θ (degrees)
Si $K\alpha$	7.126	8.7518 (PET)	109.02
Si $K\beta$	6.769	8.7518 (PET)	101.33
P $K\alpha$	6.155	8.7518 (PET)	89.38
P $K\beta$	5.804	8.7518 (PET)	83.09
S $K\alpha$	5.373	8.7518 (PET)	75.75
S $K\beta$	5.032	8.7518 (PET)	70.19
Cr $K\alpha$	2.291	4.028 (LiF200)	69.33
Cr $K\beta$	2.085	4.028 (LiF200)	62.35
Mn $K\alpha$	2.103	4.028 (LiF200)	62.90
Mn $K\beta$	1.910	4.028 (LiF200)	56.61
Fe $K\alpha$	1.937	4.028 (LiF200)	57.49
Fe $K\beta$	1.757	4.028 (LiF200)	51.72

QUALITATIVE WAVELENGTH SCANS - ELEMENTS

The values obtained during these calculations will now be compared with the wavelength scans which are shown in Figures 3.2 – 3.4. Any additional lines appearing in the wavelength scans will be identified by comparing the 2θ degree value obtained in the scan to 2θ degree values commonly available in literature tables (Willis, 2008 and White and Johnson, 1970). This was be done to try and identify unknown lines in the wavelength scans, keeping in mind the known composition of the sample.



Identification Report:

```

Scan 1
Sample Number: 2497
Operator Name: NIE08049
Sample Type: CCR
XRF9800316
Goniometer: XRF 1
Crystal: PET
Detector: FPC
Collimator: 0.60
PBD: None
kV/mA: 50/50
    
```

Line	Intensity (Kcps)			Angle (deg)
	Scan 1	Scan 2	Scan 3	
SiKB1	0.2103			101.5139
SiKa1,2	1.7248			109.0285

Figure 3.2: Si wavelength scan

The lines, 2θ angles and line intensities obtained during the Si wavelength scan are summarised in Table 3.3.

QUALITATIVE WAVELENGTH SCANS - ELEMENTS

Table 3.3: Summary of the Si wavelength scan

Spectral line	2 θ (degrees)	Intensity (kcps)
SiK β 1	101.51	0.21
A	103.55	2.33
SiK α 1,2	109.03	1.72

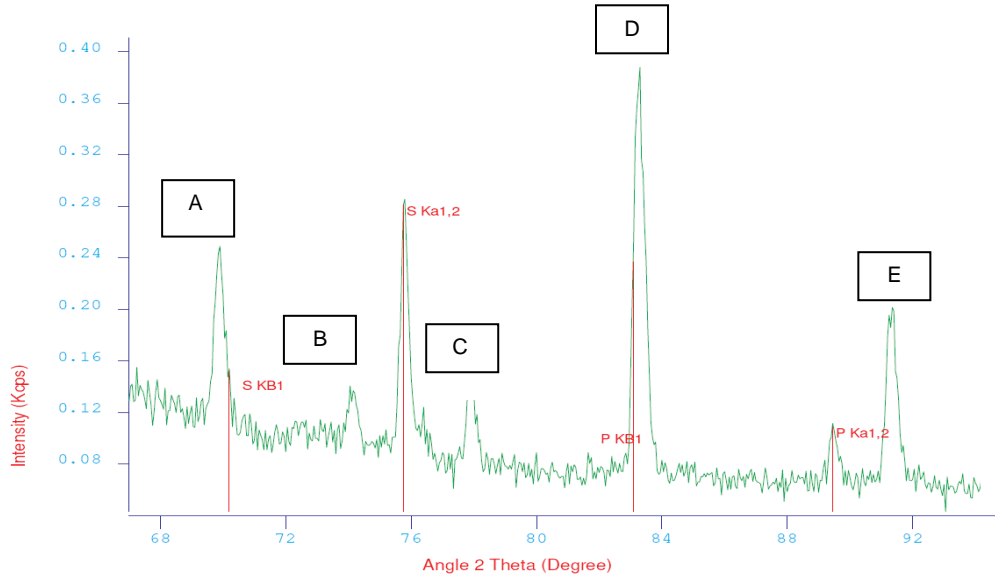
The Si wavelength scan was done over the range 97 – 115 2 θ degrees which should include the K α and K β lines. These two lines are well identified on the wavelength scan at 109.03 and 101.51 2 θ degrees. These values compare well with the calculated 2 θ values shown in Table 3.3. A very prominent line, labelled line “A”, appears right next to the SiK β 1 line at 103.55 2 θ degrees. The intensity of this line (2.33 kcps) is more than twice the intensity of the SiK β 1 line. According to available literature tables this line can be identified as most probably a CrK α 1 line (which appears at 103.58 2 θ degrees on the PET crystal). This will explain the high intensity of the line. Cr is a major element in charge chrome.

The appearance of this line next to the SiK β 1 line is of little importance because only the SiK α 1,2 line will be used during the eventual quantitative analysis. On the Si wavelength scan it is evident that there is no overlap affecting the SiK α 1,2 line, which means that no overlap correction on the line is needed.

A wavelength scan for P and S (Figure 3.3) was done over a 67 – 95 degree 2 θ range on a PET crystal. All the lines, 2 θ angles and line intensities obtained during this wavelength scan are summarised in Table 3.4.

QUALITATIVE WAVELENGTH SCANS - ELEMENTS

Scan 1: 2497PS (CCRPS), from: 2497PS, XRF Gonio: 1, 560 steps



Identification Report:

```

Scan 1
Sample Number: 2497
Operator Name: NIE08049
Sample Type: CCR
XRF9800316
Goniometer: XRF 1
Crystal: PET
Detector: PFC
Collimator: 0.25
PBD: None
kV/mA: 50/50
    
```

Line	Intensity (Kcps)			Angle (deg)
	Scan 1	Scan 2	Scan 3	
S KB1	0.1525			70.1883
S Ka1,2	0.2810			75.7500
P KB1	0.2369			83.0819
P Ka1,2	0.1087			89.4374

Figure 3.3: P and S wavelength scan

Table 3.4: Summary of the P and S wavelength scan

Spectral line	2θ (degrees)	Intensity (kcps)
A	69.91	0.247
SKβ1	70.19	0.153
B	74.1	0.14
SKα1,2	75.75	0.281
C	77.9	0.143
PKβ1	83.08	0.237
D	83.3	0.389
PKα1,2	89.44	0.109
E	91.3	0.202

QUALITATIVE WAVELENGTH SCANS - ELEMENTS

On this wavelength scan no spectral overlaps seem to appear on the $PK\alpha_{1,2}$ (89.44 2θ degrees) and $SK\alpha_{1,2}$ (75.75 2θ degrees) lines. Thus no correction for overlaps needs to be made on these lines.

Line "A" at 69.91 2θ degrees is very close to the $SK\beta_1$ line at 70.19 2θ degrees. The 0.247 kcps intensity of line "A" is higher than the 0.153 kcps intensity of the $SK\beta_1$ line. According to wavelength tables this line may well be a $VK\alpha_{1,2}$ line which appears at 69.93 2θ degrees on a PET crystal. This could indicate the possibility of low amounts of V in the charge chrome sample.

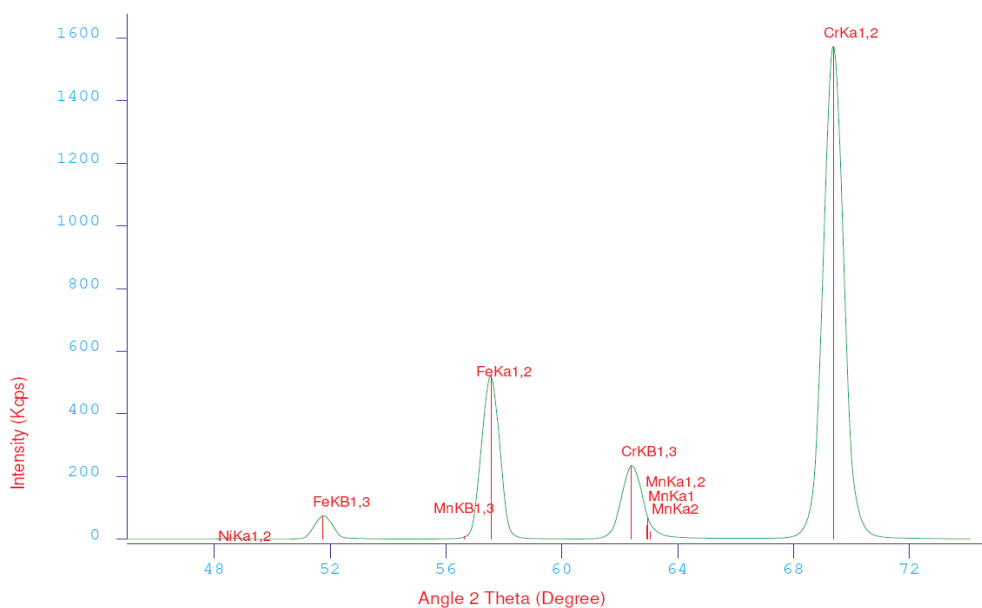
Line "D" at 83.3 2θ degrees seems to be overlapping with the $PK\beta_1$ line. This line has a significantly higher intensity of 0.389 kcps compared to the 0.237 kcps of the $PK\beta_1$ line. Line "D" is most probably a $FeK\alpha_{1,2}$ line (83.34 2θ degrees on a PET crystal). This conclusion is further supported by the fact that the composition of charge chrome is made up of high amounts of Fe (> 30%).

Lines "B", "C" and "E" are identified as $FeK\beta_1$, $TiK\alpha_{1,2}$ and $CrK\beta_{1,3}$ respectively according to wavelength tables. These lines have no influence on the $PK\alpha_{1,2}$ and $SK\alpha_{1,2}$ analyte lines.

The last wavelength scan involves the elements Cr, Mn and Fe. This scan was done using a LiF200 crystal over a 45 – 75 2θ degrees wavelength range. This scan is illustrated in Figure 3.4. Table 3.5 summarises the results of this wavelength scan.

QUALITATIVE WAVELENGTH SCANS - ELEMENTS

Scan 1: 2497CRFE (CCRCRMNFE), from: 2497CRFE, XRF Gonio: 1, 600 steps



Identification Report:

```

Scan 1
Sample Number: 2497
Operator Name: NIE08049
Sample Type: CCR
XRF9800316
Goniometer: XRF 1
Crystal: LiF200
Detector: FPC
Collimator: 0.60
PBD: None
kV/mA: 50/50
    
```

Line	Intensity (Kcps)			Angle (deg)
	Scan 1	Scan 2	Scan 3	
NiKa1,2	3.8458			48.7000
FeKB1,3	75.8179			51.7500
FeKa1,2	520.1334			57.5500
CrKB1,3	235.1291			62.4000
CrKa1,2	1572.3860			69.4000
MnKa1	81.2283			62.9291
MnKa1,2	68.0575			62.9731
MnKa2	48.6898			63.0613
MnKB1,3	7.1527			56.6388

Figure 3.4: Cr, Mn and Fe wavelength scan

Table 3.5: Summary of the Cr, Mn and Fe wavelength scan

Spectral line	2θ (degrees)	Intensity (kcps)
NiKa1,2	48.7	3.85
FeKβ1,3	51.75	75.82
MnKβ1,3	56.64	7.15
FeKa1,2	57.55	520.13
CrKβ1,3	62.4	235.13
MnKa1,2	62.97	68.06
CrKa1,2	69.4	1572.39

QUALITATIVE WAVELENGTH SCANS - ELEMENTS

The purpose of doing wavelength scans for Fe and Mn as well was to see if any of these element lines overlap with the CrK α _{1,2} analyte line. On the wavelength scan the CrK α _{1,2} line appears at 69.4 2 θ degrees, which correlates well with the theoretical value of 69.33 2 θ degrees obtained during calculation according to Bragg's Law (refer to Table 3.2).

On the wavelength scan it can be seen that the CrK β _{1,3} line overlaps with the MnK α _{1,2} line. Another overlap is found between the FeK α _{1,2} and MnK β _{1,3} lines. These overlaps are of no significance since none of these lines form part of the quantitative analysis of charge chrome. A NiK α _{1,2} line with a low intensity appears at 48.7 2 θ degrees on the wavelength scan which indicates the possible presence of very low amounts of Ni in charge chrome.

After investigation of all the wavelength scans the conclusion can be drawn that no significant spectral overlaps occur at the element lines of interest for the quantitative analysis of charge chrome. Corrections for spectral overlaps are therefore unnecessary and have not been implemented.

3.3 Energy profiles

When X-ray photons from the sample enter the detector it causes ionization of the detector gas, Ar. This forms an electron pair and the number of electron pairs formed is a function of the energy of the sample photon. This process leads to the formation of electric charges which are amplified to measure the intensity of the sample photon which corresponds to a specific spectral line (the K α -spectral line for example) from the sample.

There is a direct proportion between the energy of the sample photon entering the detector and the number of electron pairs formed. The

QUALITATIVE WAVELENGTH SCANS - ELEMENTS

number of electron pairs produced by a sample photon has a random distribution and is not a fixed value, even for monochromatic (single wavelength) X-rays. Not only the number of electron pairs produced, but also the time intervals over which the electron pairs are produced are not uniform. The distribution of electrical pulses from the element photon generated in the detector is therefore a factor of both the number of electron pairs formed during ionization of the detector gas, as well as the time distribution over which these electron pairs, and hence the pulses, are formed.

As a general rule, the amount and intensity of pulses produced inside the detector gives a Gaussian, or normal distribution about a mean height value directly proportional to the energy of the sample photons. A plot of the number of pulses (in terms of intensity) versus the pulse height is known as the pulse-height distribution (PHD). This plot is also referred to as the energy profile of a specific spectral line (Hollas, 1990).

According to the factory-calibrated parameters of the XRF spectrometer used during this study, the ideal energy profile of an element line will generate a count rate of > 10 kcps and the mean of the PHD scale (steps) should be roughly 70 - 75 V. The values obtained during the energy profile runs of Si, P, S and Cr are summarised in Table 3.6 and the energy profile spectra are attached in Appendices A – D.

Table 3.6: Summary of the Si, P, S and Cr energy profile runs

Spectral line	Count rate (kcps)	PHD steps
SiK α	12.9705	74.04
PK α	49.5725	74.04
SK α	47.5935	72.14
CrK α	23.7625	72.14

CHAPTER 4 CALIBRATION LINES - ELEMENTS

4.1 Setting up of calibration lines for the analysis of Si, P, S and Cr

For the accurate analysis of silicon, phosphorus, sulphur and chromium it is necessary to set up individual calibration lines on the XRF for each element because the response between line intensity and concentration is only relative (Bremser and Hässelbarth, 1997).

Any calibration should be traceable to standards with known concentrations. Empirical data obtained from these standards will be used to calculate unknown quantitative information from measurements being done during the analytical procedure using mathematical models that should be relevant to the actual calibration data to preclude unreliable and imprecise predictions (Martens 1989).

In setting up calibration lines for the elements, standards with known concentrations of each element were scanned on the XRF spectrometer to determine the spectral-line intensity (kcps) related to the known concentration (%) for each element. These values were used to set up a calibration line (response curve) relating the intensity of the spectral lines to the individual concentrations of the elements. When a sample with an unknown concentration is analysed the concentration can be determined by relating the intensity of the element spectral line obtained from the sample back to the calibration line because on the calibration line the spectral-line intensity is a function of concentration (François *et al.*, 2004).

It is important to use standards that will cover the complete concentration range for each element to be determined to prevent extrapolation during quantitative analysis which may cause erroneous results, especially when second-order calibration lines are used. With this in mind as well as the fact that all the calibration lines will be validated for specific quality control

parameters using relevant statistical methods, the focus point was to set up linear response curves for each element. Mathematical expressions used to calculate the uncertainty in an analytical result involving linear response curves cannot be applied when nonlinear response curves are evaluated because the results obtained may be inaccurate (Tellinghuisen, 2005).

The ideal for setting up good calibration lines is to use Certified Reference Materials (CRMs). The precise concentration of an element, as well as the uncertainty related to the concentration, are known for CRMs. This is important because the accuracy of any calibration depends on the accuracy of the standards used. It is unfortunately not always possible to use CRMs due to the limited availability of these standards. In these cases secondary standards (also known as artificial standards or reference standards) were prepared and the concentrations of the relevant elements were determined using an alternative validated analytical procedure. These secondary standards were prepared from charge chrome production samples. Standards used to set up calibration lines should also contain the elements necessary to determine and correct for possible matrix effects in the sample. This greatly enhances the advantage of using production samples as secondary standards because the matrix of the secondary standards is the same as the matrix of the samples to be analysed.

4.2 Matrix effects

Matrix effects can be divided into two categories: spectral interactions between different elements in the sample; and the physical state of the sample. Elemental interactions involve absorption and enhancement effects between elements in the sample itself (Calvert *et al.*, 1985). When elements in the sample are excited by primary X-rays all the excited elements release characteristic X-ray photons. Some of these secondary

photons might be able to excite other elements in the sample if they have a high enough excitation potential. These photons that have enough energy to cause excitement of elements in the sample may lead to absorption and enhancement effects inside the sample matrix itself, hence the term 'matrix effects'.

For this study particle size is the critical matrix effect due to the physical state of the sample. Absorption is by far the most prominent source of error due to matrix effects in XRF analysis and it is therefore essential to make the necessary corrections for absorption when setting up calibration lines, but only if analysis could be significantly affected.

The general equation used during quantitative analysis in XRF spectroscopy relating to a linear response between concentration and net spectral-line intensity is as follows:

$$C_i = K_i \times I_i \times M_i \times S \quad (4.1)$$

Where C_i = weight fraction of element 'i' ($C_i = \%C_i / 100$)
 K_i = slope of the calibration line for element 'i' (% / kcps)
 I_i = net line intensity for element 'i' (kcps)
 M_i = matrix correction term for element 'i'
 S = sample preparation term (S_s / S_{STD})

This is clearly a linear response. The sample preparation term S , is only significant when there is a difference in the preparation between the samples and standards. During this study both the samples and standards will be prepared as powder briquettes, therefore this term will have a value of 1 and can be eliminated from the equation.

The matrix correction term M_i , is relevant where matrix effects occur due to elemental interactions in the sample. These correction terms are calculated using mathematical equations, with due allowance for spectral line intensity, the concentration of the various elements in the sample, and

the influence coefficients of other elements in the sample on the specific element analysed for (Han *et al.*, 2006).

Using influence coefficients therefore enables the use of matrix correction terms to quantify inter-element matrix effects. The influence coefficients can then be used to calculate correction terms to convert the measured intensity of the analyte spectral line into accurate concentrations.

Absorption can best be described by looking at the relation between the excitation potential of an element and the energy of an emitted photon. Excitation potential is defined as the minimum energy needed to expel an electron from an inner-orbital in an atom, while photon energy is defined as the amount of energy of the expelled photon when the atom returns to its original energy state. This minimum excitation potential, also referred to as the absorption edge of a specific element, is slightly higher in energy, meaning shorter in wavelength, than the energy of the emitted photon. The excitation potential and photon energy values for the analyte elements are summarised in Tables 2.1 and 2.2 from where it is evident that the excitation potential of an electron in a specific energy level in an element, and hence the absorption edge for that electron, is higher in energy than the photon that will be emitted after initial excitation and relaxation of the atom.

Matrix effects may have a lesser influence on the lighter elements, which include Si, P and S during this study. It is possible therefore that no corrections, especially regarding spectral interferences, need to be made for these elements. The elements are also present as minor or trace elements. The low concentrations may further minimize the influence of matrix effects. However, this can only be confirmed by setting up calibration lines and studying the mathematical fit of all the calibration points on the lines. If the mathematical fit seems to be fairly satisfactory, the calibration line will be validated for accuracy to see if any corrections for matrix effects need to be made.

For the heavier elements, Cr and Fe in this case, matrix effects will have a significant influence on analytical results, especially since they are also present as major elements in charge chrome. As mentioned earlier, excitation is most efficient when the wavelength of the exciting element is just shorter (i.e. just higher in energy) than the K-line absorption edge of the element to be excited. In the case of Fe and Cr, the wavelength of the principle FeK α -line is 1.937 Å while the CrK α absorption edge has a wavelength of 2.07 Å. It is clear that the absorption of Fe by Cr is very large. Relating this back to equation 4.1, the matrix correction term M_i , for the effect where Fe will be absorbed by Cr, needs to be implemented in the equation giving equation 4.2:

$$C_{Fe} = K_{Fe} I_{Fe} [1 + \alpha_{FeCr} C_{Cr}] \quad (4.2)$$

The influence coefficient α_{FeCr} , is the coefficient correcting for the magnitude of the amount of absorption of Fe by Cr. The matrix correction term is expressed as $[1 + \alpha_{FeCr} C_{Cr}]$ in equation 4.2. Values of influence coefficients are usually expressed as mass absorption coefficients (MAC). In this specific example the MAC of Cr on FeK α equals 480.83. These values are available in various sources of XRF literature. Equation 4.2 is derived from the Lechance-Trail algorithm for the correction of matrix effects (www.icdd.com).

This correction, however, needs to be done where Fe is the analyte and Cr forms part of the sample matrix. Both Fe and Cr are present as major elements in charge chrome, but the focus will be on Cr as analyte and not Fe. Taking account of absorption as matrix effect during this study, where Cr absorbs FeK α , this implies that Cr is actually enhanced (or excited) by FeK α . The effect of enhancement as a systematic error in XRF is less pronounced compared to absorption. The effect of absorption far exceeds that of enhancement (by an order of >10). Since the effect of enhancement on systematic errors is relatively insignificant compared to absorption, it is not expected to have a major influence during this study given that Cr is the analyte element enhanced by FeK α (Willis, 2008).

When setting up calibration lines for the analyte elements no matrix corrections on calibration lines were considered at first because, as discussed, the influence of matrix effects on light elements (Si, P and S) is relatively insignificant. This observation is supported by the fact that these elements are only present in minor or trace levels. No correction on the calibration line for Cr was considered because of enhancement of Cr by FeK α which might have an insignificant effect. The main indicator of the suitability of the calibration lines for analysis at this stage will be the mathematical fit of all the calibration points on the line which will be discussed when setting up each line.

During this procedure important mathematical and statistical parameters need to be taken into account to ensure that the lines will be able to produce accurate results when used during analysis. These parameters will be investigated and discussed during the setting-up phase for each line where relevant. The actual validation for accuracy and other various parameters influencing the suitability of the calibration lines for analysis will be discussed in detail in Chapter 5.

A total of sixteen standards of which only seven are CRMs were used, emphasising the limited availability of CRMs. The specific standards chosen for each calibration line depended mostly on the concentration range of the element that needs to be covered on the line. These standards are all listed in Table 4.1 and are identified as CRMs or as secondary standards.

Table 4.1 Standards used during the setting up of calibration lines

Standard	Type of standard
BS 130/1	CRM
BS 130/2	CRM
BS 130/3	CRM
CMSI 1622	CRM
METAL A	CRM
METAL E	CRM
204/4	CRM
10	Secondary Standard
14	Secondary Standard
16	Secondary Standard
18	Secondary Standard
20	Secondary Standard
M31685	Secondary Standard
M31688	Secondary Standard
M32509	Secondary Standard
M33103	Secondary Standard

4.3 Setting up a calibration line for the analysis of Si

The expected Si-concentration in charge chrome samples is <1%. This may cause a problem setting up a calibration line because the available CRM with the lowest concentration of Si contains 4.06% Si (METAL E). It is therefore evident that the concentration range of Si <1% cannot be adequately represented on the calibration line with the available CRMs.

It was decided to take three ordinary production samples (M31685, M31688 and M33101) of which the Si concentration is expected to be <1%, and determine the % Si in these samples by using validated Inductively Coupled Plasma - Optical Emission Spectroscopy (ICP-OES) as an analytical method.

Si is regarded as a minor element and therefore ICP-OES was used as the analytical method due to the good sensitivity of the technique. The analytical procedure includes fusion of the sample in a closed muffle furnace. This is done by weighing 0.200 g (\pm 0.009 g) sample into a Zr crucible. To the sample, 2.5 g sodium peroxide and 0.5 g sodium carbonate are added. The sample is then fused in a closed muffle furnace at 650 °C for 30 minutes. The result of this decomposition is the formation of a melt which is leached with deionised water into a 250 ml glass beaker, followed by the slow addition of 20 ml concentrated hydrochloric acid which serves to dissolve the melt. After cooling to room temperature, the sample is transferred quantitatively into a 200 ml volumetric flask. The solution is diluted if necessary, and the % Si is determined against calibration standards. All chemicals used during this analytical procedure were of Analytical Grade or equivalent. The limit of quantification (LOQ) of this analytical procedure for the analysis of Si is 0.18% which is less than the lowest CRM concentration (4.06%) that will be used on the calibration line.

After analysing these production samples they were used as secondary standards for setting up a calibration line, and the % Si obtained from the ICP-OES analysis was incorporated as true values (therefore treating them as CRMs) on the line. These secondary standards, as well as the rest of the standards used to set up a Si calibration line, are summarised in Table 4.2. As mentioned earlier, the standards were selected to represent the concentration range of the analyte on the calibration line. Table 4.2 also shows statistical values obtained from the calibration line without any matrix corrections being made. These values were used as parameters to make a preliminary decision on the effectiveness of the calibration line for analysis. The values are automatically calculated by the instrumental software during the setting up of the calibration line. Figure 4.1 shows the calibration line for Si. During this discussion the concentration values depicted on the calibration curves are expressed as percentage (%) values.

Table 4.2: Standards and statistical values for the SiK α calibration line

Standard	I (kcps)	μ (%)	x (%)	Δ (%)
M33101	6.112	0.139	0.156	0.01655
M31685	11.66	0.431	0.437	0.00561
M31688	25.16	1.16	1.12	-0.03885
METAL E	85.09	4.06	4.16	0.09808
BS 130/1	91.17	4.46	4.47	0.00622
20	92.47	4.62	4.53	-0.08760

From this table the following values are obtained:

- spectral line intensity, I
- true analytical value of CRM or secondary standard, μ
- value of the standard calculated according to the linear equation of the calibration line, x
- absolute difference, Δ (difference between μ and x)

Analyte: SiKa_mC LOD (1 s): 83.9 ppm BEC: 0.154 % Q: 19.731 Kcps/% SEE: 0.0692

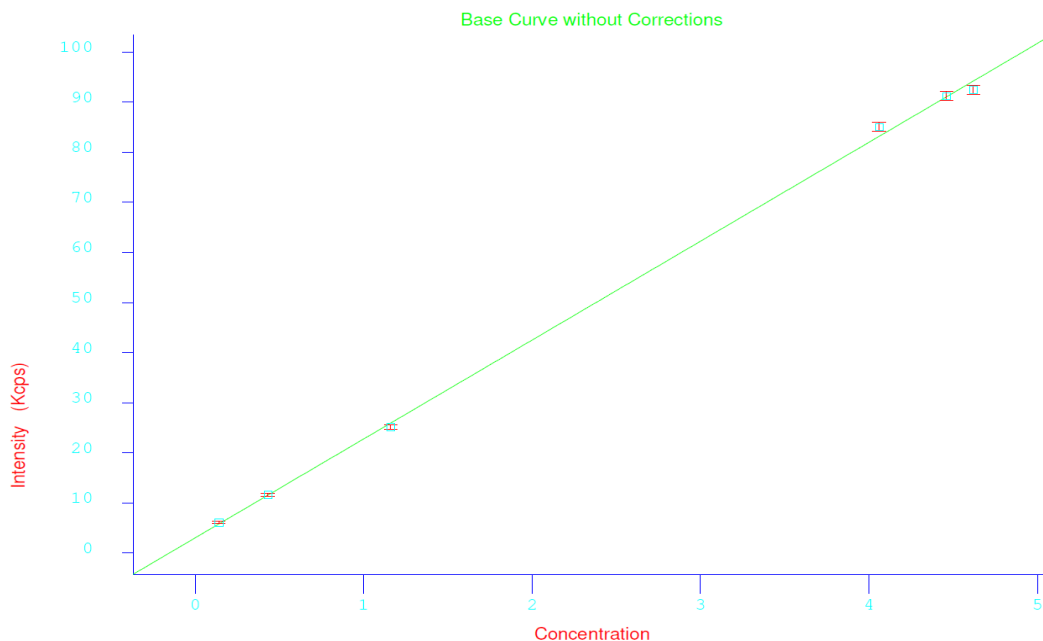


Figure 4.1: SiK α calibration line without corrections

The equation obtained for this linear function ($C = A_1 I + A_0$) is:

$$C = 0.0507 I - 0.154 \quad (4.3)$$

Where C = concentration (%)
 I = net peak intensity (kcps)
 A₀ = intercept
 A₁ = slope

For any calibration line a SEE value (Standard Error of Estimate) can be calculated. This value gives an indication of the quality of the correlation fit of all the standards used on the calibration line and takes into account the absolute difference (Δ) between the true concentration value (μ) and the calculated value (x), as well as the number of calibration standards used. Although limited, it is essential to use a sufficient number of calibration standards which will represent the full concentration range of the element on the calibration line. The equation for calculating the SEE is:

$$SEE = (\Sigma \Delta^2 / n-2)^{1/2} \quad (4.4)$$

In this equation, $\Sigma \Delta^2$ equals the sum of the square of the absolute difference for all standards, and 'n' is the number of standards used on the calibration line. The lower the SEE value, the better the correlation fit of the standards on the calibration line.

As can be seen from equation 4.4, SEE is a function of the values of the difference between the true analytical value of the standard and the value calculated by using the linear function of the calibration line (x in Table 4.2, calculated by using equation 4.3). It is also a function of the number of standards used to set up the calibration line (Martens,1989). It is important to note that this value only describes the mathematical fit of the standards on the calibration line and is by no means an indication of the capability of the line to produce accurate results when applied during analysis. This

capability will only be determined when, amongst other parameters, the calibration line is validated for accuracy.

The SEE does, however, give a good indication of the covariance between spectral line intensity and analyte concentration. The smaller the value of SEE, the higher is the probability that the response between C and I on the calibration line is indeed a linear response and suitable for quantitative analysis. For the Si-calibration line $SEE = 0.069$, which is fairly low.

The value of the absolute difference of each calibration point on the line was evaluated to see if the individual calibration points have a good mathematical fit with regard to the calibration line. This value is very much concentration-dependent. This implies that the absolute difference must be evaluated taking into account the concentration level of the standards represented on the calibration line.

The value obtained for Δ is very small in the sense that the difference between the true value of the standard and the value calculated according to the linear response equation of the calibration line is low.

Referring back to Table 4.2, it is evident that the concentration differences between the true analytical value and the calculated value is significantly small, especially considering the low concentration level of the standards. The lowest calibration standard, which is a production sample analysed by ICP-OES, has an estimated value of 0.139%. This value is lower than the LOD of the ICP-OES technique, which is 0.18% for Si. This value is therefore an extrapolated value, but nevertheless, and because Δ for this standard is small, it will still be used on the calibration line. This concentration is very low and if the standard has a good enough fit on the calibration line and does not reduce the accuracy of the results obtained when using the calibration line for analysis, it will lower the detection limit of Si. These criteria will be established and discussed during the validation of the Si calibration line.

4.4 Setting up a calibration line for the analysis of P

The standards chosen to set up a P-calibration line are summarised in Table 4.3. Again, these standards were chosen taking into account the concentration range of P in charge chrome, which is expected to be relatively constant at around 0.02%. The calibration line for P is illustrated in Figure 4.2.

Table 4.3: Standards and statistical values for the PK α calibration line

Standard	I (kcps)	μ (%)	x (%)	Δ (%)
BS 130/2	0.690	0.0130	0.01313	0.00013
10	0.744	0.0150	0.01505	0.00005
18	0.849	0.0190	0.01875	-0.00025
20	1.052	0.0260	0.02597	-0.00003
14	1.169	0.0300	0.03010	0.00010

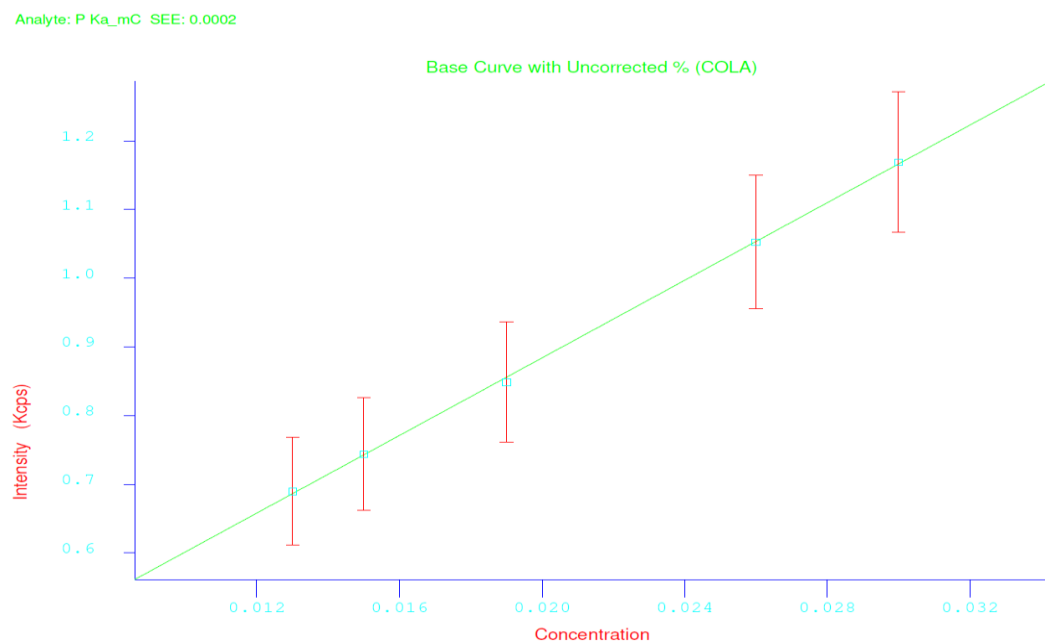


Figure 4.2: PK α calibration line without corrections

After interpretation of the Δ values in Table 4.3 it is again evident that the difference between μ and Δ is very small. This indicates a good covariance between C and I, an observation that is supported by the low SEE of 0.0002. The good mathematical fit of the individual standards on the calibration line can also be seen on Figure 4.2. These results lead to the decision that no matrix corrections regarding spectral interferences will be made for P at this stage.

Equation 4.5 represents the linear response between C and I for the P- calibration line:

$$C = 0.0354 I - 0.0113 \quad (4.5)$$

4.5 Setting up a calibration line for the analysis of S

The standards chosen to set up and represent the concentration range of S in charge chrome are summarised in Table 4.4. The calibration line for S is illustrated in Figure 4.3.

Table 4.4: Standards and statistical values for the SK α calibration line

Standard	I (kcps)	μ (%)	x (%)	Δ (%)
M31685	0.572	0.011	0.0116	0.00064
CMSI 1622	0.632	0.013	0.0124	-0.00065
BS 130/3	2.005	0.029	0.0284	-0.00065
18	2.228	0.030	0.0310	0.00095
METAL-A	2.636	0.036	0.0357	-0.00029

CALIBRATION LINES - ELEMENTS

Analyte: S Ka_mC Q: 87.528 Kcps/% SEE: 0.0009

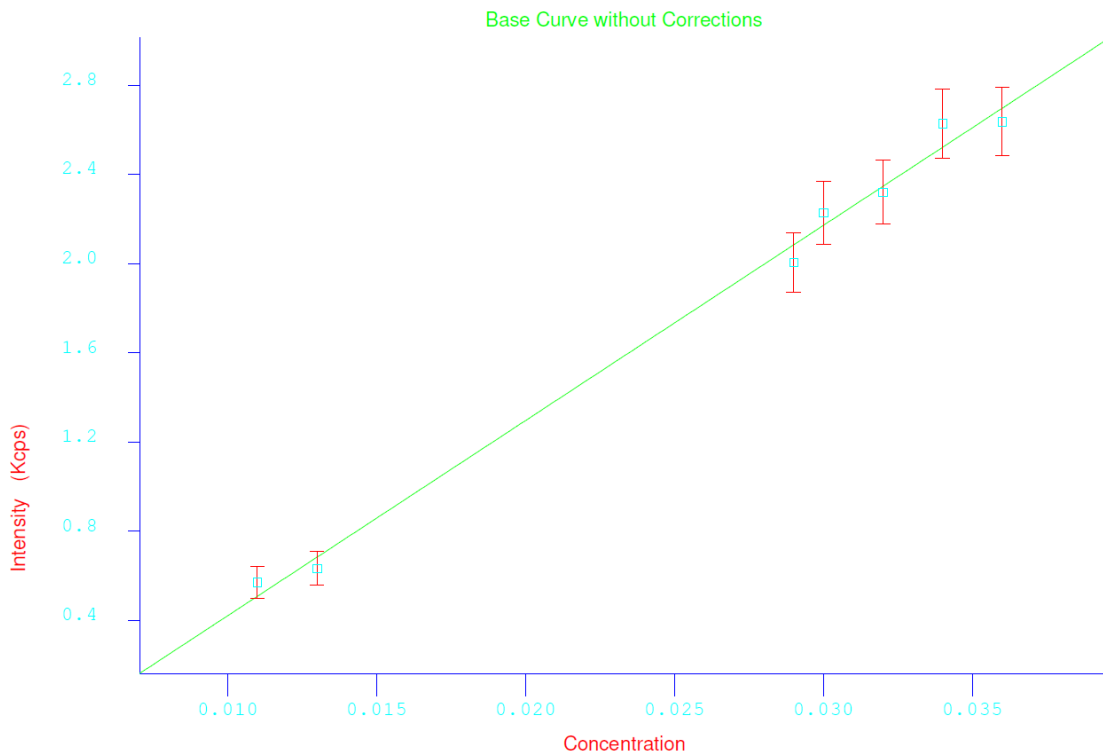


Figure 4.3: SK α calibration line without corrections

The SEE for the S-calibration line is 0.0009 and equation 4.6 represents the linear response between C and I.

$$C = 0.0117 I - 0.00498 \quad (4.6)$$

As mentioned in Table 1.1, the expected concentration of S in charge chrome is < 0.04%. The highest calibration point on the line is CRM METAL-A with a S concentration of only 0.036%. This is not much lower than the expected concentration, and if the line shows acceptable linearity during the validation procedure, a small amount of extrapolation beyond 0.036% should not have a significant influence on the accuracy of results. As with P, the S concentration is expected to be relatively constant in charge chrome samples, and this value might be lower than 0.036%, which will eliminate the need for extrapolation further than the highest calibration point.

The Δ values for S are low enough to assume a good mathematical fit. As can be seen on the calibration line (Figure 4.3) none of the calibration points has a perfect fit on the line itself. The uncertainty of each calibration point (illustrated by the red uncertainty range on the calibration point) all falls on the calibration line which indicates a good enough mathematical fit.

4.6 Setting up a calibration line for the analysis of Cr

The standards for the Cr-calibration line are summarised in Table 4.5. The calibration line is illustrated in Figure 4.4.

Table 4.5: Standards and statistical values for the CrK α calibration line

Standard	I (kcps)	μ (%)	x (%)	Δ (%)
METAL –A	246.43	50.65	50.9171	0.257
18	249.50	51.58	51.6707	0.091
10	250.15	51.90	51.8308	-0.069
M31688	251.12	52.10	52.0704	-0.030
M32509	255.27	53.10	53.1009	-0.001
20	260.66	54.44	54.4381	-0.302
204/4	331.25	71.95	71.9519	0.0519

CALIBRATION LINES - ELEMENTS

Analyte: CrKa_mC LOD (1 s): 1511.3 ppm BEC: 10.230 % Q: 4.031 Kcps/% SEE: 0.1865

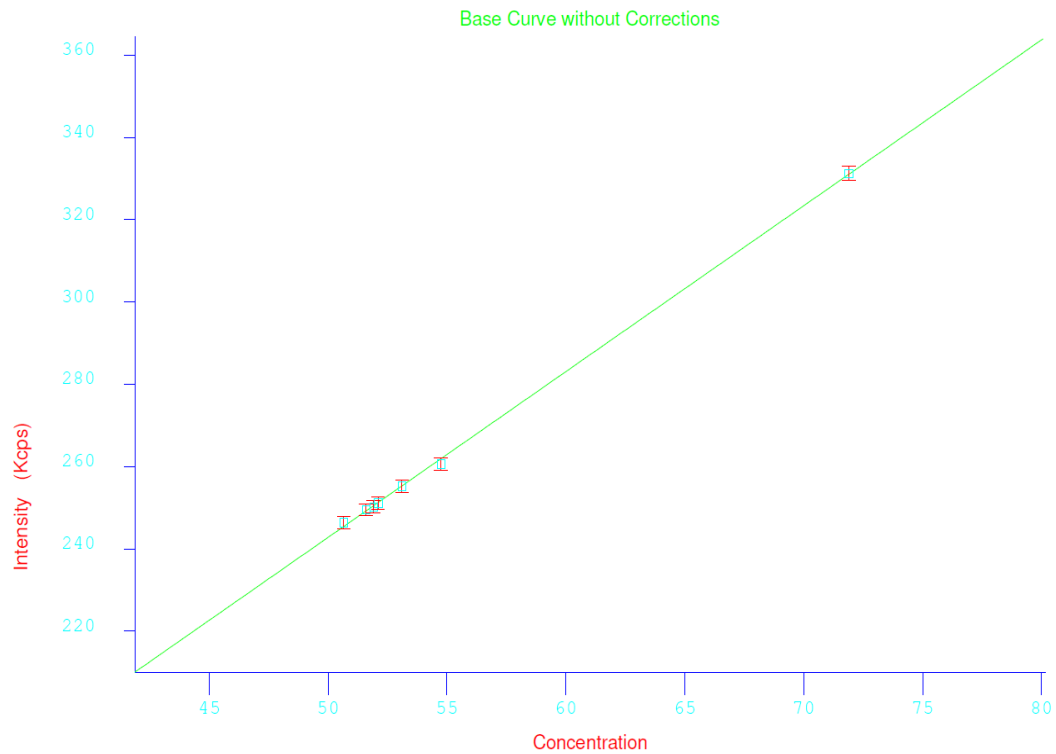


Figure 4.4: CrK α calibration line without corrections

As mentioned earlier, the Δ values should be evaluated taking into account the concentration range of the elements on the calibration line. The concentration of Cr in the samples is much higher than the concentrations of Si, P and S. This is also evident from the very high CrK α -line intensities. Although the Δ values for Cr seem much higher than those determined for the minor and trace elements, they are actually rather low as a proportion of the high Cr concentration.

Given the high Cr concentrations, the SEE value of 0.1865 is low enough to indicate a good covariance between C and I. The equation relating the linear response between C and I for Cr is as follows:

$$C = 0.248 I - 10.23 \quad (4.7)$$

The Δ values for all four calibration lines are low enough to indicate a fairly good correlation between μ and x . Further, the SEE for each line is also low enough to assume a good mathematical fit for all the standards on the individual lines. Equations 4.3, 4.5, 4.6 and 4.7 represent the linear response between spectral-line intensity and concentration for each line. The equations are models used to describe the relation between C and I and can be used to predict the concentration of an element if the $K\alpha$ -line intensity of the element is measured by the instrument.

At this stage the calibration lines have only been evaluated using a mathematical fit (according to the SEE and Δ values). This is not good enough, however, to assume that each line will be able to give accurate results during an analysis. This and other validation parameters will now be determined using specific statistical calculations to prove that all the lines are able to give accurate and trustworthy results and are fit for the intended analysis of each of the charge chrome samples.

CHAPTER 5 METHOD VALIDATION – ANALYSIS OF ELEMENTS

5.1 Method validation for the analysis of Si, P, S and Cr

Errors occur unavoidably regardless of whatever analytical method is used. In fact, errors form part of almost every aspect of analysis, from sampling and sample preparation, right up to the final result, errors are generated in the process of instrumental detection or the generation and interpretation of results during a wet chemical analysis.

Errors are classifiable into gross, random or systematic errors. Gross errors are of such a nature that the entire analysis has to be abandoned. When multiple analysis is done on a sample and a systematic error occurs, all individual results will be biased, yielding values that are either higher or lower than the true analytical value, with the result that the true value is not included in the results range, implying that systematic errors have a direct influence on the accuracy of the results.

Random errors are spread over a range higher and lower than the average analytical value, in other words on both sides of the average result. Random errors effectively influence the precision of results due to the wide range over which the results appear. Given that errors form part of any analysis and are a critical factor leading to uncertainties in analytical results, these errors must be identified and quantified wherever possible. One of the main purposes of analytical-method development is to try and minimize systematic and random errors as far as possible so that application of the method can yield acceptably accurate results. Gross errors should obviously be strictly avoided. In fact, minimising errors is integral to the validation of an analytical procedure.

Validation of an analytical method helps to determine whether results obtained during analysis are sufficiently interpretable and reliable. A good

validation procedure will ensure a good predictive ability of the method in terms of results obtained. A validated method will also facilitate the identification of errors. The primary aim of validating an analytical method is therefore to ensure and provide the evidence to prove that the chosen analytical method can yield correct and trustworthy results in conformity with standards and specifications laid down by the test laboratory.

In the process of validating the method used to analyse Si, P, S and Cr in charge chrome various statistical methods were used to validate relevant parameters to prove the reliability and efficiency of the test method. The analytical parameters validated include the following:

- accuracy and precision of the results
- analytical range
- determination of detection and quantitation limits
- determination of the linear regression
- calculation of uncertainties in the analytical measurements.

For the purpose in hand accuracy can be defined as the deviation of the measured analytical result obtained during analysis from the true concentration value of the analyte in the sample. The accuracy of this XRF method was validated against CRMs with known concentrations. Precision, which can be defined as the spread or variation between results for the multiple analysis of one homogeneous sample, was validated with the interpretation of standard deviation and relative standard deviation values as validation criteria.

Analysing variances with the aid of the ANOVA function of Microsoft Excel[®] was used to determine the detection and quantitation limits as well as the validation of regression and the measurement of uncertainties in the analytical results. The calculation of the uncertainty associated with an analytical result is of extreme importance during method validation (Hosogaya *et al.*, 2008). The theory and implementation of statistical techniques relevant to the analysis of charge chrome applied during this

validation procedure are methods almost exclusively drawn from Martens and Næs (1989) and from Miller and Miller (2005).

5.2 Validating accuracy for the analysis of Si, P, S and Cr

As noted, accuracy can be defined as the variation of an analytical result obtained during an analysis, with the true analyte concentration in the sample. In validating the accuracy of the XRF method for the analysis of the various elements, the accuracy was validated by analysing CRMs with known concentration values (obtained from the CRM certificate of analysis) for each element. The average of the values obtained during analysis was evaluated for accuracy by comparing it to the CRM value using the statistical t-test. The aim of the t-test is to determine statistically whether there is a significant difference between the average analytical result (x_{avg}) and the true value (μ) of the analyte in the sample.

Final assessment of the accuracy of a result after performing the t-test proceeds from a comparison of hypotheses, first being the null hypothesis (H_0) which assumes that the average analytical value x_{avg} , for an element in the CRM is not significantly different from the true value μ , of that element in the CRM. The value of x_{avg} can therefore be regarded as accurate. The second or alternative hypothesis (H_1) assumes that there is a significant difference between x_{avg} and μ hence x_{avg} cannot be deemed accurate.

Multiple measurements of CRMs were made and the x_{avg} value of these measurements was calculated in order to validate accuracy. This value will provide an estimate of μ , the true value. Multiple measurements lead to a range (or population) of results that are likely to contain the true value. The width or spread of this range depends on the precision (repeatability) of the results and on the number of measurements (n) done.

This range determines the confidence interval, and the extreme values (lowest and highest) define the limits of this interval. The term ‘confidence’ implies that assumptions can be made only up to a certain level which is determined by the population of results. This means that there is a certain probability that the confidence interval will contain the true value. The larger the confidence interval, the higher the certainty that the true value will be present within the confidence limits.

During this validation statistical assumptions are made that fall within the 95% confidence interval. A set of analytical measurements (n) made around the value μ usually gives a Gaussian (normal) distribution around μ , that is if no systematic errors occur during analysis that may cause the results to be biased higher or lower than μ . It is generally accepted that if the measurements falls within a normal distribution around μ , then 95% of the sample measurements will lie within the range expressed in equation 5.1:

$$\mu - 1.96 (\sigma / n^{1/2}) < x_{\text{avg}} < \mu + 1.96 (\sigma / n^{1/2}) \quad (5.1)$$

Where μ = true analytical value
 x_{avg} = average value of measurements
 n = number of measurements
 σ = standard deviation of n measurements
 1.96 = z value over a 95% confidence interval range
 (obtainable from statistical tables)

The z value, also known as the standard normal cumulative distribution function, is usually rounded off to a value of 2. Only one CRM was used for the accuracy validation for each element, which means that a range around μ is required. The above equation can therefore be rearranged to give equation 5.2:

$$x - 1.96 (\sigma / n^{1/2}) < \mu < x_{\text{avg}} + 1.96 (\sigma / n^{1/2}) \quad (5.2)$$

A multiple repetition of measurements implies a higher confidence in the average of the analytical values obtained. This would mean that the estimate of x_{avg} with regard to μ will improve with a larger number of measurements.

For accuracy validation the null hypothesis wants to be retained, which means no significant difference between x_{avg} and μ , and the alternative hypothesis wants to be rejected. The null hypothesis was tested on a 95% (0.05) confidence level as mentioned earlier, meaning that the chances of the null hypothesis to be rejected if it is indeed true, is less than 5%, therefore very small.

H_0 was subjected to the t-test where a calculated t-value ($|t|_{calc}$, regardless of the sign) will be evaluated against a critical t-value (t_{crit}). If $t_{calc} < t_{crit}$, H_0 will be accepted and the method will be regarded as accurate. If $t_{calc} > t_{crit}$, H_0 will be rejected and H_1 will be accepted, meaning the method cannot be deemed as accurate. The equation to calculate the t-value is as follows:

$$t_{calc} = (x_{avg} - \mu) n^{1/2} / \sigma \quad (5.3)$$

Where

- t_{calc} = calculated t-value
- x_{avg} = sample average
- μ = true concentration
- n = number of analytical measurements
- σ = standard deviation of 'n' analytical measurements

During validation, the calculated t-value was compared to a critical t-value, which is a function of n, the number of analytical measurements made, as well as the degrees of freedom (DF). This value refers to a number of independent deviations used to calculate the value of σ . The values of t_{crit} for different values of DF are available in numerous statistical tables. All the available statistical values and constants used during this validation were obtained from a training manual by De Beer (2006).

METHOD VALIDATION – ANALYSIS OF ELEMENTS

Two CRMs, one applicable to Si and Cr and the other to P and S, were analysed five times each. Note that these must be independent CRMs with regard to the element calibration line; that is these CRMs may not appear on the calibration line of the specific element validated for accuracy. After analysis x_{avg} , σ and t_{calc} were calculated for each element. The analytical results obtained are summarised in Table 5.1 while the statistical values obtained after calculations using these analytical values are compared in Table 5.2.

Table 5.1: Results (% concentration) obtained during the elemental analysis of CRMs for accuracy

Element	CRM	1	2	3	4	5
Si	BS 130/2	2.121	2.119	2.117	2.118	2.115
P	METAL E	0.0110	0.0108	0.0110	0.0110	0.0110
S	METAL E	0.0540	0.0540	0.0536	0.0539	0.0540
Cr	BS 130/2	49.31	49.31	49.23	49.32	49.30

Table 5.2: Summary of the statistical values obtained after the elemental analysis of CRMs for accuracy validation

Element	μ (%)	x_{avg} (%)	σ	n	DF	t_{crit}	t_{calc}
Si	2.120	2.118	0.00224	5	4	2.78	1.9
P	0.011	0.0108	0.00009	5	4	2.78	2.5
S	0.0540	0.0539	0.0002	5	4	2.78	1.1
Cr	49.30	49.29	0.0365	5	4	2.78	0.6

It is evident from the results summarised in Table 5.2 that $t_{calc} < t_{crit}$ for all elements. The calculations were done at the 95% confidence limit; therefore the value is 2.78 for t_{crit} . This means that the null hypothesis, H_0 , assuming that there is no significant difference between x_{avg} and μ , may be accepted and the conclusion can be drawn that the XRF method for the

analysis of Si, P, S and Cr, using the calibration lines developed in Chapter 4, yields accurate results.

5.3 Validating precision for the analysis of Si, P, S and Cr

The repeatability of results is an indication of the precision of a method. The more repeatable the results, the more precise the method. Note that precision is not an indication of accuracy. Results may have good repeatability and precision but may nevertheless be completely inaccurate.

A production sample (2497) was analysed five times to validate the precision of this method. The standard deviation for these five results will be used as an indication of the precision. By multiple analysis of the same sample the analytical values obtained will vary across a range extending between the lowest and highest extremes (if no biased systematic error occurs). For good precision the difference between the highest and lowest values should be as small as possible.

The standard deviation value (σ) is chosen as an indication of the precision because this value represents all the results obtained during a multiple analysis of the same sample for the same element(s). For the precision to be good, the standard deviation should be minimal indicating little deviation between results falling within the results population. The standard deviation is calculated using the following equation:

$$\sigma = [\sum_i (x_i - x_{\text{avg}})^2 / (n - 1)]^{1/2} \quad (5.4)$$

- Where
- σ = standard deviation
 - \sum_i = summation of all measurements
 - x_i = individual analytical result (out of 'n' results)
 - x_{avg} = average of measurements
 - n = number of analytical measurements

METHOD VALIDATION – ANALYSIS OF ELEMENTS

The relative standard deviation (%RSD) will also give an indication of the precision of the results. The %RSD is given by $100(\sigma / x_{avg})$. A value of < 2% for the %RSD is usually considered an acceptable measure of good precision. The results obtained by analysing a production sample to get an indication of the precision of the method are all summarised in Table 5.3.

Table 5.3: Summary of the five analytical results (% concentration) and the precision indicators for Si, P, S and Cr (production sample 2497)

Element	1	2	3	4	5	x_{avg}	σ	%RSD
Si	0.374	0.381	0.384	0.384	0.392	0.383	0.00648	1.69
P	0.0200	0.0197	0.0196	0.0196	0.0197	0.0197	0.000164	0.833
S	0.0154	0.0154	0.0155	0.0155	0.0154	0.0154	0.0000548	0.355
Cr	54.45	54.47	54.48	54.45	54.43	54.46	0.0195	0.0358

On examining the results shown in Table 5.3 it is obvious that the standard deviation for all elements is very low. This indicates good precision for all the elements analysed. All the %RSD values are below 2%, which further supports the assumption that the analytical method is capable of giving repeatable results, therefore good precision.

For Si, the %RSD value is relatively high compared to the values for the other elements. The first (0.374%) and last (0.392%) concentration values seem to be a bit lower and higher respectively than the other three results. There is always a possibility that some results may be regarded as outliers, meaning that they do not form part of the measurement population (analytical range). The validity of a result (or results) can be tested by using the Dixon Q-test to determine the possible outlier status of a result (or results).

As with the accuracy validation, this test also uses hypothesis statements to determine whether results can be regarded as outliers. A statistical Q-value (Q_{calc}) is calculated and compared to a critical Q-value (Q_{crit})

METHOD VALIDATION – ANALYSIS OF ELEMENTS

obtained from statistical tables. The value of Q_{crit} is determined by the number of analytical measurements in the population (n). The equation for the calculation of Q_{calc} is as follows:

$$Q_{calc} = |\text{suspect value} - \text{nearest value}| / R \quad (5.5)$$

'R' represents the range of the population, the absolute difference (regardless of sign) between the highest and lowest values. The analytical values 1 and 5 obtained during the precision determination for Si will be tested as possible outliers using the Q-test. The results are summarised in Table 5.4.

Table 5.4: Dixon Q-test results for possible Si outliers

Suspect value	Nearest value	R	n	Q_{crit}	Q_{calc}
0.374	0.381	0.018	5	0.71	0.389
0.392	0.384	0.018	5	0.71	0.444

The null hypothesis H_0 , states that all the measurements come from the same population and therefore cannot be regarded as outliers. This hypothesis is true when $Q_{calc} < Q_{crit}$. As can be seen from Table 5.4, this is the case with both the suspected values, therefore they cannot be regarded as outliers. This means that all five values used during the analysis of Si will be retained in the operations done to calculate σ and the %RSD. Although the %RSD value for Si is higher than those obtained for the other elements, it is still within the < 2% range which implies good precision for the results obtained during the analysis of Si. As mentioned earlier, this assumption is supported by the low σ value obtained for Si.

5.4 The analytical range and the detection and quantitation limits

The analytical range (or working range) is determined by the lowest and the highest calibration points (in terms of concentration) on the calibration line for a specific element. It is essential that the expected concentration value of the analyte must be included in the concentration range of the standards on the calibration line to exclude the possibility of extrapolation during analysis, which may lead to erroneous results. During the setting up of the calibration lines to analyse the elements (Chapter 4) measures were taken to ensure coverage of the analytical range for each element. Refer back to Table 1.1 for the expected concentration values of each element to be analysed in charge chrome.

A major advantage using XRF as an analytical method, is that the method can analyse elements at very low concentration levels. This is also true for other quantitative instrumental techniques where the analysis of trace and ultratrace ($\mu\text{g/L}$ and ng/L) quantities of elements are possible. The limit of detection (LOD) of an analyte can be described as the lowest instrumental signal produced by the analyte that is significantly distinct from a signal that is attributable to a blank sample or instrumental background. The limit of quantitation (LOQ) is regarded as the lowest concentration of the analyte that can be analysed with satisfactory accuracy.

All the statistical parameters and equations required to determine an acceptable analytical range and to calculate the LOD and LOQ values, as well as the calculation of regression and uncertainty values, was done using the ANOVA function on Excel as mentioned earlier.

In the calibration phase of the analytical method development, an empirical model was used to investigate the relation between two variables, the spectral line intensity (I , measured in kcps) and the concentration of the analyte (C , measured as percentage). The relation between these variables was found to be linear, without the use of

correction factors. The mathematical model used to represent this relation is the general linear regression model $y = bx + a$ where the value of 'b' represents the slope of the linear calibration line and 'a' the intercept of the line on the y-axis.

The calibration data for each element was used to do a statistical analysis of all the variances that are influential on the analytical range, LOD, LOQ and regression and uncertainty measurements to be determined and validated. The analysis of variance (abbreviated as ANOVA) is a very useful statistical technique which can be applied to separate and estimate the parameters that cause variances in analytical results. As mentioned, all these parameters and the equations required to do the calculations will be discussed during the ANOVA evaluation for each element. The discussion will be started by using Si as a foundation, and the same principles will be used during the validation of the elements P, S and Cr.

5.5 Statistical results and interpretation for the Si calibration line

The intensity (I) and concentration (C) values as represented on the Si calibration line (Table 4.2 and Figure 4.1) were used to set up regression statistics for the line. The values obtained during the determination of the statistical values are summarised in Table 5.5. The functions and necessary values to calculate the statistical parameters for validation are obtained from this data spread sheet as shown in Table 5.6.

Table 5.5: Regression statistics for the Si-calibration line

<i>Regression Statistics</i>	
Multiple R	0.9997
R Square	0.9993
Adjusted R Square	0.9991
Standard Error	1.2259
Observations	6

ANOVA				
	<i>df</i>	<i>SS</i>	<i>MS</i>	<i>F</i>
Regression	1	8714.136	8714.135973	5798.47741
Residual	4	6.011	1.502831753	
Total	5	8720.147		

	<i>Coefficients</i>	<i>Standard Error</i>	<i>t Stat</i>	<i>P-value</i>
Intercept	2.7824	0.8169	3.4062	0.027121565
X Variable 1	19.8360	0.2605	76.1477	1.78248E-07

Table 5.6: Functions for the calculation of statistical parameters for validation of the Si calibration line (obtained from Table 5.5):

Function	Description	Value
Multiple R (r)	Regression value	0.999
Standard error ($S_{y/x}$)	Random calibration uncertainty	1.23
Observations (n)	Number of standards analysed	6
Intercept (a)	Calibration line intercept	2.78
X Variable 1 (b)	Calibration line slope	19.8
Intercept Standard Error (S_a)	Uncertainty in intercept	0.817
X Variable 1 Standard Error (S_b)	Uncertainty in slope	0.260

Since ANOVA will mainly be used as a tool in determining LODs, LOQs, regression factors and measuring of the uncertainty in terms of the regression factor and analyte concentrations, the functions and values obtained from Table 5.5 will now be discussed and formulated to illustrate the dependence between the parameters and equations for proper statistical evaluation.

5.5.1 The regression value

The aim in setting up calibration lines in Chapter 4 was to get the best linear response between line intensity and concentration for the standards used on the various lines. The correlation coefficient, in other words the linear correlation between C and I, can be calculated to estimate how well the line linearly fits all the calibration points, For this study this value will be referred to as the regression value r , which is calculated using equation 5.6:

$$r = \frac{\sum_i \{(x_i - x_{\text{avg}})(y_i - y_{\text{avg}})\}}{\sigma} \quad (5.6)$$

The value r is a function of all the individual values of C and I for all the standards used on the calibration line as well as the average of these values. The regression value of these values (refer to equation 5.4) is also a function of the standard deviation. When $r = 1$, it will imply perfect positive correlation between C and I. For any calibration line this will be the ideal situation but is highly exceptional during instrumental analysis due to, amongst others, instrumental drift, slight variations in detector response caused by electrical noise that influence line intensities (I), and uncertainties in the concentration of the standards used (C). The value of r should be as close as possible to 1.

5.5.2 Random calibration uncertainty

The random calibration uncertainty $S_{y/x}$, is an indication of the random errors in the y-axis (I) of the calibration line. This value incorporates y-residuals $y_i - \hat{y}_i$, where the \hat{y}_i -value is calculated directly from the relevant linear function $y = bx + a$ of the regression line where the individual x-values (x_i) are used to calculate the fitted \hat{y}_i -value (\hat{y}_i). Random calibration uncertainty is calculated using equation 5.7:

$$S_{y/x} = [\sum_i (y_i - \hat{y}_i)^2 / n-2]^{1/2} \quad (5.7)$$

$S_{y/x}$ is a function of the sum of all the y residuals represented on the calibration line.

5.5.3 Uncertainty in the intercept and slope

The uncertainty in the intercept S_a , of the calibration line is calculated taking into account the random calibration uncertainty (y-axis random errors), the individual x-values on the calibration line and x_{avg} . This value is expressed as a standard deviation and can be calculated using equation 5.8:

$$S_a = S_{y/x} [\sum_i x_i^2 / n \sum_i (x_i - x_{avg})^2]^{1/2} \quad (5.8)$$

The uncertainty in the slope is also expressed as a standard deviation value S_b and is a function of $S_{y/x}$, the individual x-values on the calibration line and x_{avg} . This is expressed in equation 5.9:

$$S_b = S_{y/x} / [\sum_i (x_i - x_{avg})^2]^{1/2} \quad (5.9)$$

To summarise, all the parameters and their values as mentioned in Table 5.6 are obtained during the ANOVA calculations using Excel; consequently the following parameters, additional to accuracy and precision, can be determined during the statistical validation phase of the analytical method:

- the analytical range
- limit of detection
- limit of quantitation
- regression value
- uncertainty values in terms of the calibration line intercept and slope
- uncertainty values in terms of analytical concentration.

5.6 Determining the analytical range and the detection and quantitation limits for Si

As explained earlier, the analytical range is the difference between the highest and lowest values on a calibration line. The calibration line is a direct indication of the concentration range in which the analytical method is capable of giving good results. It is logical to assume that the calibration uncertainties influencing the line will also influence the analytical range represented by the calibration line.

The three calibration uncertainties discussed so far are:

- random calibration uncertainty ($S_{y/x}$)
- uncertainty in the slope of the calibration line (S_a)
- uncertainty in the intercept of the calibration line (S_b).

$S_{y/x}$ is an indication of the random error in the y-axis of the calibration line. This axis therefore represents the intensity variable on the calibration line. The analytical range is an expression of the concentration values of the

standards used in the calibration. This determines S_a and S_b and these values should be used as indices from which to infer whether the analytical range is wide enough to prevent extrapolation during concentration analysis. The general rule for the analytical range to be considered wide enough is $S_b < S_a$. Referring back to the values summarised in Table 5.6 where $S_a = 0.817$ and $S_b = 0.260$ it becomes clear that the concentration range represented by the Si-calibration line is wide enough for the levels of Si to be analysed in charge chrome. All the calculations that follow will be based on the calibration data in Table 5.6.

The regression line for Si according to the calibration data can be expressed by equation 5.10:

$$y = 19.8x + 2.78 \quad (5.10)$$

With this equation the LOD-value can be determined using equations 5.11 and 5.12:

$$y_{LOD} = a + 3S_a \quad (5.11)$$

The y_{LOD} value represents the lowest signal produced by the analyte that can be distinguished from instrumental background. With this value the lowest distinguishable analyte concentration x_{LOD} can be calculated using the following equation:

$$x_{LOD} = (y_{LOD} - a) / b \quad (5.12)$$

Substituting the values a , b and S_a in Table 5.6 into equations 5.11 and 5.12, it follows that for Si the $LOD = 0.124\%$.

The following equations are used to calculate the LOQ for Si:

$$y_{LOQ} = a + 10S_a \quad (5.13)$$

$$x_{LOQ} = (y_{LOQ} - a) / b \quad (5.14)$$

By again substituting the values in Table 5.6 into these equations, for Si the calculated LOQ = 0.412%.

Since the %Si in charge chrome is expected to be < 1%, it may be possible to analyse a sample with a Si content < 0.412%, which will be below the LOQ-value. The accuracy validation for the analysis of Si was done using a CRM with Si content = 2.12%. Since it seems from the foregoing discussion that the concentration range for the Si-calibration line is satisfactory ($S_b < S_a$), it can be readily assumed that the analysis of Si below the LOQ value should still produce acceptable results. Further, the lowest point on the calibration line is 0.156% Si, which is lower than the LOQ value.

The ideal would be to have a lower LOQ value for the analysis of Si than the calculated one. This can be achieved, for example, by introducing more Si standards on the calibration line with Si < 1%. But as mentioned earlier, CRMs representing a charge chrome matrix are not readily available. For future improvement of the method more secondary standards with low Si concentrations (production samples analysed by an alternative technique) can be added to the calibration line. This will lead to a lower LOQ value and make the method used to analyse Si in the concentration range of < 1% more effective.

5.7 Regression and the calculation of uncertainty in the analytical concentration of Si

As discussed earlier, regression can be described as the best fit of a calibration line between all the calibration points on the line. The ideal will be to obtain perfect linearity for the regression line, meaning that all calibration points fit the line perfectly. For the determination of the value of r , refer back to equation 5.6. It has been stressed that perfect linearity is

highly unlikely and the aim was to obtain a value of r as close as possible to 1.

The regression analysis done using ANOVA expresses r as Multiple R. During the calculation of the regression statistics summarised in Table 5.5 and Table 5.6 the value of $r = 0.999$ which indicates almost perfect linearity for the Si-calibration line.

Because analytical measurements are made in terms of concentration, estimates of the possible occurrence of errors are essential. This has been discussed earlier. Analytical results cannot be exact. An approximation of the uncertainty of the result, that is the range within which the true value lies, must be determined. This is referred to as the measurement of uncertainty of an analytical value.

The regression uncertainty is the largest contribution of uncertainty in an analytical value. To report a trustworthy analytical result it is therefore essential to calculate this uncertainty and include it in the concentration value to be reported. The calculation of the x value relating to a certain value of y (equation 5.10) involves the value of the slope (b) and the intercept (a). Since both these values are prone to error it follows that the final analytical value will be affected by the regression uncertainty S_{x0} , (notated as U(r)) which is calculated using equation 5.15:

$$S_{x0} = S_{y/x} / b [1/m + 1/n + \{ (y_0 - y_{avg})^2 / b^2 \sum_i (x_i - x_{avg}^2) \}]^{1/2} \quad (5.15)$$

It is clear from equation 5.15 that U(r) is a function of the following parameters:

- random calibration uncertainty, $S_{y/x}$
- slope of the calibration line, b
- total of individual sample analysis, m (usually m = 5)
- number of standards on the calibration line, n

METHOD VALIDATION – ANALYSIS OF ELEMENTS

- relation between an individual y-value and the average of all the y values on the calibration line, $y_0 - y_{avg}$
- sum of the relation between an individual x value and the average of all the x values on the calibration line, $\sum_i (x_i - x_{avg})$.

U(r) was calculated by analysing a representative production sample, (sample 2497 in this study) to obtain the values of x_0 and y_0 . For reasons of simplicity it is easier to determine the values of all the different parameters as mentioned above and do individual calculations of the factors represented in equation 5.15. The individual values are substituted back into equation 5.15 to calculate U(r). A copy of these calculations is shown below:

Data obtained from Si-calibration line:

	<u>x_i</u>	<u>y_i</u>	<u>$(x_i - x_{avg})$</u>	<u>$(x_i - x_{avg})^2$</u>
M33101	0.156	6.112	-2.322	5.394
M31685	0.463	11.658	-2.015	4.062
M31688	1.140	25.165	-1.339	1.793
METAL E	4.065	85.087	1.587	2.518
BS 130/1	4.439	91.170	1.961	3.845
20	4.608	92.470	2.129	4.534

x_i and y_i avg	2.48	51.94		
$\sum(x_i - x_{avg})^2$				22.147

Sy/x =	1.230
b =	19.830
m =	5
n =	6
y_0 =	9.811
x_0 =	0.374
y_{avg} =	51.944
b^2 =	393.626
$\sum(x_i - x_{avg})^2$	22.147

$$U_{reg} = Sy/x/b \sqrt{1/m + 1/n + (y_0 - y_{avg})^2 / b^2 \sum(x_i - x_{avg})^2}$$

$b^2 \sum(x_i - x_{avg})^2 =$	8717.63
$(y_0 - y_{avg})^2 =$	1775.15
$(y_0 - y_{avg})^2 / b^2 \sum(x_i - x_{avg})^2 =$	0.204 {1}
$1/m + 1/n =$	0.367 {2}
{1} + {2} =	0.570
$\sqrt{1 + 2} =$	0.755 {3}
Sy/x/b =	0.064 {4}
(Ur) = {3} x {4}	0.048 (%)

METHOD VALIDATION – ANALYSIS OF ELEMENTS

The value of $U(r)$ obtained during the calculations therefore implies an uncertainty value of $\pm 0.048\%$ relating to the analytical value of Si obtained by analysis. Since all the previous calculations of parameters, such as LOD and LOQ were done on a 95% confidence level, the concentration uncertainty is also based on that level. Sample 2497 gave a concentration value of 0.374% Si (x_0 , refer to the above data sheet). The uncertainty of this value is therefore $0.374\% \pm 0.048\%$, which implies that the true analytical value will be in the order of 0.326 – 0.422% Si. All the necessary parameters identified and calculated for the validation of the Si analysis are summarised in Table 5.7:

Table 5.7: Summary of the validation parameters and values for the Si analytical method

Validation parameter	Value	Description/Conclusion
Analytical range	$S_a = 0.817$ $S_b = 0.260$	$S_b < S_a$ Range satisfactory
Slope (b)	19.8	Regression line slope
Intercept (a)	2.78	Regression line intercept
Regression line	$y = 19.8x + 2.78$	Regression line equation
LOD	0.124%	Lowest distinguishable signal
LOQ	0.412%	LOQ < lowest calibration point (0.431%); still within analytical range
r	0.999	Almost perfect linearity
$U(r)$	0.048%	$x_0 \pm 0.048\%$

All the necessary validation parameters and criteria, as well as the necessary equations to calculate validation parameters, were discussed in detail as the validation procedure for the analysis of Si proceeded. To validate these parameters for the elements P, S and Cr the parameters and conclusions will only be summarised in tables according to the ANOVA and Excel calculations. The relevant data spread sheets will be attached as appendices.

From the results summarised in Table 5.2 it is evident that $t_{\text{calc}} < t_{\text{crit}}$ for all elements. The calculations were done at the 95% confidence limit, therefore the value for t_{crit} is 2.78. This means that, assuming that there is no significant difference between x_{avg} and μ , the null hypothesis, H_0 , obtains and it follows therefore that the XRF method of analysing Si, P, S and Cr yields accurate results.

The results summarised in Table 5.3 indicate satisfactory precision for the XRF analysis of the analyte elements in charge chrome.

5.8 Statistical results and analysis for the P calibration line

Table 4.3 and Figure 4.2 summarise the calibration parameters and calibration line for P which will be used to determine the regression statistics. Table 5.8 summarises the results obtained by calculating the validation data. Refer to Appendices E.1 and E.2 for the data spreadsheets.

Table 5.8: Validation parameters and values for the P analytical method

Validation parameter	Value	Description/Conclusion
Analytical range	$S_a = 0.0072$ $S_b = 0.334$	$S_b > S_a$ Range could be improved
$S_{y/x}$	0.00483	Calibration uncertainty
n	5	Number of standards
Slope (b)	28.2	Regression line slope
Intercept (a)	0.32	Regression line intercept
Regression line	$y = 28.2x + 0.32$	Regression line equation
LOD	0.0008%	Lowest distinguishable signal
LOQ	0.0026%	LOQ < lowest calibration point $0.0026\% < 0.013\%$
r	0.999	Almost perfect linearity
U(r)	0.00011%	$x_0 \pm 0.00011\%$

Actually the analysis of P can only be improved by widening the analytical range. For P, $S_b > S_a$ which implies that the analytical range can be extended. This will only be a minor improvement since the average concentration of P in charge chrome is constantly less than 0.02% and this value is represented on the calibration line range.

5.9 Statistical results and analysis for the S calibration line

Table 4.4 and Figure 4.3 show the calibration detail and calibration line for S. Table 5.9 summarises the regression statistics for S. The data spreadsheets are attached as Appendices E.3 and E.4.

Table 5.9: Validation parameters and values for the S analytical method

Validation parameter	Value	Description/Conclusion
Analytical range	$S_a = 0.0896$ $S_b = 3.19$	$S_b > S_a$ Range could be improved
$S_{y/x}$	0.0794	Calibration uncertainty
n	7	Number of standards
Slope (b)	87.2	Regression line slope
Intercept (a)	-0.444	Regression line intercept
Regression line	$y = 87.2x - 0.444$	Regression line equation
LOD	0.0031%	Lowest distinguishable signal
LOQ	0.0103%	LOQ < lowest calibration point $0.0103\% < 0.011\%$
r	0.997	Almost perfect linearity
U(r)	0.00065%	$x_0 \pm 0.00065\%$

As with P, the analytical range of S can eventually be improved by adding more calibration standards on the line using production samples. The average concentration of S in the charge chrome matrix (<0.04%) is represented in the range of the calibration line, which is therefore not a main concern at this stage.

5.10 Statistical results and analysis for the Cr calibration line

Table 4.5 and Figure 4.4 show the calibration detail and calibration line that will be used to determine the regression statistics for Cr, which are summarised in Table 5.10. The data spreadsheets are attached as Appendices E.5 and E.6.

Table 5.10: Validation parameters and values for the Cr analytical method

Validation parameter	Value	Description/Conclusion
Analytical range	$S_a = 2.27$ $S_b = 0.0409$	$S_b < S_a$ Range satisfactory
$S_{y/x}$	0.752	Calibration uncertainty
n	7	Number of standards
Slope (b)	4.03	Regression line slope
Intercept (a)	41.4	Regression line intercept
Regression line	$y = 41.4x + 4.03$	Regression line equation
LOD	1.69%	Lowest distinguishable signal
LOQ	5.64%	LOQ < lowest calibration point $5.64\% < 50.65\%$
r	0.999	Almost perfect linearity
U(r)	0.110%	$x_0 \pm 0.110\%$

5.11 Conclusions

During the validation stage it was proven that the method for charge chrome analysis is capable of producing satisfactory and trustworthy results, especially regarding:

- accuracy and precision
- analytical range
- linear response
- limit of detection and quantitation
- regression uncertainty

A wide enough analytical range ensures that all the analytical results obtained for a specific element fall within the confidence limits for that specific element. The validation of the analytical ranges Si and Cr shows satisfactory results. According to the statistical values the ranges for both P and S can be improved. The only way to improve the analytical range for

an element is to incorporate more standards on the calibration line. This has already been identified as a shortcoming during the analytical method development due to the low availability of CRM standards with a matrix compatible with that of charge chrome. The fact that the ranges for S and P do not seem satisfactory according to the statistical evaluation ($S_b < S_a$) is not of great concern because the expected concentration of these elements in charge chrome samples falls within the calibration range, and extrapolation beyond the highest or lowest calibration point is unlikely due to the fairly constant matrix of charge chrome. This implies little variation in the concentration of the elements contained by different samples.

Evaluation of the response between line intensity and element concentration shows a very good coherent linear response with almost perfect linearity for all elements.

Regarding detection and quantitation limits the only concern may be with regard to Si. The LOQ for Si is higher than the lowest point on the calibration line. The only way to improve the LOQ value for Si is to add more <1% Si standards on the line. This can be done by analysing production samples using an alternative analytical technique and by then introducing the results of the analysis as secondary standards on the calibration line. There is still a possibility, however, of extrapolating a result if the concentration falls short of 0.4%. The lower LOD value (0.12%) may offset this problem to a slight degree. For the other elements, the LOD and LOQ values are much lower than the expected concentration of these elements in charge chrome.

The uncertainty in the final analytical value is mostly a factor of the regression uncertainty. Given all the available data, it was possible to calculate the uncertainty related to concentration for each element. The uncertainties for all the elements are very low. It will be possible to lower the uncertainty value for especially Si when more low concentration standards become available to add to the calibration line.

METHOD VALIDATION – ANALYSIS OF ELEMENTS

Validation of the accuracy and precision of the method, together with the good analytical ranges, linear responses, low LOD and LOQ values, and minor uncertainties in concentration measurements, show to yield satisfactory and trustworthy results developed to analyse Si, P, S and Cr in charge chrome.

CHAPTER 6 QUALITATIVE WAVELENGTH SCANS - OXIDES

6.1 Qualitative wavelength scans for oxides

It was noted in Chapter 1 that metallised charge chrome ore is smelted in a direct-current plasma arc furnace where Cr and Fe oxides in the form of Cr_2O_3 and FeO , as well as other unwanted minerals, are reduced, yielding Cr and Fe in their metal form, while the other unwanted minerals are removed in the form of slag. Since the slag has a lower density than the reduced metals it separates from the metallic phase and can be removed by scraping.

However, incomplete reduction of Cr_2O_3 and FeO leaves remains that are separated out with the slag. The slag content of a production heat is analysed to determine its content of unreduced Cr_2O_3 and FeO with a view to maximising reduction and therefore maximising the gain of Cr and Fe from the relevant oxides. The other unwanted minerals in their oxide form that will be analysed in the slag are MgO , Al_2O_3 , SiO_2 , CaO , TiO_2 and MnO .

XRF analysis of oxides is actually an indirect form of analysis because XRF spectroscopy is only used to analyse elements. Using Cr_2O_3 as an example, the oxide is analysed as elemental Cr. The software available on the instrument is used as an aid to convert the concentration result of the analysed $\text{CrK}\alpha$ elemental line into the oxide form using the molar ratios of chromium and oxygen in Cr_2O_3 . Consequently, throughout the rest of this discussion, references to elemental analysis must be interpreted as analysis of the pertinent oxide.

As with the elements Si, P, S and Cr, qualitative wavelength scans were done on a slag sample to identify the presence of any spectral overlaps. The same principles used during the wavelength scans of the elements

QUALITATIVE WAVELENGTH SCANS - OXIDES

will pertain to the scans of the oxides. A sample was scanned over predetermined wavelength ranges and the 2θ angles of diffraction were determined by applying the Bragg Law. No real overlaps are expected for the light elements Mg, Al, Si and Ca, but overlaps will almost certainly occur between the heavier elements Ti, Cr, Mn and Fe.

It is expected that the slag composition will not vary significantly between production heats. Due to the consistency of the charge chrome smelting process, only small variations in the oxide content may occur. Table 6.1 gives a summary of the general composition of slag samples.

Table 6.1: Chemical composition of charge chrome slag

Oxide	Estimated concentration (%)
MgO	> 20
Al ₂ O ₃	> 30
SiO ₂	> 20
CaO	> 20
TiO ₂	< 1.5
Cr ₂ O ₃	< 3
MnO	< 0.5
FeO	< 1

The composition of the slag samples as well as the expected concentrations of the oxides is known. This simplifies the choice of analytical parameters which will be used during the scans. The analytical parameters used during the wavelength scans are summarised in Table 6.2.

QUALITATIVE WAVELENGTH SCANS - OXIDES

Table 6.2: Analytical parameters to be used during wavelength scans for Mg, Al, Si, Ca, Ti, Cr, Mn and Fe

Element	Crystal	Collimator	Detector	Voltage (kV)/Current (mA)
Mg	AX06	Coarse (0.6)	FPC	50/50
Al	PET	Medium (0.25)	FPC	50/50
Si	PET	Coarse (0.6)	FPC	50/50
Ca	LiF200	Medium (0.25)	FPC	50/50
Ti	LiF200	Medium (0.25)	FPC	50/50
Cr	LiF200	Medium (0.25)	FPC	50/50
Mn	LiF200	Medium (0.25)	FPC	50/50
Fe	LiF200	Medium (0.25)	FPC	50/50

The theoretical 2θ angles of the $K\alpha$ lines (the principal lines to be analysed) for the elements were calculated using the Bragg Law (equation 3.1). The calculations were done using first-order lines ($n = 1$), the wavelength of the principal $K\alpha$ line (in Å units) and the crystal spacing of the various crystals used. The results obtained during these calculations are summarised in Table 6.3.

Table 6.3: Theoretical 2θ angles for Mg, Al, Si, Ca, Ti, Cr Mn and Fe

Spectral line	λ (Å)	$2d$ (Å)	2θ (degrees)
MgK α	9.889	57.3 (AX06)	19.88
AlK α	8.339	8.7518 (PET)	144.66
SiK α	7.126	8.7518 (PET)	109.02
CaK α	3.360	4.028 (LiF200)	113.06
TiK α	2.750	4.028 (LiF200)	86.11
CrK α	2.291	4.028 (LiF200)	69.33
MnK α	2.103	4.028 (LiF200)	62.90
FeK α	1.937	4.028 (LiF200)	57.49

QUALITATIVE WAVELENGTH SCANS - OXIDES

The wavelength scans for Mg, Al, Si and Ca are attached as Appendices F, G, H and I. The single-wavelength scan for Ti, Cr, Mn and Fe are shown in Figure 6.1. (Energy profiles for the elements Mg, Al, Ca, Ti, Mn and Fe are attached as Appendices J, K, L, M, N, and O). The primary $K\alpha$ -line 2θ values obtained for each element during the scans were compared with the calculated theoretical values. The results are summarised in Table 6.4.

Table 6.4: Comparison between theoretical 2θ angles and experimental 2θ angles

Spectral line	Theoretical 2θ (degrees)	Experimental 2θ (degrees)
MgK α	19.88	20.05
AlK α	144.66	144.71
SiK α	109.02	109.03
CaK α	113.06	113.09
TiK α	86.11	86.14
CrK α	69.33	69.35
MnK α	62.90	62.97
FeK α	57.49	57.52

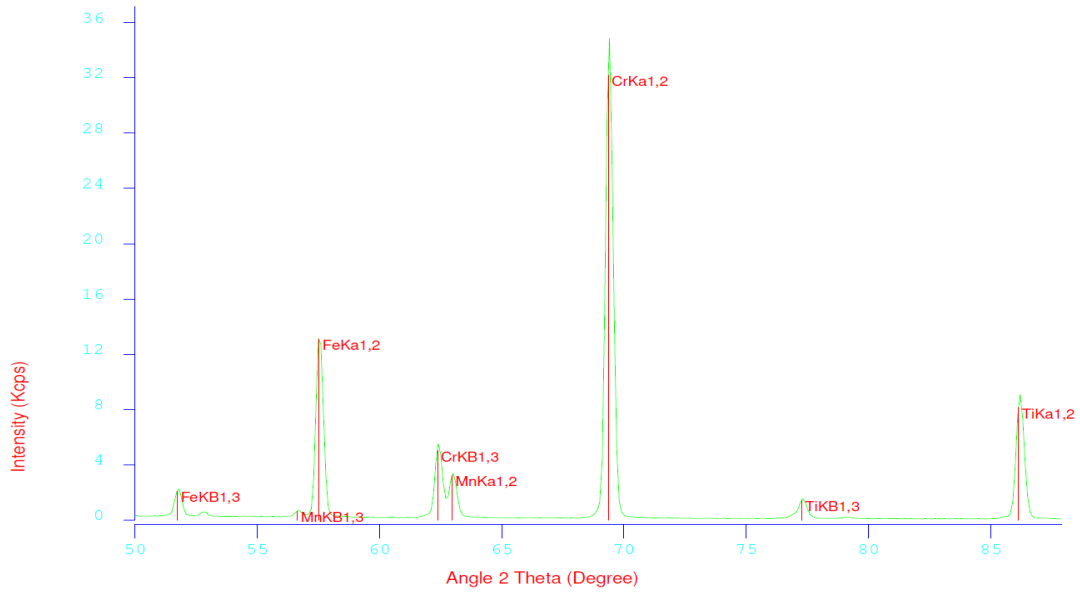
It is clear from Table 6.4 that the theoretical and experimental 2θ values for the elements are very similar. As expected, the wavelength scans for Mg, Al, Si and Ca show single lines with no overlaps. The wavelength scan for Ti, Cr, Mn and Fe (Figure 6.1) shows the following overlaps:

- CrK β _{1,3} on the primary MnK α _{1,2} line
- MnK β _{1,3} on the primary FeK α _{1,2} line.

When analysing for the Mn and Fe oxides it may be necessary to correct for these overlaps. No overlaps occur at the primary TiK α and CrK α lines.

QUALITATIVE WAVELENGTH SCANS - OXIDES

Scan 1: TICRMNFE (M3SLAG), from: TICRMNFE, XRF Gonio: 1, 380 steps



Identification Report:

```

Sample Identifier: Scan 1
                  SLAG
Sample Number:   M37815
                  XRF9800051
Goniometer:     XRF 1
Crystal:        LiF200
Detector:       FPC
Collimator:     0.25
kV/mA:          50/50
    
```

Line	Intensity (Kcps)			Angle (deg)
	Scan 1	Scan 2	Scan 3	
FeKB1,3	2.0946			51.7285
MnKB1,3	0.6321			56.6388
FeKa1,2	13.0748			57.5179
CrKB1,3	5.0132			62.3644
MnKa1,2	3.2258			62.9731
CrKa1,2	32.1629			69.3544
TiKB1,3	1.4225			77.2632
TiKa1,2	8.1373			86.1373

Figure 6.1: Ti, Cr, Mn and Fe wavelength scan

During this phase of the study all the oxides (indirectly analysed as elements) were identified using wavelength scans, thus assisting identification of the possible instrumental parameters (Table 6.2) that can be used during the analysis of charge chrome slag. The next step is to set up calibration lines for each oxide to be analysed. In light of the confirmed possibility of overlaps, when setting up the calibration lines, the possibility of spectral interferences has to be identified as well.

CHAPTER 7 CALIBRATION LINES - OXIDES

7.1 Setting up calibration lines for the analysis of oxides

As with the elements, it is necessary to set up individual calibration lines for the accurate analysis of the specific oxides mentioned in Chapter 5. These calibration lines should also be traceable to standards with known concentrations. Regarding standards for the eight oxides to be analysed, the scarcity of CRMs is of even greater concern than was the case with the elements. A total of 48 standards were used to set up the individual calibration lines of which only 10 were CRM standards. The remaining 38 standards were prepared from production slag and were analysed with ICP-OES, much the same as with the secondary standards used for the elements.

Matrix differences between the calibration standards and the samples may lead to a substantial amount of spectral overlaps and spectral interferences that must be corrected for (Martin *et al.*, 2002). However, there is a big advantage when implementing production samples as secondary standards when setting up calibration lines for analysis. Minimising, or even eliminating the need for correction for spectral overlaps and matrix effects is a possibility if the matrix of the standards closely match the matrix of the samples to be analysed. Consequently, the implementation of production samples as secondary standards causes a matrix similarity between standards and samples, which is referred to as matrix matching.

7.2 Matrix matching

For matrix matching to occur between standards and samples the matrices must be sufficiently close together in the sense that the standards have much the same chemical composition as the samples. For the purpose of this study, therefore it means that the oxides in the samples must also be present in the standards used for calibration. There may actually be one limitation in the sense that the concentration differences of the oxides in the standards and samples must be small, for the standards within a few percent compared to the same oxides in the sample (Sieber, 2002).

During the setting up of calibration lines for the analysis of the oxides the purpose was to be able to exert a certain amount of control over spectral overlaps and matrix effects by closely matching the matrices of standards and samples. As noted, this exercise is simplified when production samples are implemented as secondary standards.

The assumption that will be tested during this study is that no corrections for spectral overlaps or matrix effects will be necessary if spectral overlaps and matrix effects in the samples occur to the same extent in the standards.

7.3 Spectral overlaps expected in the oxide samples

With reference to Figure 6.1 the following spectral overlaps are expected:

- CrK β _{1,3} on the MnK α _{1,2} line
- MnK β _{1,3} on the FeK α _{1,2} line.

Both the MnK α and FeK α lines will be measured to determine the concentrations of MnO and FeO in the samples. The overlaps in the

samples and standards will occur to the same extent. Therefore, to prove the theory that during the analysis of charge chrome slag no corrections due to matrix matching will be necessary, overlap corrections will not be made.

7.4 Spectral interferences expected in the oxide samples

The possibility that spectral interference (specifically absorption) will occur in the samples was again predicted using the values of mass absorption coefficients (MACs) and absorption edges.

For absorption to take place, the wavelength of the element to be absorbed must be shorter than that of the element to be enhanced. For every element there is an absorption edge which is the minimum energy necessary to excite an electron to the point of producing characteristic spectral lines (K-lines in this study). Table 7.1 summarises the wavelengths of the absorption edges of the K-lines of the elements to be analysed in the sample in order to eventually determine the concentration of the relevant oxides.

Table 7.1: Wavelength of the K-absorption edges for the slag matrix elements

Element	Element K-absorption edge (Å)
Mg	9.512
Al	7.951
Si	6.745
Ca	3.070
Ti	2.497
Cr	2.070
Mn	1.896
Fe	1.743

It is evident from the data in Table 7.1 that a FeK α line may be absorbed by Cr because of its shorter wavelength, TiK α can be absorbed by Ca and so on. For absorption of the spectral-line intensity of an analyte element by another matrix element, the matrix element must absorb the analyte wavelength significantly more than the analyte absorbs its own wavelength.

The absorption coefficient of the FeK α line by Fe itself (notated $\mu_{\text{Fe,FeK}\alpha}$) is 70.21, clearly much lower than that of the FeK α line by Cr ($\mu_{\text{Cr,FeK}\alpha}$), which amounts to 480.83, thus indicating strong absorption of the FeK α line intensity by Cr. Insignificant absorption can be illustrated using Mn and Fe as examples. Although $\mu_{\text{Mn,FeK}\alpha} > \mu_{\text{Fe,FeK}\alpha}$ (refer to Table 7.1), this does not necessarily mean that Mn will be a strong absorber of the FeK α -line intensity:

$$\mu_{\text{Fe,FeK}\alpha} = 70.21 \text{ and } \mu_{\text{Mn,FeK}\alpha} = 69.81$$

This absorption coefficient is insubstantial compared to the absorption of FeK α line intensity by Cr, which means that the absorption of the FeK α line intensity by Mn is insignificant.

According to tables summarising MAC values (Willis, 2008), and taking due account of the oxide matrix and analytes, the following conclusions can be drawn:

- $\mu_{\text{Al,AlK}\alpha} = 387.07$; $\mu_{\text{Mg,AlK}\alpha} = 4339.6$; strong absorption of AlK α by Mg
- $\mu_{\text{Si,SiK}\alpha} = 325.37$; $\mu_{\text{Al,SiK}\alpha} = 3472.6$; strong absorption of SiK α by Al
- $\mu_{\text{Ti,TiK}\alpha} = 113.74$; $\mu_{\text{Ca,TiK}\alpha} = 782.2$; strong absorption of TiK α by Ca
- $\mu_{\text{Cr,CrK}\alpha} = 88.18$; $\mu_{\text{Ti,CrK}\alpha} = 607.4$; strong absorption of CrK α by Ti

Spectral interferences in charge chrome slag samples will therefore definitely occur according to the above-mentioned information. With this now confirmed, calibration lines were set up for each element. Possible matrix effects in the form of spectral overlaps and spectral interferences

were ignored to test the theory that overlaps and interferences can be ignored in the main if matrix matching can be done between charge chrome slag standards and samples.

All the oxides in the secondary standards used during the setting up of the calibration lines were analysed by using the same ICP-OES method applied to analyse Si (refer to section 4.3). Standards were chosen to represent a large concentration range. The use of an asterisk (*) indicates the CRMs on the calibration lines.

In each case, all the standards and statistical parameters and values that will assist in evaluating the significance of the calibration line (μ , x , and absolute differences, Δ) will be summarised in a table. Following the illustration of calibration lines, a conclusion regarding each line will be discussed at the end of the chapter, followed in the next chapter by the validation of analytical results using the calibration lines developed for analysis.

7.5 Setting up a calibration line for the analysis of MgO

Table 7.2: Standards and statistical values for the MgK α calibration line

Standard	I (kcps)	μ (%)	x (%)	Δ (%)
BS 101/5*	8.647	5.50	5.58	0.080
135	14.088	6.50	6.62	0.125
124	17.536	7.20	7.29	0.087
149/S	20.571	7.80	7.87	0.069
151/S	22.057	8.20	8.15	-0.045
956V	26.762	9.00	9.06	0.059
110	33.677	10.58	10.39	-0.195
338993VS	34.779	10.70	10.60	-0.103
339106PS	36.837	11.00	10.99	-0.008
114	37.481	11.22	11.12	-0.103
CDR14	66.161	16.60	16.62	0.021
123/S	79.852	19.40	19.25	-0.150
57/S	81.311	19.65	19.53	-0.120
52/S	82.851	19.83	19.83	-0.004
119/S	83.120	19.90	19.88	-0.023
55/S	99.162	22.75	22.96	0.207
19/69*	99.932	23.00	23.10	0.105

Analyte: MgKa1,2 Q: 5.209 Kcps/% SEE: 0.1180

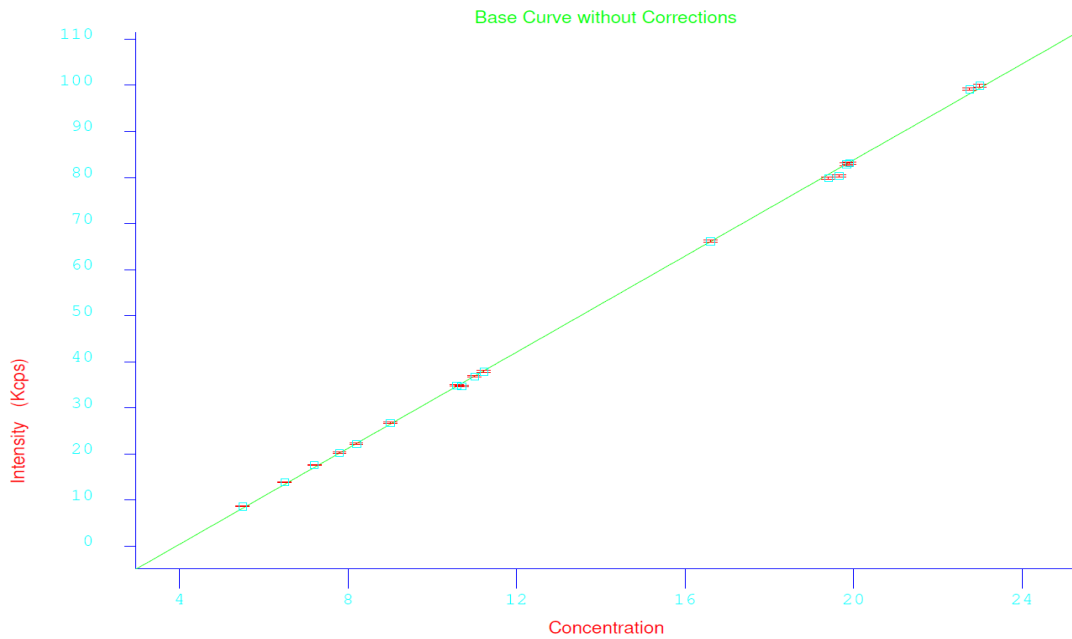


Figure 7.1: MgK α (for MgO) calibration line without corrections

7.6 Setting up a calibration line for the analysis of Al₂O₃

Table 7.3: Standards and statistical values for the AlK α calibration line

Standard	I (kcps)	μ (%)	x (%)	Δ (%)
NHKG-152*	4.01	2.60	2.59	-0.010
NHKG-142*	4.59	3.13	2.94	-0.192
637PS	7.86	5.00	4.91	-0.093
636PS	8.77	5.60	5.45	-0.151
113	14.91	9.02	9.14	0.124
110	15.48	9.27	9.49	0.220
114	16.93	10.08	10.36	0.282
53/S	33.20	20.20	20.14	-0.056
52/S	34.29	20.85	20.80	-0.054
19/69*	47.64	28.90	28.83	-0.071

Analyte: AlKa1,2 Q: 1.663 Kcps/% SEE: 0.1669

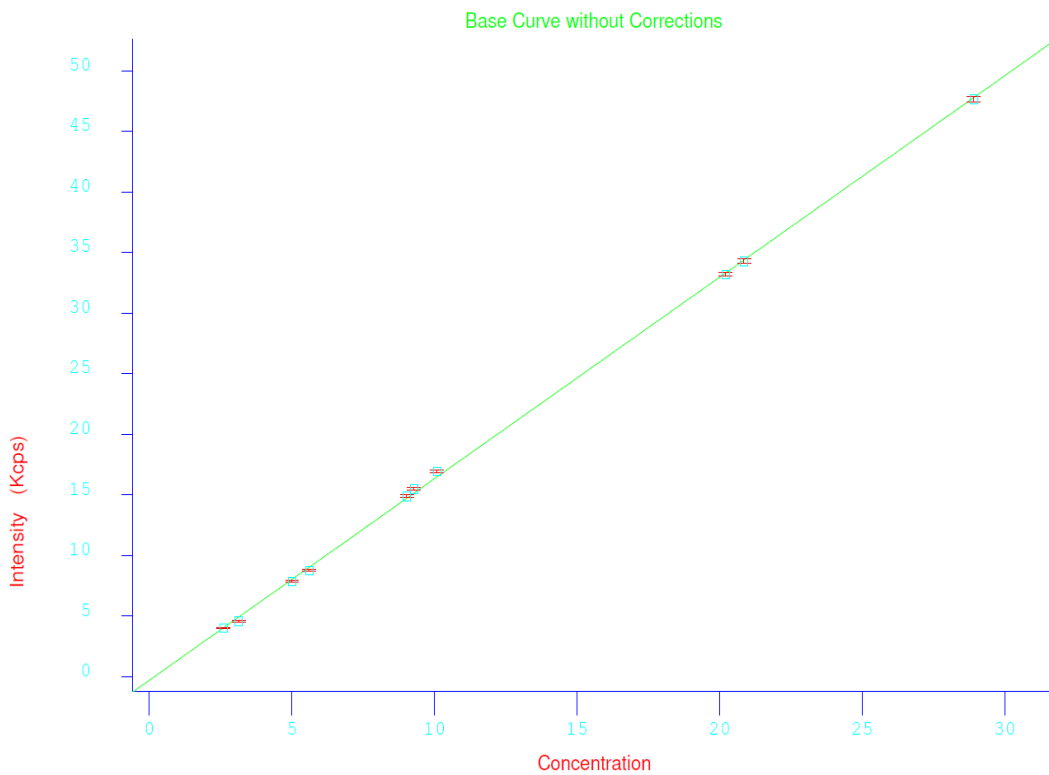


Figure 7.2: AlK α (for Al₂O₃) calibration line without corrections

7.7 Setting up a calibration line for the analysis of SiO₂

Table 7.4: Standards and statistical values for the SiK α calibration line

Standard	I (kcps)	μ (%)	x (%)	Δ (%)
149/S	21.13	0.90	0.89	-0.014
151/S	22.36	1.00	0.96	-0.042
BCS 396*	29.70	1.37	1.39	0.015
BCS 369*	51.70	2.59	2.67	0.075
338990LS	131.69	7.40	7.32	-0.079
N-STD*	352.34	19.90	20.16	0.263
123/S	357.32	20.23	20.45	0.223
134/S	373.20	21.33	21.38	0.047
50/S	379.68	21.92	21.75	-0.166
NHKG-142*	384.76	22.16	22.05	-0.110
777	414.46	23.90	23.78	-0.122
CDR14	449.75	26.10	25.83	-0.268
956V	532.95	30.50	30.67	0.175

Analyte: SiKa_m LOD (30 s): 24.5 ppm BEC: 0.343 % Q: 17.182 Kcps/% SEE: 0.1651

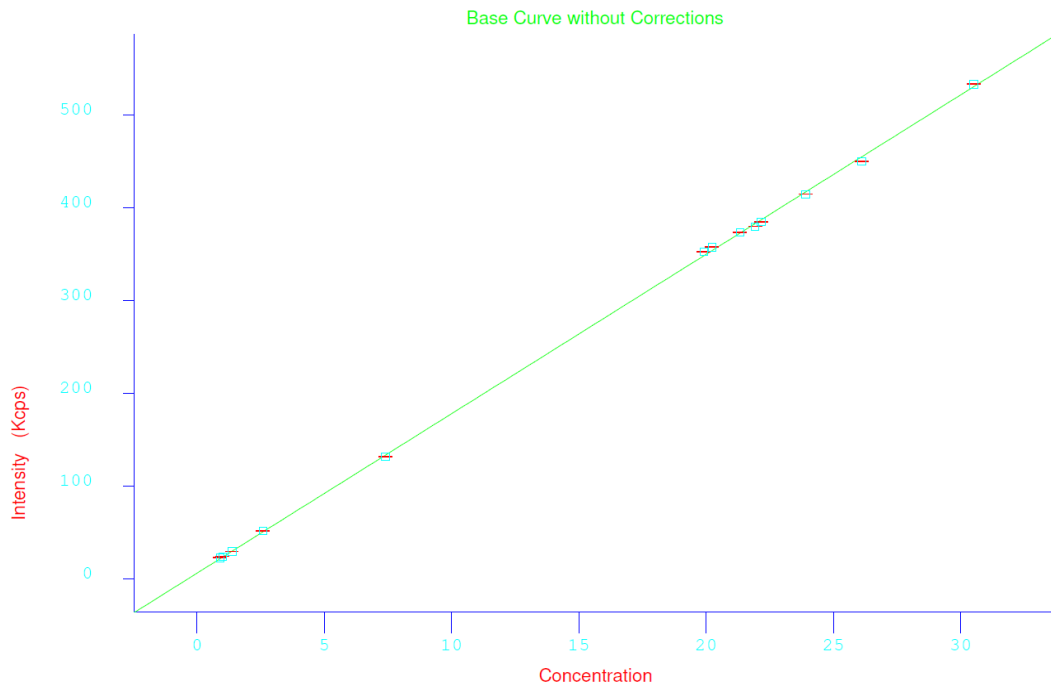


Figure 7.3: SiK α (for SiO₂) calibration line without corrections

7.8 Setting up a calibration line for the analysis of CaO

Table 7.5: Standards and statistical values for the CaK α calibration line

Standard	I (kcps)	μ (%)	x (%)	Δ (%)
134/S	62.33	6.31	6.22	-0.087
N-STD*	71.46	7.10	7.26	0.157
CDR18/19	125.44	13.10	13.38	0.276
CDR26	143.67	15.50	15.44	-0.057
CDR21	148.76	15.80	16.02	0.219
JK-S8*	326.54	36.50	36.17	-0.329
BCS 382-1*	356.87	40.10	39.61	-0.491
957P	394.13	44.50	43.83	-0.668
BS 101/5*	412.10	46.00	45.87	-0.131
955V	467.02	51.80	52.09	0.294
130/S	486.63	53.50	54.32	0.817

Analyte: CaKa1,2 LOD (10 s): 92.7 ppm BEC: 0.843 % Q: 8.822 Kcps/% SEE: 0.4364

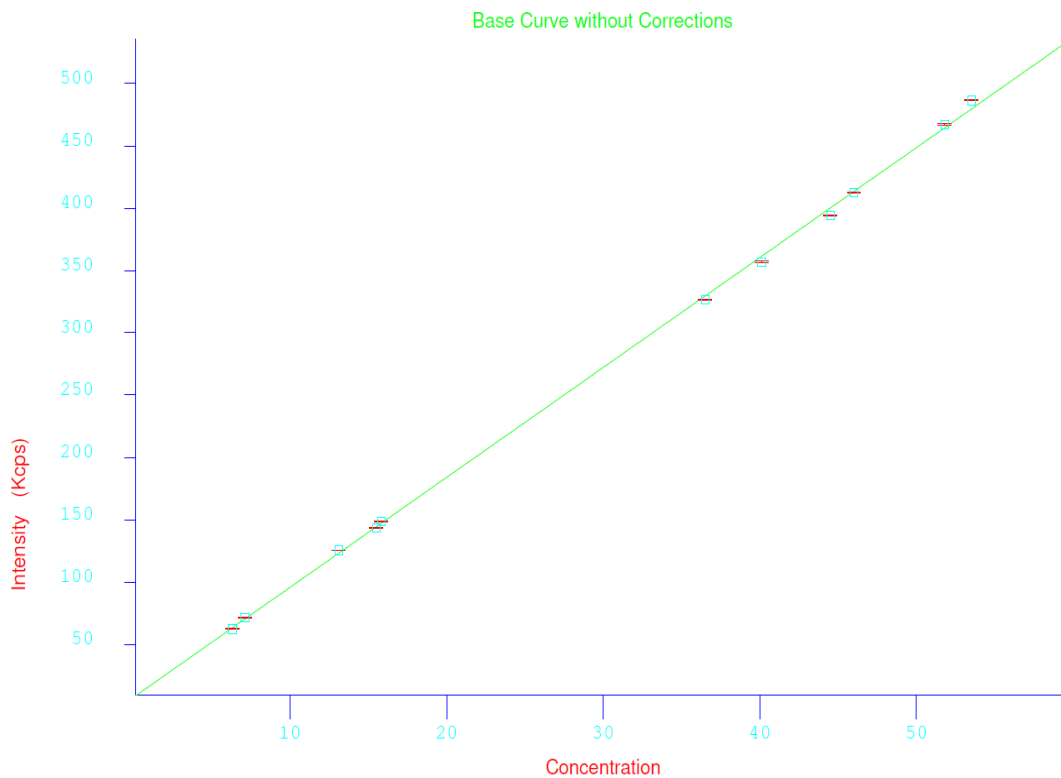


Figure 7.4: CaK α (for CaO) calibration line without corrections

7.9 Setting up a calibration line for the analysis of TiO₂

Table 7.6: Standards and statistical values for the TiK α calibration line

Standard	I (kcps)	μ (%)	x (%)	Δ (%)
JK-S8*	2.16	0.26	0.27	0.007
PREG*	2.72	0.33	0.32	-0.017
143/S	5.23	0.56	0.57	0.014
NHKG-142*	6.30	0.69	0.68	-0.010
CDR16/17	8.22	0.86	0.87	0.012
CDR26	12.45	1.30	1.29	-0.006

Analyte: TiKa_m Q: 10.022 Kcps/% SEE: 0.0133

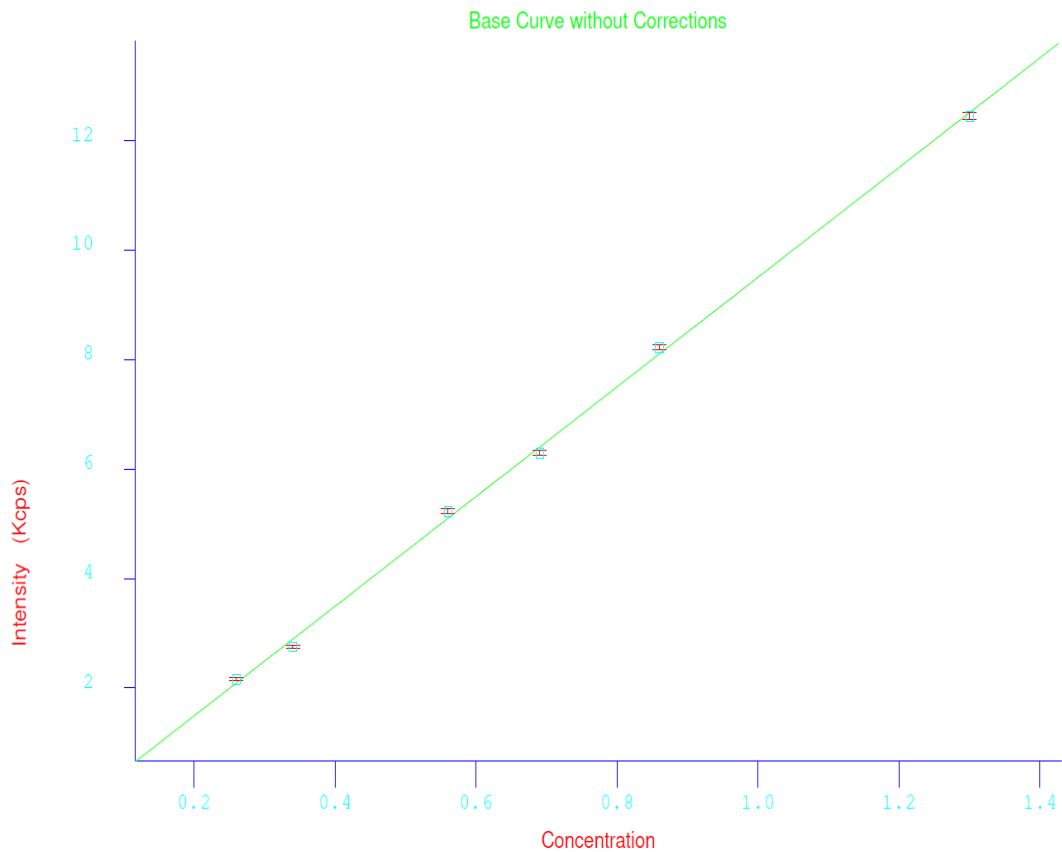


Figure 7.5: TiK α (for TiO₂) calibration line without corrections

7.10 Setting up a calibration line for the analysis of Cr₂O₃

Table 7.7: Standards and statistical values for the CrK α calibration line

Standard	I (kcps)	μ (%)	x (%)	Δ (%)
130/S	13.44	1.440	1.429	-0.0111
508VS	18.94	1.700	1.713	0.0126
636PS	22.99	1.900	1.922	0.0219
777	40.28	2.900	2.815	-0.0852
CDR16/17	73.40	4.430	4.525	0.0951
CDR21	73.58	4.490	4.534	0.0445
CDR26	88.26	5.290	5.293	0.0026
122/S	200.06	11.200	11.067	-0.1334
123/S	358.61	19.200	19.253	0.0531

Analyte: CrKa1,2 Q: 19.365 Kcps/% SEE: 0.0753

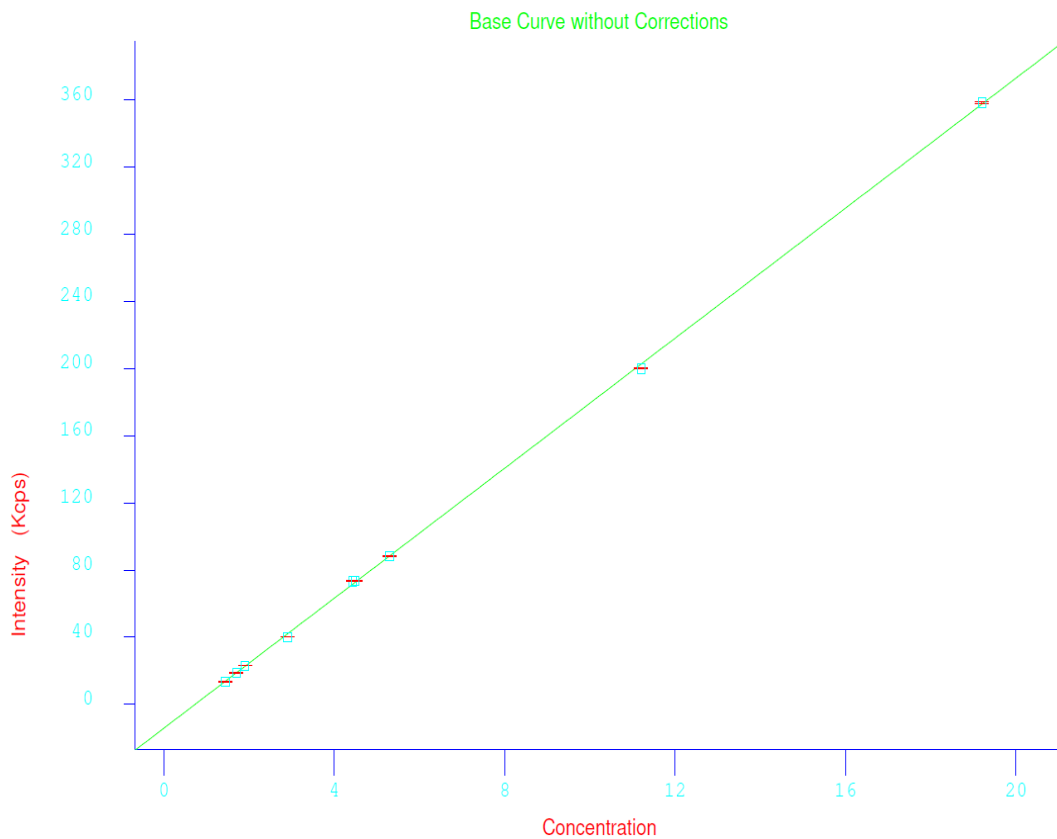


Figure 7.6: CrK α (for Cr₂O₃) calibration line without corrections

7.11 Setting up a calibration line for the analysis of MnO

Table 7.8: Standards and statistical values for the MnK α calibration line

Standard	I (kcps)	μ (%)	x (%)	Δ (%)
338993VS	10.03	0.32	0.36	0.040
508VS	15.32	0.50	0.49	-0.006
110	18.90	0.59	0.58	-0.006
135	22.81	0.69	0.68	-0.008
636PS	32.14	0.95	0.92	-0.032
NHKG-152*	189.43	4.85	4.88	0.028
133/S	284.99	7.30	7.28	-0.015

Analyte: MnKa_m Q: 39.708 Kcps/% SEE: 0.0249

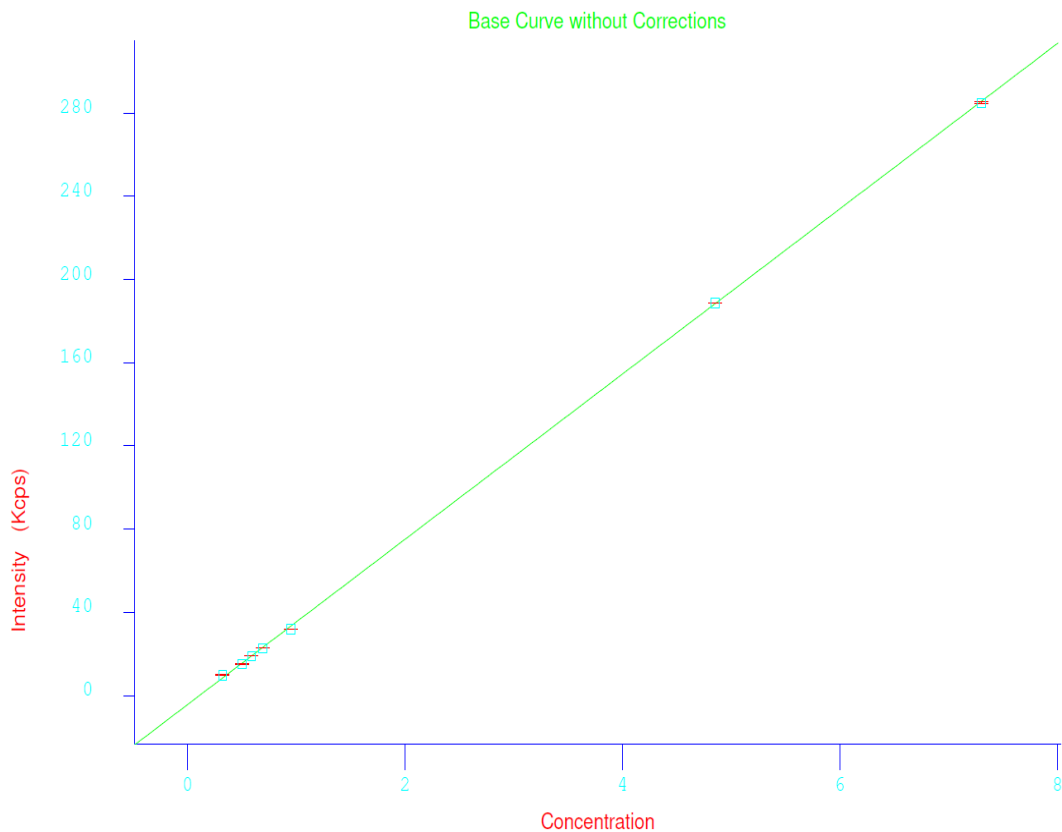


Figure 7.7: MnK α (for MnO) calibration line without corrections

7.12 Setting up a calibration line for the analysis of FeO

Table 7.9: Standards and statistical values for the FeK α calibration line

Standard	I (kcps)	μ (%)	x (%)	Δ (%)
141/S	5.17	0.18	0.25	0.069
135	7.38	0.38	0.37	-0.009
143/S	11.06	0.54	0.57	0.034
JK-S8	16.61	0.80	0.88	0.080
CDR16/17	50.82	2.94	2.77	-0.174
SLAG-5	129.14	7.17	7.08	-0.089
57/S	196.22	10.80	10.78	-0.022
123/S	204.09	11.10	11.21	0.111

Analyte: FeKa1,2 LOD (10 s): 13.3 ppm BEC: 0.036 % Q: 18.146 Kcps/% SEE: 0.1064

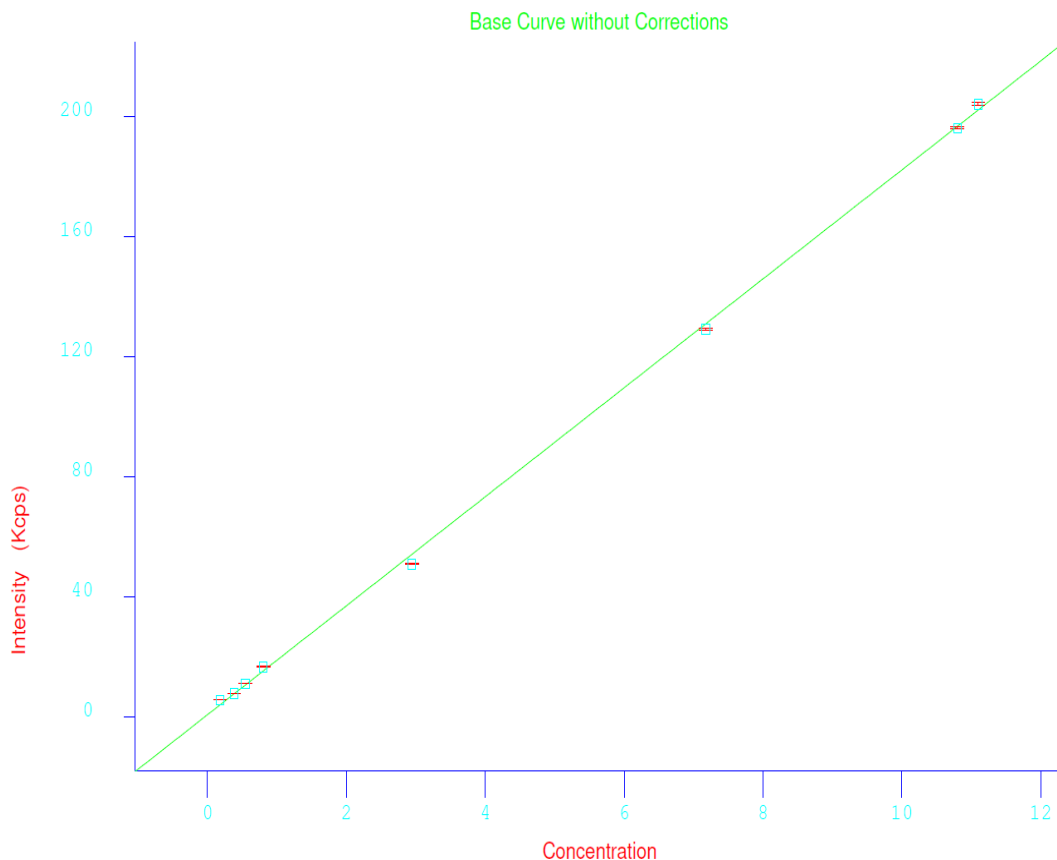


Figure 7.8: FeK α (for FeO) calibration line without corrections

7.13 Interpretation of the calibration line data

Calibration lines for each oxide have been set up using CRMs and mostly secondary standards. As discussed earlier, the aim during the development of the calibration lines for each element was to match the matrix of the calibration standards used on each calibration line with the matrix of the slag samples that will eventually be analysed using these calibration lines. The simplest way to do this was to implement production samples as secondary standards. This will ensure good matrix matching between the standards and the samples.

The calibration lines for each oxide are illustrated in Figures 7.1 – 7.8. By just visually looking at the lines it is quite evident that the response between spectral line intensity and the concentration of the oxide standards seems to be linear. The Δ -values for each standard used on the individual lines (summarised in Tables 7.2 – 7.9) is significantly low which indicates good linear response between line intensity and concentration. The SEE values obtained for each line are summarised in Table 7.10 along with the concentration ranges covered by the samples for each line.

Table 7.10: SEE values and concentration ranges for the oxide calibration lines

Calibration line	SEE	Concentration range (%)
MgO	0.118	Approximately 5 – 23
Al ₂ O ₃	0.167	Approximately 2 – 28
SiO ₂	0.165	Approximately 1 – 30
CaO	0.436	Approximately 6 – 54
TiO ₂	0.0133	Approximately 0.3 – 1.3
Cr ₂ O ₃	0.0753	Approximately 1 – 19
MnO	0.0249	Approximately 0.3 – 7
FeO	0.106	Approximately 0.2 - 11

According to the data in Table 7.10 it is clear that the SEE value for each calibration line is very low, especially when the wide concentration range for the different oxides is taken into account. Upon evaluation of the Δ -values and the SEE for each calibration line it seems that there is a significant linear response between line intensity and concentration without any corrections with regard to spectral overlaps or spectral interferences being made. This already gives a good indication that the theory in terms of matrix matching between standards and samples will eliminate the need for any corrections on the calibration lines, might be substantial.

As with the elements, the Δ -values and SEE cannot be used as the only parameters to prove significant linearity. This will be done by calculation of the regression value for each line during the validation phase in the next chapter.

CHAPTER 8 METHOD VALIDATION – ANALYSIS OF OXIDES

8.1 Method validation for the analysis of the oxides

When a new analytical method is developed it is done to minimise the possibility of errors that may lead to inaccurate results. During the validation of the method for the analysis of the oxides it was determined if the method is fit for the intended purpose of analysis (Garfield, Klesta and Hirsch, 2000).

Since the reduction of Cr and Fe oxides during the charge chrome manufacturing process is incomplete, slags (metals and other minerals in their oxide form) are analysed to determine the Cr and Fe losses sustained during the reduction phase of the manufacturing process. There will be slight variations in the oxide content of slags from different heats. Table 8.1 gives a summary of the expected oxide content and the approximate variations that may be expected in the oxide concentrations.

Table 8.1: Expected oxide content and possible variations in concentration

Oxide	Expected content (%)	Approximate variation (%)
MgO	> 20	± 1
Al ₂ O ₃	> 30	± 1
SiO ₂	> 20	± 1
CaO	> 20	± 1
TiO ₂	< 1.5	± 0.25
Cr ₂ O ₃	< 3	± 0.5
MnO	< 0.5	± 0.25
FeO	< 1	± 0.25

These variations in concentration must be taken into account when the method is validated. Certain tolerance levels in the variation of the concentrations are allowed and will be kept in mind during the quality specifications that will be determined during the validation procedure. The method for the analysis of the oxides will be validated within these allowed tolerances for:

- accuracy and precision
- analytical range
- determination of detection and quantitation limits
- determination of the linear regression
- calculation of uncertainties in the analytical measurements.

The definition and the way of calculating each of these parameters have already been explained in detail in Chapter 4. The same principles will be applied during this discussion. The results obtained for each parameter will be summarised and investigated to see if the analytical method is fit for purpose and able to deliver acceptable analytical results.

8.2 Validating accuracy for the analysis of the oxides

For the validation of the accuracy of the analytical method an independent CRM (a CRM not used on the line to be validated) was analysed five times. The average obtained for each oxide was evaluated for accuracy using the t-test (see equation 4.3). The null hypothesis (H_0) which states that there is no significant difference between x_{avg} and μ was tested by comparing the t_{calc} value obtained using equation 5.3 with the t_{crit} value ($t_{crit} = 2.78$; $n = 5$). The condition for H_0 to be accepted is that $t_{calc} < t_{crit}$. The values obtained during this validation are summarised in Tables 8.2 and 8.3.

METHOD VALIDATION – ANALYSIS OF OXIDES

Table 8.2: Results (% concentration) obtained during the oxide analysis of CRMs for accuracy validation

Oxide	CRM	1	2	3	4	5
MgO	BS 101/1	9.17	9.14	9.15	9.14	9.15
Al ₂ O ₃	DIL 3905	29.13	29.12	29.19	29.23	29.16
SiO ₂	DIL 3905	25.40	25.43	25.43	25.44	25.46
CaO	DIL 3905	34.47	34.44	34.47	34.46	34.49
TiO ₂	DIL 3905	0.504	0.503	0.503	0.505	0.502
Cr ₂ O ₃	NHKG 142	0.550	0.551	0.551	0.551	0.550
MnO	BCS396	0.500	0.499	0.499	0.500	0.499
FeO	DIL 3905	2.24	2.24	2.241	2.24	2.25

Table 8.3: Summary of the statistical values obtained after the oxide analysis of CRMs for accuracy

Oxide	μ (%)	x_{avg} (%)	σ	n	DF	t_{crit}	t_{calc}
MgO	9.15	9.150	0.0131	5	4	2.78	0.1
Al ₂ O ₃	29.1	29.16	0.0548	5	4	2.78	2.4
SiO ₂	25.4	25.43	0.0212	5	4	2.78	1.1
CaO	34.5	34.47	0.0182	5	4	2.78	0.5
TiO ₂	0.50	0.5018	0.0020	5	4	2.78	2.0
Cr ₂ O ₃	0.55	0.5506	0.00054	5	4	2.78	2.5
MnO	0.50	0.4994	0.00054	5	4	2.78	2.5
FeO	2.24	2.239	0.0039	5	4	2.78	0.6

According to the data in Table 8.3, the t-test shows $t_{calc} < t_{crit}$ for all the oxides. The H_0 hypothesis will therefore be accepted as true and the conclusion can be made that the method for the analysis of oxides is capable of yielding accurate results.

8.3 Validating precision for the analysis of the oxides

The repeatability of the results, hence the precision, was validated by analysing a production sample five times. The standard deviation (equation 5.4) and the %RSD will be used to evaluate the precision of the method. The results obtained for the validation of precision are summarised in Table 8.4.

Table 8.4: Summary of the five analytical results (% concentration) and the precision indicators for the oxides

Oxide	1	2	3	4	5	\bar{x}_{avg}	σ	%RSD
MgO	18.998	18.971	18.997	18.987	18.989	18.988	0.0109	0.057
Al ₂ O ₃	25.877	25.865	25.869	25.896	25.889	25.879	0.0131	0.051
SiO ₂	14.757	14.752	14.765	14.767	14.768	14.762	0.0070	0.047
CaO	17.238	17.227	17.254	17.264	17.221	17.241	0.0180	0.105
TiO ₂	1.377	1.373	1.376	1.376	1.376	1.376	0.0015	0.110
Cr ₂ O ₃	12.104	12.142	12.112	12.120	12.126	12.121	0.0145	0.119
MnO	0.380	0.380	0.380	0.381	0.380	0.3802	0.0004	0.118
FeO	7.944	7.935	7.948	7.957	7.957	7.948	0.0093	0.117

Table 8.4 clearly shows very low σ and %RSD values for all the oxides. This, together with the conclusion made during the validation of accuracy, implies that the method is capable of producing both accurate and repeatable results, indicating good precision.

8.4 Validation of the remaining parameters for oxide analysis

The remaining parameters necessary to complete the validation for the analysis of the oxides were done using the ANOVA function on Excel as a tool, as well as the relevant equations needed to calculate each parameter. All these functions are discussed in detail in Chapter 5.

The parameters which include the analytical range, linear regression, LOD and LOQ values, as well as the uncertainty of the final analytical value, were determined using the functions and principles applied to validate the elements Si, P, S and Cr in charge chrome.

During this discussion the statistical results and the values of the above-mentioned parameters will be summarised for each oxide. The analytical range was evaluated to see if the concentration range on each calibration line is wide enough to prevent extrapolation during the calculation of analytical results. The LOD and LOQ values will indicate the lowest quantifiable concentration levels, and the calculation of the regression uncertainty was used to determine uncertainties in the analytical values obtained.

One of the main parameters to be evaluated is the regression value, r . As explained earlier, one of the main aims of developing the analytical method for the analysis of the oxides is to show that no corrections in terms of spectral overlaps or elemental interferences need to be made if the matrix of the standards used on the calibration lines and the matrix of the samples can be closely matched. This assumption has already been proved by validating the accuracy of the method to a large extent. Linear covariance between spectral line intensity and concentration without the need for corrections will be further supported when the regression value of each calibration line has a value tending to be as close to 1 as possible, which will indicate almost perfect linearity.

METHOD VALIDATION – ANALYSIS OF OXIDES

Table 8.5: Results and summary of the validation parameters for MgO

<i>Regression Statistics</i>				
Multiple R	0.9998			
R Square	0.9997			
Adjusted R Square	0.9997			
Standard Error	0.5868			
Observations	17			

ANOVA				
	<i>df</i>	<i>SS</i>	<i>MS</i>	<i>F</i>
Regression	1	16279.1	16279.1	47283.1
Residual	15	5.2	0.3	
Total	16	16284.2		

	<i>Coefficients</i>	<i>Standard Error</i>	<i>t Stat</i>	<i>P-value</i>
Intercept	-20.3944	0.3524	-57.88051	4.73876E-19
X Variable 1	5.2071	0.0239	217.44680	1.16434E-27

Validation parameter	Value	Description/Conclusion
Analytical range	$S_a = 0.352$ $S_b = 0.024$	$S_b < S_a$ Range satisfactory
Slope (b)	5.21	Regression line slope
Intercept (a)	-20.4	Regression line intercept
Regression line	$y = 5.21x - 20.4$	Regression line equation
LOD	0.203%	Lowest distinguishable signal
LOQ	0.676%	LOQ < lowest calibration point (5.50%)
r	0.999	Almost perfect linearity
U(r)	0.0661%	$x_0 \pm 0.0661\%$

METHOD VALIDATION – ANALYSIS OF OXIDES

Table 8.6: Results and summary of the validation parameters for Al₂O₃

<i>Regression Statistics</i>				
Multiple R	0.9999999			
R Square	0.9999999			
Adjusted R Square	0.9999999			
Standard Error	0.0052839			
Observations	10			
<i>ANOVA</i>				
	<i>df</i>	<i>SS</i>	<i>MS</i>	<i>F</i>
Regression	1	1949.6	1949.639	69830453.74
Residual	8	0.0002	2.79196E-05	
Total	9	1949.6		
	<i>Coefficients</i>	<i>Standard Error</i>	<i>t Stat</i>	<i>P-value</i>
Intercept	-0.2971	0.0028	-105.0556	7.5289E-14
X Variable 1	1.6629	0.0002	8356.4618	4.71019E-29

Validation parameter	Value	Description/Conclusion
Analytical range	S _a = 0.0028 S _b = 0.0002	S _b < S _a Range satisfactory
Slope (b)	1.66	Regression line slope
Intercept (a)	-0.297	Regression line intercept
Regression line	y = 1.67x – 0.297	Regression line equation
LOD	0.0051%	Lowest distinguishable signal
LOQ	0.017%	LOQ < lowest calibration point (2.60%)
r	0.999	Almost perfect linearity
U(r)	0.0031%	x ₀ ± 0.0031%

METHOD VALIDATION – ANALYSIS OF OXIDES

Table 8.7: Results and summary of the validation parameters for SiO₂

<i>Regression Statistics</i>				
Multiple R	0.99999998			
R Square	0.99999996			
Adjusted R Square	0.99999995			
Standard Error	0.04131490			
Observations	13			
<i>ANOVA</i>				
	<i>df</i>	<i>SS</i>	<i>MS</i>	<i>F</i>
Regression	1	420360.2	420360.20	246268165
Residual	11	0.019	0.00	
Total	12	420360.2		
	<i>Coefficients</i>	<i>Standard Error</i>	<i>t Stat</i>	<i>P-value</i>
Intercept	5.8398	0.0203	287.2937	1.14068E-22
X Variable 1	17.1858	0.0011	15692.9336	8.83692E-42

Validation parameter	Value	Description/Conclusion
Analytical range	S _a = 0.020 S _b = 0.001	S _b < S _a Range satisfactory
Slope (b)	17.2	Regression line slope
Intercept (a)	5.84	Regression line intercept
Regression line	y = 17.2x + 5.84	Regression line equation
LOD	0.0035%	Lowest distinguishable signal
LOQ	0.0118%	LOQ < lowest calibration point (0.90%)
r	0.999	Almost perfect linearity
U(r)	0.0014%	x ₀ ± 0.0014%

METHOD VALIDATION – ANALYSIS OF OXIDES

Table 8.8: Results and summary of the validation parameters for CaO

<i>Regression Statistics</i>				
Multiple R	0.99999999			
R Square	0.99999998			
Adjusted R Square	0.999999978			
Standard Error	0.024278959			
Observations	11			
<i>ANOVA</i>				
	<i>df</i>	<i>SS</i>	<i>MS</i>	<i>F</i>
Regression	1	266133.6	266133.6	451481172.7
Residual	9	0.0053	0.0006	
Total	10	266133.6		
	<i>Coefficients</i>	<i>Standard Error</i>	<i>t Stat</i>	<i>P-value</i>
Intercept	7.4283	0.0145	513.8945	2.03678E-21
X Variable 1	8.8224	0.0004	21248.0863	5.76756E-36

Validation parameter	Value	Description/Conclusion
Analytical range	$S_a = 0.014$ $S_b = 0.0004$	$S_b < S_a$ Range satisfactory
Slope (b)	8.82	Regression line slope
Intercept (a)	7.43	Regression line intercept
Regression line	$y = 8.82x + 7.43$	Regression line equation
LOD	0.0049%	Lowest distinguishable signal
LOQ	0.0164%	LOQ < lowest calibration point (6.31%)
r	0.999	Almost perfect linearity
U(r)	0.0015%	$x_0 \pm 0.0015\%$

METHOD VALIDATION – ANALYSIS OF OXIDES

Table 8.9: Results and summary of the validation parameters for TiO₂

<i>Regression Statistics</i>				
Multiple R	0.999984			
R Square	0.999967			
Adjusted R Square	0.999959			
Standard Error	0.024280			
Observations	6			
<i>ANOVA</i>				
	<i>df</i>	<i>SS</i>	<i>MS</i>	<i>F</i>
Regression	1	72.5210	72.5210	123019.975
Residual	4	0.0024	0.0006	
Total	5	72.5234		
	<i>Coefficients</i>	<i>Standard Error</i>	<i>t Stat</i>	<i>P-value</i>
Intercept	-0.5250	0.0215	-24.3822	1.67881E-05
X Variable 1	10.0576	0.0287	350.7420	3.96439E-10

Validation parameter	Value	Description/Conclusion
Analytical range	S _a = 0.022 S _b = 0.029	S _b > S _a Range could be improved
Slope (b)	10.1	Regression line slope
Intercept (a)	-0.53	Regression line intercept
Regression line	y = 10.1x – 0.53	Regression line equation
LOD	0.0064%	Lowest distinguishable signal
LOQ	0.0214%	LOQ < lowest calibration point (0.26%)
r	0.999	Almost perfect linearity
U(r)	0.0023%	x ₀ ± 0.0023%

METHOD VALIDATION – ANALYSIS OF OXIDES

Table 8.10: Results and summary of the validation parameters for Cr₂O₃

<i>Regression Statistics</i>				
Multiple R	0.9999999			
R Square	0.9999997			
Adjusted R Square	0.9999997			
Standard Error	0.0624668			
Observations	9			
<i>ANOVA</i>				
	<i>df</i>	<i>SS</i>	<i>MS</i>	<i>F</i>
Regression	1	101982.8	101982.8	26135361.6
Residual	7	0.0273	0.0039	
Total	8	101982.8		
	<i>Coefficients</i>	<i>Standard Error</i>	<i>t Stat</i>	<i>P-value</i>
Intercept	-14.1782	0.0304	-466.860	5.46292E-17
X Variable 1	19.3635	0.0038	5112.276	2.89384E-24

Validation parameter	Value	Description/Conclusion
Analytical range	S _a = 0.030 S _b = 0.004	S _b < S _a Range satisfactory
Slope (b)	19.4	Regression line slope
Intercept (a)	-14.2	Regression line intercept
Regression line	y = 19.4x – 14.2	Regression line equation
LOD	0.0047%	Lowest distinguishable signal
LOQ	0.0157%	LOQ < lowest calibration point (1.44%)
r	0.999	Almost perfect linearity
U(r)	0.0019%	x ₀ ± 0.0019%

METHOD VALIDATION – ANALYSIS OF OXIDES

Table 8.11: Results and summary of the validation parameters for MnO

<i>Regression Statistics</i>				
Multiple R	0.9999995			
R Square	0.9999989			
Adjusted R Square	0.9999987			
Standard Error	0.124989			
Observations	7			
<i>ANOVA</i>				
	<i>df</i>	<i>SS</i>	<i>MS</i>	<i>F</i>
Regression	1	72344.2	72344.2	4630867.19
Residual	5	0.078	0.016	
Total	6	72344.3		
	<i>Coefficients</i>	<i>Standard Error</i>	<i>t Stat</i>	<i>P-value</i>
Intercept	-4.2382	0.0619	-68.4327	1.26181E-08
X Variable 1	39.7154	0.0185	2151.9450	4.11289E-16

Validation parameter	Value	Description/Conclusion
Analytical range	$S_a = 0.062$ $S_b = 0.018$	$S_b < S_a$ Range satisfactory
Slope (b)	39.7	Regression line slope
Intercept (a)	-4.24	Regression line intercept
Regression line	$y = 39.7x - 4.24$	Regression line equation
LOD	0.0047%	Lowest distinguishable signal
LOQ	0.0156%	LOQ < lowest calibration point (0.32%)
r	0.999	Almost perfect linearity
U(r)	0.002%	$x_0 \pm 0.002\%$

METHOD VALIDATION – ANALYSIS OF OXIDES

Table 8.12: Results and summary of the validation parameters for FeO

<i>Regression Statistics</i>				
Multiple R		0.9999998		
R Square		0.9999997		
Adjusted R Square		0.9999996		
Standard Error		0.0522104		
Observations		8		
<i>ANOVA</i>				
	<i>df</i>	<i>SS</i>	<i>MS</i>	<i>F</i>
Regression	1	51768.24	51768.24	18991088.62
Residual	6	0.016	0.003	
Total	7	51768.26		
	<i>Coefficients</i>	<i>Standard Error</i>	<i>t Stat</i>	<i>P-value</i>
Intercept	0.6490	0.0255	25.4118	2.44653E-07
X Variable 1	18.1450	0.0042	4357.8766	9.85494E-21

Validation parameter	Value	Description/Conclusion
Analytical range	$S_a = 0.026$ $S_b = 0.004$	$S_b < S_a$ Range satisfactory
Slope (b)	18.1	Regression line slope
Intercept (a)	0.649	Regression line intercept
Regression line	$y = 18.1x + 0.649$	Regression line equation
LOD	0.0042%	Lowest distinguishable signal
LOQ	0.014%	LOQ < lowest calibration point (0.18%)
r	0.999	Almost perfect linearity
U(r)	0.002%	$x_0 \pm 0.002\%$

8.5 Conclusions

The calibration range for all the lines are satisfactory ($S_b < S_a$) except for the TiO_2 calibration line. The range for this line can be improved by introducing more standards on the line when production samples become available to be analysed by ICP-OES and used as secondary standards. For the rest of the lines, due to the acceptable ranges, extrapolation on the lines to get analytical values should present no difficulty.

The LOQ values for all the oxides are very low, lower than the lowest calibration point on each line. The method for the analysis of the oxides is therefore sensitive enough to give good results for the expected concentration ranges of each oxide.

All the calibration lines show almost perfect linearity (i.e. r equals almost 1). The assumption made at the beginning of the method development for the analysis of oxides that matrix matching between standards and samples may eliminate the need for overlap corrections or corrections for spectral interferences is therefore valid. This statement is now supported after validation of all the calibration lines, especially the parameters regarding the accuracy of the method and the good regression values, which indicates that although no corrections have been made on any line, the lines show an almost perfect linear response between spectral line intensity and concentration, and yields accurate results when analysing CRMs.

CHAPTER 9 SAMPLE PREPARATION

9.1 Sampling

During the charge chrome manufacturing process a sample is taken during the scraping of the slag when separated from the melt for oxide analysis, and a sample is taken from the charge chrome melt itself for elemental analysis. Samples are taken from the melt or the slag as spoon samples with an average mass of 350 g. These samples will represent a production heat of roughly 100 tons.

From an analytical point of view there is no control on the taking of the original sample during the production stage. The preparation of the subsample for analytical purposes should however be investigated to minimise any factors that may cause erroneous results.

It is known that particle size effects in samples have an influence on the intensity of X-rays produced during analysis. This can be attributed to the fact that the penetration depths of X-rays vary, in the sense that for longer wavelengths the penetration depth is much less than the penetration depths will be for shorter wavelength X-rays. These effects might be minimised when there is matrix matching between samples and standards (as discussed in Chapter 7) and by grinding or milling the sample to obtain very small particle sizes. In general, for samples in the range of 20 – 50 g, when the largest amount of the sample have particle sizes of $<75 \mu\text{m}$, particle size effects can be minimised to a large extent (Willis, 2008).

One sample preparation technique involves the preparation of a button sample by melting the charge chrome (for elemental analysis) at a high temperature ($>1000 \text{ }^\circ\text{C}$) in an alumina-silica crucible. After melting the sample is moulded in a small container and cooled. The sample surface is polished to ensure a surface suitable for XRF analysis. The surface should

be smooth and even to ensure effective penetration of X-rays over the whole sample area. The main disadvantages of this method are that the method is time consuming, and contamination of the sample may occur, especially Si contamination from the alumina-silica crucible used during the melting process. A more convenient way of sample preparation involves the making of a powder briquette. This method is less time consuming and Si contamination can be avoided.

This technique is already applied for the sample preparation of the slag samples. The physical state of these samples (soft and brittle) makes the preparation of briquettes ideal and the procedure is fairly simple. The slag samples are milled to obtain small particle sizes and after milling the sample is pressed into a briquette by adding a cellulose binder to the milled sample (Anzelmo *et al.*, 2001). The preparation of charge chrome samples as briquettes similar to the briquettes prepared for slag analysis will be investigated.

During this discussion the main focussing points will be the following:

- influence of sample milling time on the particle size of charge chrome
- influence of sample particle size on analysis by XRF
- homogeneity of the sample preparation technique
- comparison between the results obtained on the analysis of a button sample and a briquette sample from the same production heat.

9.2 Effect of milling time on particle size

During this investigation a 350 g spoon sample (obtained from a production heat) was first crushed using a jaw crusher to obtain sample pieces with sizes <10 mm. After this, the sample was further crushed on an automatic Herzog HP crushing machine further decreasing the sample size to <3 mm. From this, five 50 g mass aliquots of the sample were

SAMPLE PREPARATION

taken and each one was milled on an automatic Herzog HP milling machine at different time intervals. This was followed by a sieving process to determine the effect of milling time on particle size. The aim will be to obtain the maximum amount of sample with particle sizes of $<75\ \mu\text{m}$. For this a sieve with an aperture of $75\ \mu\text{m}$ was used. The 50 g sample aliquots were weighed before milling. After milling the samples were sieved and the mass retained on the sieve ($>75\ \mu\text{m}$) was subtracted from the mass that passed through the sieve ($<75\ \mu\text{m}$). This calculation was used to determine the percentage sample with particle sizes $<75\ \mu\text{m}$. This experiment was done in duplicate using samples from two different production heats. The results obtained are shown in Table 9.1.

Table 9.1: The effect of milling time on particle size

Production sample 3344					
Milling time (sec)	30	60	90	120	150
Initial sample mass (g)	50.3	50.5	50.5	50.0	49.5
Mass retained ($<75\ \mu\text{m}$)	1.0	0.7	0.5	0.3	0.8
Sample $<75\ \mu\text{m}$ (%)	98.0	98.6	99	99.4	98.4
Production sample 3410					
Milling time (sec)	30	60	90	120	150
Initial sample mass (g)	50.2	50.2	49.8	50.2	50.1
Mass retained ($<75\ \mu\text{m}$)	4.2	0.7	0.3	0.1	0.1
Sample $<75\ \mu\text{m}$ (%)	91.6	98.6	99.4	99.8	99.8

From the data in Table 9.1 it is evident that more than 90% of the sample already have a particle size of $<75\ \mu\text{m}$ after just 30 seconds of milling. After 90 seconds of milling, more than 99% of the sample has a particle size of $<75\ \mu\text{m}$. From these two different samples the conclusion can be made that 90 seconds of milling time is sufficient enough to obtain more than 99% of the sample with particle sizes $<75\ \mu\text{m}$.

9.3 Influence of particle size on XRF analysis

It has now been established that 90 seconds milling time is sufficient to give the largest amount of sample with particle sizes $<75\ \mu\text{m}$, the desired particle size for XRF analysis when the mass of the samples that will be analysed is in the range of 20 – 50 g. The next step after milling will be to make a powder briquette of the sample.

While milling the sample (50 g) a cellulose binder (2 g) is added to the sample to press the milled sample into a briquette. The sample is pressed using an automatic Herzog HP pressing machine. During the pressing process, the pressure on the sample is increased from ambient pressure to 110 kN. The ramp-up to this pressure is done over 30 seconds. Once this pressure is reached, it is maintained for a further 30 seconds. The pressure on the sample is then decreased to ambient pressure over 30 seconds. This method results in a pressed briquette with a smooth and even sample surface.

During the previous experiment the sample was milled over different time intervals to establish the effect of milling time on particle size. The next experiment will focus on the effect of particle size on the actual XRF analysis, using production sample 3410 as an example. The five sample aliquots milled over the different time intervals were pressed into briquettes using the method described above. Each sample was then analysed to see if particle size will have any significant influence on the analysis of the charge chrome briquette. The parameter that will be used as an expression of particle size is the milling time. The samples were analysed using the method validated in Chapter 5 and the results are summarised in Table 9.2. Figures 9.1 – 9.4 illustrates the effect of milling time (hence particle size) on the concentration of each element.

Table 9.2: The effect of particle size on XRF analysis

Element	30 sec	60 sec	90 sec	120 sec	150 sec
Si (%)	1.28	0.394	0.362	0.314	0.284
P (%)	0.0114	0.0125	0.0129	0.0134	0.0138
S (%)	0.0242	0.0210	0.0212	0.0204	0.0200
Cr (%)	53.32	55.20	56.18	56.56	56.70

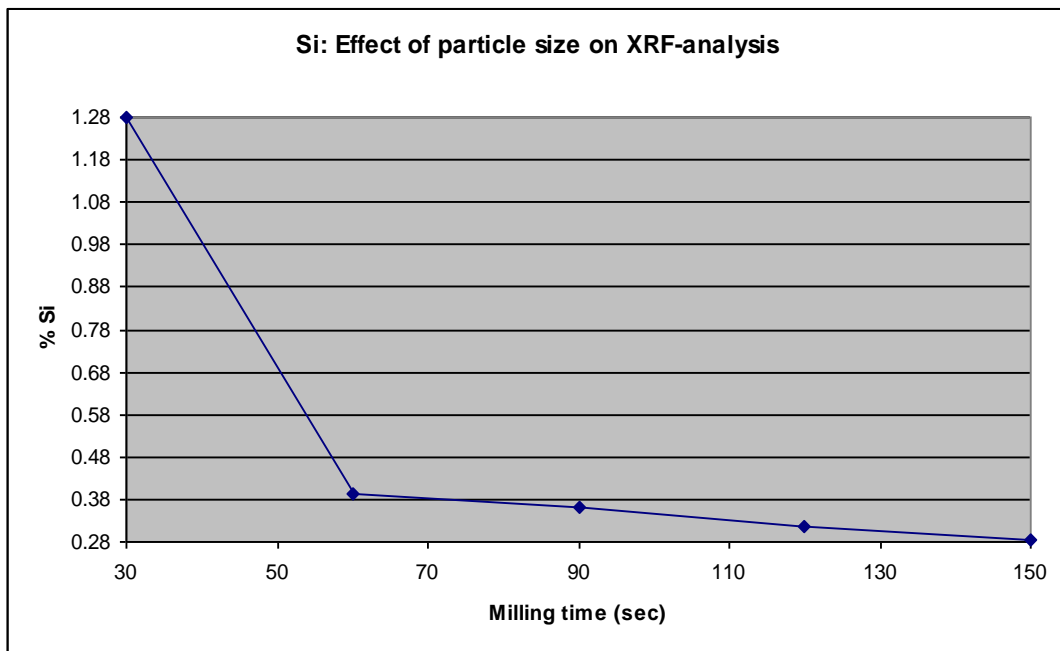


Figure 9.1: The effect of particle size on the analysis of Si

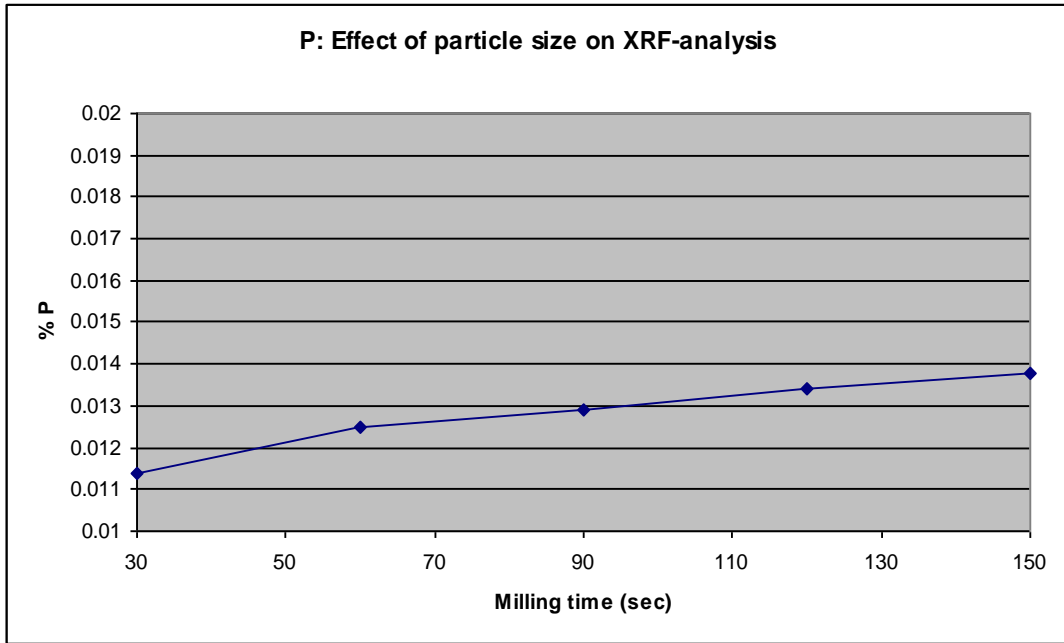


Figure 9.2: The effect of particle size on the analysis of P

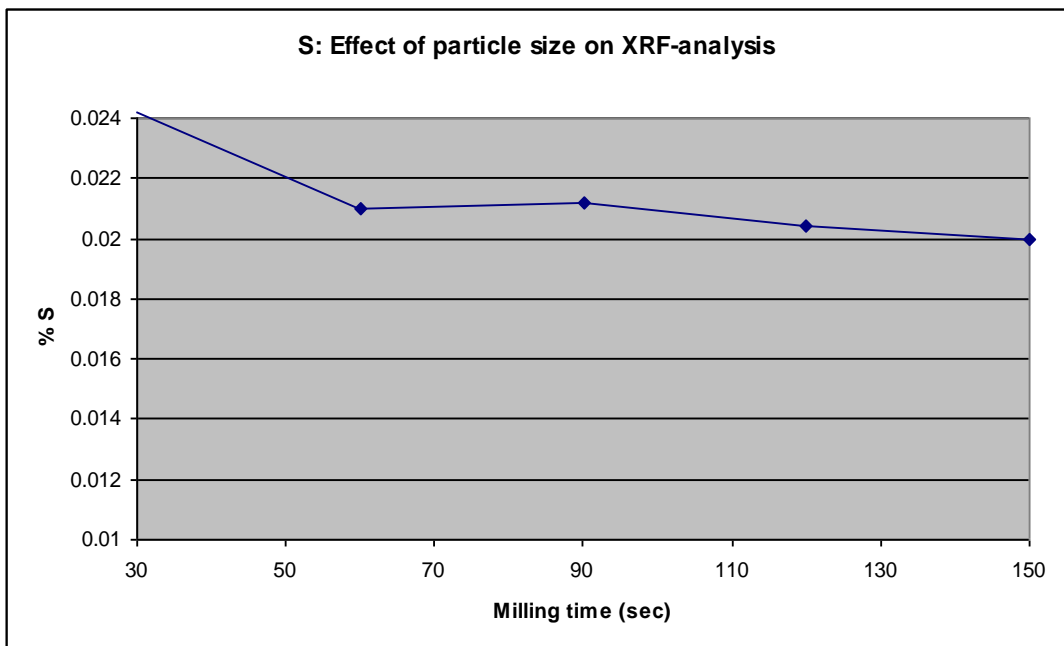


Figure 9.3: The effect of particle size on the analysis of S

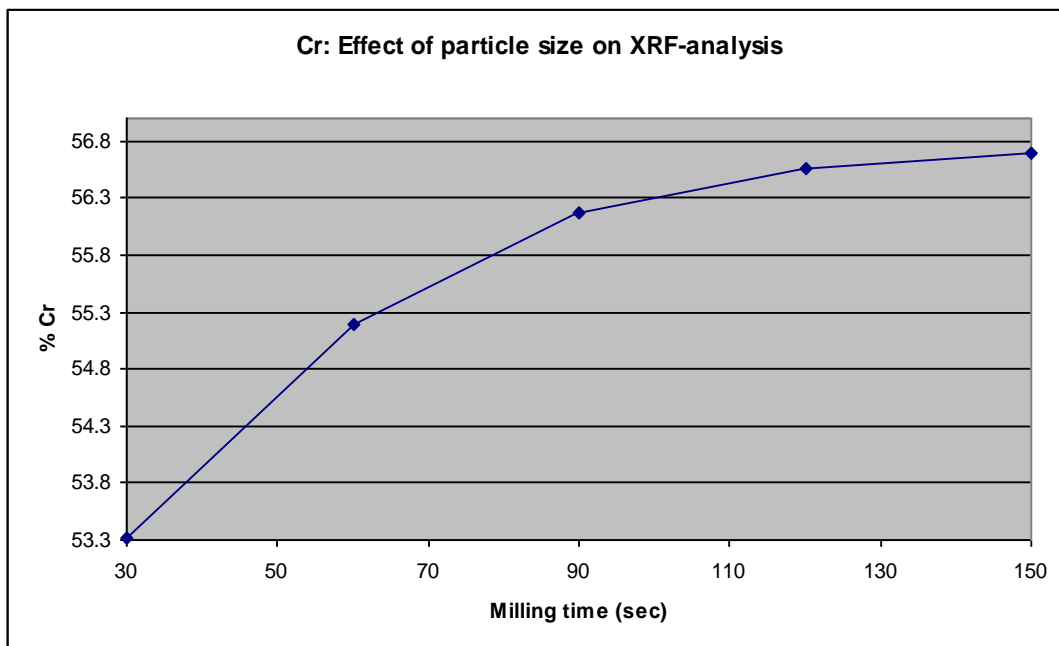


Figure 9.4: The effect of particle size on the analysis of Cr

When examining the values in Table 9.2 and the graphs represented by Figures 9.1 – 9.4 it is clear that milling time does have an influence on the chemical analysis of the sample briquettes. The assumption can be made that milling time has an influence on the distribution of particles throughout the sample.

For Si, there is an obvious decrease in concentration with an increase in milling time. A possible explanation for this is that 30 seconds of milling time is not sufficient enough to mill the Si in the sample to obtain a small enough particle size. Due to the larger Si particles and the low density of the element, segregation of Si to the sample surface may take place leading to higher Si concentrations being analysed. Between the 60 seconds and 150 seconds time intervals there is only a slight variation in the Si concentration, only 0.11% between the two mentioned time intervals. At this stage the conclusion can be made that 60 seconds milling time is sufficient to produce Si-particles with an acceptable size not to significantly influence the concentration with an increase in milling time.

For the elements P and S the change in concentration levels between the 30 seconds and 150 seconds time interval is very small. For P there is only a 0.0024% increase in concentration and for S a 0.0042% decrease in concentration, which is low when taking the 2 minute difference between the shortest and longest milling times into account.

Cr shows an increase in concentration with an increase in milling time. As discussed earlier, the Si concentration decreases with an increase in milling time leading to smaller particles which prohibits the possible segregation of the element to the sample surface. The largest amount of Cr in the sample now also has a particle size of $<75 \mu\text{m}$. At 150 seconds milling time it is likely that there is a more evenly distribution of all the elements through the briquette resulting in a more homogenous sample.

This conclusion can be supported by the fact that the difference in concentration values for all the elements between the 120 seconds and 150 seconds milling time interval is very small. For Cr the concentration difference is only 0.1% which is insignificant on a Cr level of $>50\%$. This is also the reason why the impact of milling times longer than 150 seconds have not been investigated. According to this results, an optimum milling time of 150 seconds for the preparation of charge chrome briquettes is suggested.

9.4 Homogeneity

During the production process a spoon sample with a mass of roughly 350 g is taken for chemical analysis. The laboratory has no influence or control on this sampling procedure.

It is very important though to ensure that the sample received by the laboratory is treated and prepared in such a way as to ensure that the results obtained after analysis are an accurate and precise indication of

the chemical composition of the sample received. One of the important parameters that has to be investigated during this stage is the homogeneity of the sample after the sample preparation stage is completed.

During this experiment two samples from different production heats have been prepared and analysed. The sample preparation technique is described below:

- 350 g sample crushed on a jaw crusher; particle size <10 mm
- sample further crushed on an automatic crusher; particle size <3 mm
- cellulose binder added and sample milled for 150 seconds; roughly 99% particles <75 μm
- sample separated into five 50 g mass aliquots, each one pressed into a briquette
- each briquette analysed using the validated XRF method.

After analysis of the five samples the standard deviation for each element was used as an indication of homogeneity. A low standard deviation (relative to the concentration level of each element) will be an indication of satisfactory homogeneity. This decision was also made based on the various tolerances allowed as indicated in Table 8.1. The results obtained during this experiment are summarised in Table 9.3.

Table 9.3: Results indicating the homogeneity of the sample preparation technique

Production sample 3336						
Element	Briquette 1 (%)	Briquette 2 (%)	Briquette 3 (%)	Briquette 4 (%)	Briquette 5 (%)	σ
Si	1.03	0.983	0.975	1.03	1.01	0.0258
P	0.0136	0.0134	0.0131	0.0135	0.0134	0.000187
S	0.0264	0.0255	0.0255	0.0268	0.0258	0.000579
Cr	55.76	55.51	55.39	55.97	55.48	0.238
Production sample 3344						
Element	Briquette 1 (%)	Briquette 2 (%)	Briquette 3 (%)	Briquette 4 (%)	Briquette 5 (%)	σ
Si	0.266	0.251	0.260	0.270	0.257	0.00746
P	0.0131	0.0125	0.0131	0.0131	0.0128	0.000268
S	0.0268	0.0251	0.0265	0.0272	0.0265	0.000792
Cr	56.28	55.37	56.39	56.27	56.41	0.437

The percentage differences between the highest and lowest values obtained during the analysis for each element are very low, hence the low σ -values. These values fall within the tolerances allowed according to laboratory specifications and the conclusion can be made that the preparation method yields satisfactory results with regard to the homogeneity of the sample.

9.5 Comparison of analysis between button and briquette samples

One of the main aims during this research project was to develop an analytical method suitable for analysing charge chrome samples as powder briquettes for the elements Si, P, S and Cr. Now that the XRF analytical method has been developed and validated and a suitable sample preparation technique for powder briquettes has been established, the last step was to compare the results obtained when the same production sample is analysed as a button and as a powder briquette. A

good agreement between the results will indicate that the analysis of charge chrome samples as powder briquettes is a suitable alternative technique for charge chrome sample preparation and analysis. It should be kept in mind that there is a possibility of Si contamination during the button preparation technique. Therefore lower results for Si in the briquette samples are expected when a button and briquette from the same production heat will be analysed.

The paired t-test was used to evaluate the comparison between the analytical results obtained from the two different sample preparation techniques. This test differs from the t-test used during the validation of accuracy (equation 5.3) in the sense that the paired t-test takes into account not only the difference between the values of two means, but also the different populations which is represented by each mean, in this case the population of values obtained from the button samples and the population of values obtained from the briquette samples (Miller and Miller, 2005). The calculated t-value is obtained using equation 9.1:

$$t_{\text{calc}} = \left| x_{\text{avg;d}} \right| n^{1/2} / \sigma_d \quad (9.1)$$

Where t_{calc} = calculated t-value
 d = difference between pair of results given by two methods
 $x_{\text{avg;d}}$ = average of Σ_d , divided by the number of measurements
 Σ_d = sum of d-values obtained for all measurements
 n = number of analytical measurements
 σ_d = standard deviation of all the d-values

The ideal will be to get the difference of the analytical results obtained during the method as close as possible to zero. The calculated t-values was again evaluated against hypothesis statements. H_0 will assume no significant difference between the results obtained from the different methods while H_1 will assume a significant difference between the results of the two different methods. For H_0 to be accepted, $t_{\text{calc}} < t_{\text{crit}}$. The value for t_{crit} was obtained from the same statistical table used during

Chapter 5. Table 9.4 shows the results obtained for each element analysed using the two different sample preparation techniques.

Table 9.4: Results (% concentration) obtained during the elemental analysis of charge chrome buttons and briquettes

Element	Method	1	2	3	4	5
Si	Button	0.824	0.821	0.826	0.823	0.825
	Briquette	0.409	0.410	0.409	0.408	0.408
	d	0.415	0.411	0.417	0.415	0.417
P	Button	0.0116	0.0115	0.0113	0.0113	0.0111
	Briquette	0.0119	0.0119	0.0118	0.0118	0.0120
	d	-0.0003	-0.0004	-0.0005	-0.0005	-0.0009
S	Button	0.0262	0.0262	0.0262	0.0258	0.0265
	Briquette	0.0265	0.0267	0.0267	0.0267	0.0266
	d	-0.0003	-0.0005	-0.0005	-0.0009	-0.0001
Cr	Button	54.34	54.10	54.28	54.12	54.15
	Briquette	54.19	54.20	54.23	54.25	54.23
	d	0.15	-0.1	0.05	-0.13	-0.08

Table 9.5: Summary of the statistical values obtained after the elemental analysis of charge chrome buttons and briquettes

Element	Σd	$x_{avg;d}$	σ_d	n	DF	t_{crit}	t_{calc}
Si	2.1	0.415	0.0024	5	4	2.78	3.87
P	-0.0027	0.00054	0.00027	5	4	2.78	4.48
S	-0.0023	0.00046	0.0003	5	4	2.78	3.43
Cr	-0.11	0.022	0.118	5	4	2.78	0.418

As can be seen from Table 9.4 there is a significant difference between the Si-values obtained when analysing a button sample compared to the values obtained when analysing a powder briquette in the sense that the briquette samples give lower results for Si. This confirms the assumption made earlier that there might well be Si contamination from the crucible used during the preparation of a charge chrome button. The very large

t_{calc} value for Si (Table 9.5) is also an indication of significant difference between the results obtained for the different samples. The lower values for Si obtained with the powder briquettes should therefore be a more accurate estimate of the Si concentration since this sample preparation procedure avoids Si contamination.

For both P and S, the values in Table 9.5 shows that $t_{\text{calc}} > t_{\text{crit}}$, which implies that the H_0 hypothesis should be rejected and the H_1 hypothesis should be accepted, which means there is a significant difference between the values obtained for the different sample preparation techniques. It should now be decided if this difference is significant enough to discard the briquette as sample preparation technique for these two elements or not.

Two factors will be taken into consideration. Firstly, when the t_{calc} values obtained for these elements are compared to their respective t_{crit} values, the difference is not that large. Secondly, when the individual analytical results obtained during the analysis of both samples are compared (Table 9.4), the percentage difference between the two samples is very small. On average there is only a 0.0005% difference in concentration for both elements. Because of these factors the decision is made that the difference between the results obtained for the button sample and the briquette sample for the analysis of P and S is not that significant and that the briquette sample still gives satisfactory results.

For Cr $t_{\text{calc}} < t_{\text{crit}}$ which indicates good similarity between the results obtained for the different sample preparation techniques. The H_0 hypothesis will therefore be accepted.

During this discussion the preparation of charge chrome as a powder briquette has been investigated. This technique is easier and quicker compared to the current technique where the sample is prepared as a button.

For the briquette method the milling time has been optimised to give a sample with adequate particle sizes (more than 99% <75 μm) for effective XRF analysis. This was shown during the analysis of samples milled over different time intervals. It has also been shown that the production sample received can be prepared homogeneously to further minimise errors during sample preparation and analysis.

The main purpose was to determine if the sample prepared as either a button or a powder briquette will give significant different results. After analysis of the two different sample types and the statistical interpretation of the results, the conclusion was made that the powder briquette does not give results significantly different from the results obtained when preparing and analysing a button. The exception in this case was Si. Contamination of this element was expected when preparing a button sample. The powder briquette showed lower levels of Si which indicates that Si contamination can be avoided during the preparation of a powder briquette.

The conclusion can therefore be made that the analysis of charge chrome samples in the form of a powder briquette is able to give results comparable to the results obtained when analysing the sample as a button. The preparation and analysis of charge chrome as a powder briquette is therefore sustainable and will be implemented as an alternative to the current button preparation technique.

CHAPTER 10 SUMMARY AND CONCLUSIONS

10.1 Qualitative wavelength scans

Charge chrome contains >50% Cr which is used as a raw material for the manufacturing of stainless steel. It is essential to know the chemical composition of this high carbon ferro-alloy before it can be used during the stainless steel manufacturing process.

The essential elements that need to be analysed for include Si, P, S and Cr. Si contributes to the elongation properties of stainless steel while high quantities of P and S cause the steel to be brittle. Cr is the element that gives stainless steel its corrosion resistant properties. These elements are present in charge chrome as trace (P and S), minor (Si) and major (Cr) elements.

During the charge chrome manufacturing process the main Cr-ore is reduced to yield Cr metal. During this reduction process other unwanted minerals are removed in the form of oxide slag. The slag is also analysed to determine the loss of Cr as Cr_2O_3 during the reduction process. The other oxides analysed for include MgO , Al_2O_3 , SiO_2 , CaO , TiO_2 , MnO and FeO .

Method development for the analysis of the elements and oxides was started by doing qualitative wavelength scans on a charge chrome production sample and a slag sample respectively. The aim of the wavelength scans was to determine if any spectral overlaps are present between the elements or oxides analysed for. The wavelength scans also verified the instrumental parameters that were used during the analytical method development phase.

During the wavelength scans for the elements no overlaps were expected since spectral overlaps is not likely to occur when lighter elements (Si, P and S) are analysed. Wavelength scans did on a production sample confirmed no overlaps on any of the elemental K α -spectral lines that will be used for the eventual quantitative analysis.

The principle K α -lines of the elements Mg, Al, Si, Ca, Ti, Cr, Mn and Fe were used to analyse the corresponding oxides. During wavelength scans of a slag production sample using a LiF200 crystal, overlaps occurred on two of the K α -lines that will be analysed: CrK β 1,3 on the MnK α 1,2 (for the analysis of MnO) and MnK β 1,3 on the FeK α 1,2 line (for the analysis of FeO). In general it will be necessary to make overlap corrections if the Mn and Fe K α -lines will be analysed. These overlap corrections were not made because of reasons discussed during the setting up of calibration lines for each oxide to be analysed.

10.2 Setting up calibration lines

During the setting up of calibration lines the two most important factors to keep in mind are that the standards should represent the charge chrome and oxide matrices of the samples to be analysed, and the standards must cover the concentration range of each element and oxide as it will be in the production samples.

This was one of the major challenges during the method development process due to the fact that CRMs representing a charge chrome or slag matrix is not readily available commercially. This problem was mainly overcome by introducing production samples as secondary standards on the calibration lines. These production samples were analysed by an alternative validated analytical technique (ICP-OES).

During the research it was found that there were two major advantageous with the introduction of production samples as secondary standards. Firstly, for the analysis of Si, these samples contain Si in the range of < 1% Si. CRMs with Si at this concentration level are not available. Secondly, using production samples as standards there is a possibility that matrix matching between calibration standards and samples may compromise for the need to make matrix corrections in terms of spectral overlaps and spectral line interferences.

For matrix effects, spectral interferences with regard to absorption in the oxide samples were predicted using mass absorption coefficient values (refer to Table 7.1). According to these values the following interferences due to absorption were predicted:

- absorption of AlK α by Mg
- absorption of SiK α by Al
- absorption of TiK α by Ca
- absorption of CrK α by Ti.

The theory that matrix matching between calibration standards and samples might eliminate the need for corrections by using correction algorithms was tested by setting up calibration lines using CRMs (where available and applicable to a certain calibration line) and secondary standards created from production samples.

The ideal situation will be to have calibration lines with a linear response between spectral line intensity and analyte concentration. This will simplify the validation of the calibration lines especially when uncertainties of analytical values will be calculated since the statistical methods and equations for calculating uncertainties and other validation parameters for linear response curves are easy to apply and interpret. The validity of the matrix matching theory was first noticed when the calibration lines of the oxides visually appear to be linear without any corrections being made.

The relative small SEE values obtained for each calibration line further strengthened the theory.

10.3 Method validation

During the method validation phase the main parameters that were validated to prove that the methods for the analysis of the elements and oxides are fit for purpose were:

- accuracy and precision of results
- analytical range
- determination of detection and quantitation limits
- calculations of uncertainties in analytical measurements.

According to the SANS 17025:2005 quality manual, these parameters are stipulated as essential indicators for the validity of any analytical method, and if the method(s) are relevant to the needs of the laboratory (SANS 17025:2005). Validations of these parameters were done using general statistical techniques relevant to linear response curves. For all the calibration lines the linearity was found to be satisfactory and showed almost perfect linearity. Accuracy was validated using CRMs independent with regard to the calibration line validated (the CRM does not form part of the calibration standards used on the line). According to the results obtained from the statistical t-test used to validate accuracy, all the calibration lines used for the analysis of the elements and the oxides gave results that could be interpreted as accurate according to the H_0 hypothesis. This hypothesis states that when t values calculated using the t-test are smaller than critical t values obtained from statistical tables (dependant upon statistical parameters such as the number of measurements made etc.), it can be accepted that the analytical method is able to give accurate and trustworthy results. For all the calibration lines

$t_{\text{calc}} < t_{\text{crit}}$. These results confirmed the theory that due to matrix matching between standards and samples no matrix corrections are necessary.

Multiple analysis of production samples were used to calculate the standard deviation obtained between analytical results. These values were used as an indication of the precision of the analytical method. For all elements and oxides the σ -values were low enough to indicate good precision.

The ANOVA function on Excel was used to validate parameters such as the analytical range, LOD and LOQ values, and linear regression. The calibration lines for P, S and TiO_2 are the only lines that can be improved with regard to the analytical ranges. The ranges for the rest of the calibration lines are satisfactory. The LOD and LOQ values for all the lines are low enough to prevent extrapolation below the lowest calibration point. The regression values for all the lines indicate almost perfect linearity.

The general conclusion made after the validation procedures was that the methods developed for the analysis of Si, P, S and Cr as elements, and the oxides MgO , Al_2O_3 , SiO_2 , CaO , TiO_2 , Cr_2O_3 , MnO and FeO are fit for purpose for the analysis of the mentioned analytes.

10.4 Areas of improvement

As mentioned earlier, according to the statistical results the analytical range for P and S and TiO_2 can be improved. This can be done by introducing more standards (in the form of analysed production samples) on the calibration lines.

It has been noticed that some of the calibration lines are not passing through the zero-intercept (origin) on the graphs illustrating the relation between spectral line intensity and analyte concentration. The calibration

lines mostly affected by this are the lines for Cr (element), and MgO and CaO. The lines for P, S and TiO₂ also do not go through zero, but only to a lesser extent when compared to the other three lines. The main reason these lines do not pass through zero might possibly be due to inadequate background corrections. To be able to correct for this will mainly depend on the availability of blank samples that need to be scanned to determine and quantify the amount of background signal that will lead to the setting up of calibration lines not going through the zero-intercept. This will form part of further research on the methods to improve the validity of results obtained. This should however not be a main concern at this stage due to the fact that the concentration ranges of every element and oxide analysed are restricted to very repetitive values and the validations showed that the analytical methods for the analysis of the elements and the oxides are able to give precise and accurate results.

APPENDIX A

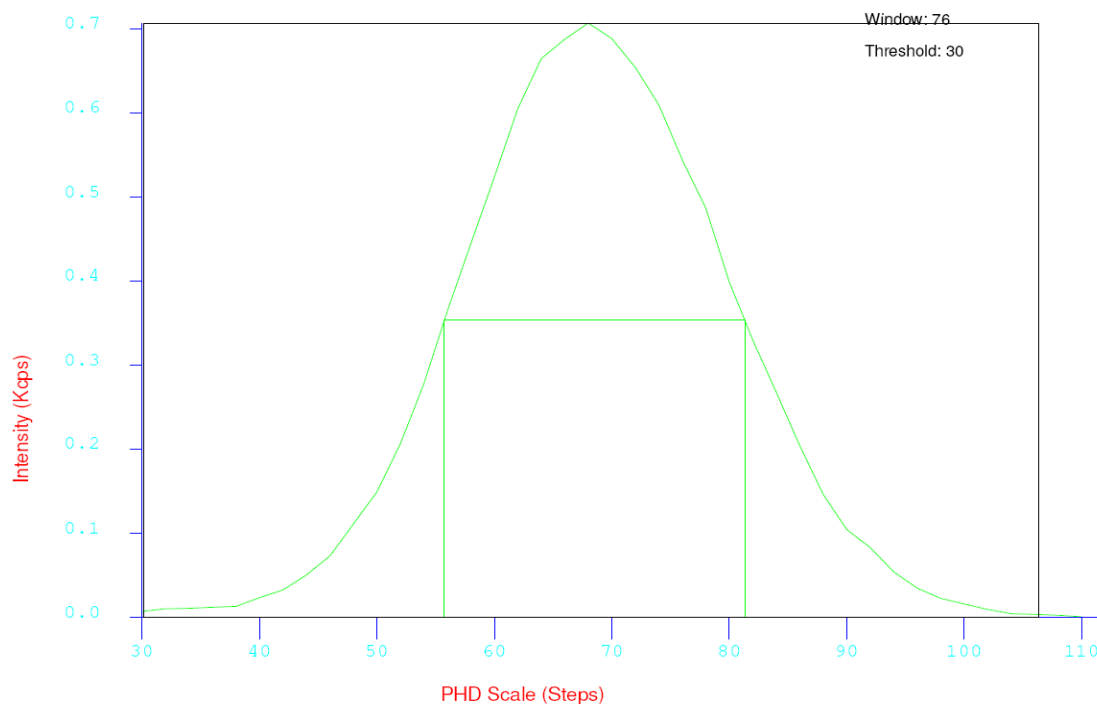
SiK α Energy Profile

Count Rate: 19.1345 kcps

PHD Scale Steps: 74.04 V

Results: SIAUG09 (200B) Monochromator: SiKa_mC

Count Rate: 19.1345 Kcps Detector Resolution: 37.62 %



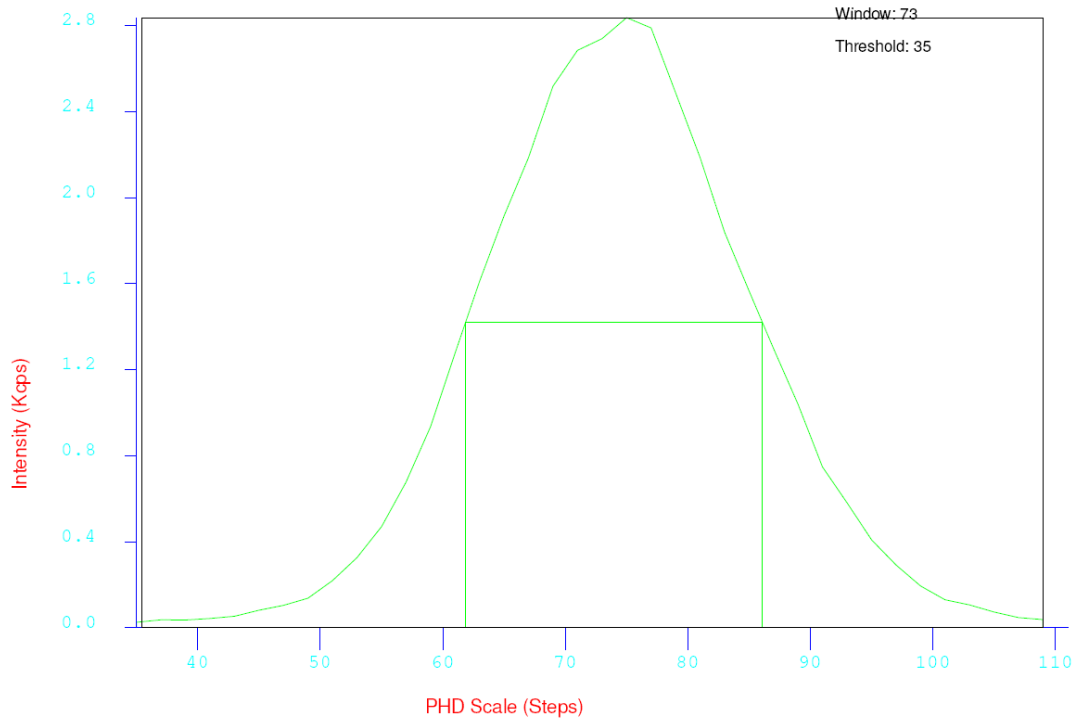
Parameters

Channel Type:	Monochromator
Element Line:	SiKa_mC
kV/mA:	20/15
PBF:	0
Monochromator Filter:	Off
Automatic Gain Control (AGC):	Off
PHD limits low/high:	30/110
Increment:	2
Integration time:	2
Counting Time/Window:	2

PKα Energy Profile

Count Rate: 72.6655 kcps
 PHD Scale Steps: 72.04 V

Results: PAUG09 (200B) Monochromator: P Ka_mC
 Count Rate: 72.6655 Kcps Detector Resolution: 32.34 %



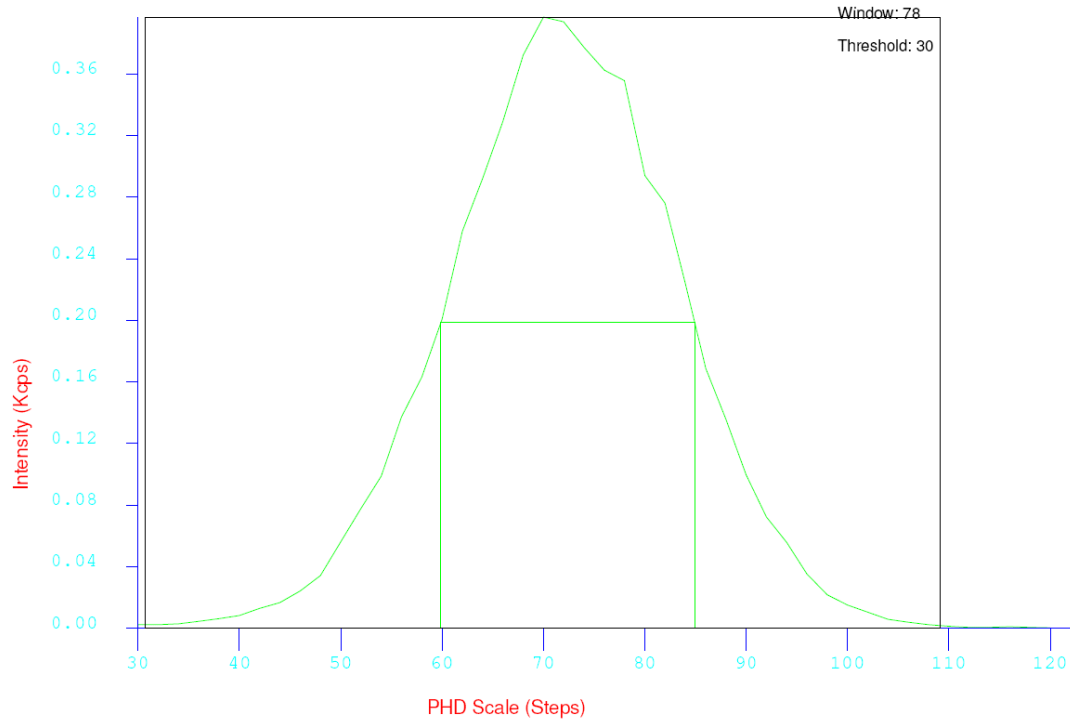
```

Parameters
-----
Channel Type:                Monochromator
Element Line:                P Ka_mC
kV/mA:                      50/60
PBF:                        0
Monochromator Filter:       On
Automatic Gain Control (AGC): On
PHD limits low/high:       35/110
Increment:                   2
Integration time:            2
Counting Time/Window:       2
    
```

SK α Energy Profile

Count Rate: 11.0435 kcps
 PHD Scale Steps: 72.14 V

Results: SAUG09 (200B) Monochromator: S Ka_mC
 Count Rate: 11.0435 Kcps Detector Resolution: 35.8 %



Parameters

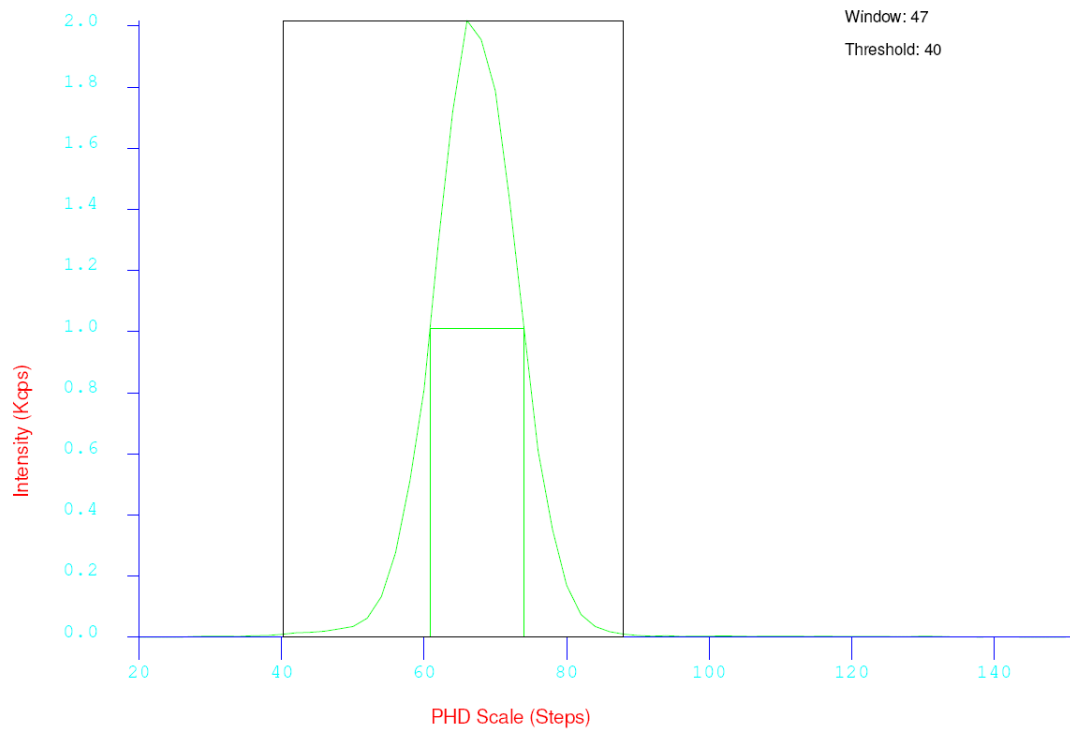
Channel Type:	Monochromator
Element Line:	S Ka_mC
kV/mA:	30/20
PBF:	0
Monochromator Filter:	On
Automatic Gain Control (AGC):	Off
PHD limits low/high:	30/120
Increment:	2
Integration time:	2
Counting Time/Window:	2

CrK α Energy Profile

Count Rate: 28.7825 kcps

PHD Scale Steps: 72.14 V

Results: CRAUG09 (200C) Monochromator: CrKa_mC
 Count Rate: 28.7825 Kcps Detector Resolution: 20.02 %



Parameters

Channel Type:	Monochromator
Element Line:	CrKa_mC
kV/mA:	50/60
PBF:	0
Monochromator Filter:	On
Automatic Gain Control (AGC):	Off
PHD limits low/high:	20/150
Increment:	2
Integration time:	2
Counting Time/Window:	2

Regression statistics for the P-calibration line

<i>Regression Statistics</i>	
Multiple R	0.9998
R Square	0.9996
Adjusted R Square	0.9994
Standard Error	0.0048
Observations	5

ANOVA				
	<i>df</i>	<i>SS</i>	<i>MS</i>	<i>F</i>
Regression	1	0.1666226	0.16662262	7135.69612
Residual	3	7.005E-05	2.33506E-05	
Total	4	0.1666927		

	<i>Coefficients</i>	<i>Standard Error</i>	<i>t Stat</i>	<i>P-value</i>
Intercept	0.3195	0.007214	44.2896	2.53378E-05
X Variable 1	28.2219	0.334093	84.4730	3.65677E-06

Data obtained from P-calibration line

Regression Uncertainty (Ur)

<u>Standard</u>	<u>xi</u>	<u>yi</u>	<u>(xi - xavg)</u>	<u>(xi - xavg)²</u>
BS 130/2	0.0130	0.690	-0.00760	0.00006
10	0.0150	0.744	-0.00560	0.00003
18	0.0190	0.849	-0.00160	0.00000
20	0.0260	1.053	0.00540	0.00003
14	0.0300	1.169	0.00940	0.00009

xi and yi avg	0.02	0.90		
∑(xi - xavg)²				0.00021

Sy/x =	0.005
b =	28.220
m =	5
n =	5
y0 =	0.8770
x0 =	0.020
yavg =	0.901
b ² =	796.368
∑(xi - xavg) ²	0.0002

$$U_{reg} = Sy/x/b \sqrt{1/m + 1/n + (y_0 - y_{avg})^2 / b^2 \sum (xi - x_{avg})^2}$$

b ² ∑(xi - xavg) ² =	0.167	
(y0 - yavg) ² =	0.001	
(y0 - yavg) ² / b ² ∑(xi - xavg) ² =	0.003	{1}
1/m + 1/n =	0.400	{2}
{1} + {2} =	0.403	
sqrt{1 + 2} =	0.635	{3}
Sy/x/b =	0.00017	{4}
(Ur) = {3} x {4}	0.00011	(%)

Regression statistics for the S-calibration line

<i>Regression Statistics</i>	
Multiple R	0.9967
R Square	0.9933
Adjusted R Square	0.9920
Standard Error	0.0794
Observations	7

ANOVA				
	<i>df</i>	<i>SS</i>	<i>MS</i>	<i>F</i>
Regression	1	4.6959	4.6959	745.71
Residual	5	0.0315	0.006297	
Total	6	4.7274		

	<i>Coefficients</i>	<i>Standard Error</i>	<i>t Stat</i>	<i>P-value</i>
Intercept	-0.4442	0.0896	-4.9596	0.00424973
X Variable 1	87.1896	3.1929	27.3076	1.23215E-06

Regression statistics for the Cr-calibration line

<i>Regression Statistics</i>	
Multiple R	0.9997
R Square	0.9995
Adjusted R Square	0.9994
Standard Error	0.7520
Observations	7

ANOVA				
	<i>df</i>	<i>SS</i>	<i>MS</i>	<i>F</i>
Regression	1	5482.2972	5482.2972	9695.62
Residual	5	2.8272	0.5654	
Total	6	5485.1244		

	<i>Coefficients</i>	<i>Standard Error</i>	<i>t Stat</i>	<i>P-value</i>
Intercept	41.3508	2.2738	18.1861	9.23923E-06
X Variable 1	4.0286	0.0409	98.4664	2.04826E-09

Data obtained from Cr-calibration line

Regression Uncertainty (Ur)

<u>Standard</u>	<u>xi</u>	<u>yi</u>	<u>(xi - xavg)</u>	<u>(xi - xavg)²</u>
METAL A	50.6500	246.43	-4.48857	20.147
18	51.5800	249.50	-3.55857	12.663
10	51.9000	250.15	-3.23857	10.488
M31688	52.1000	251.12	-3.03857	9.233
M32509	53.1000	255.27	-2.03857	4.156
20	54.7400	260.66	-0.39857	0.159
204/4	71.9000	331.25	16.76143	280.945

xi and yi avg	55.14	263.48		
Σ(xi - xavg)²				337.792

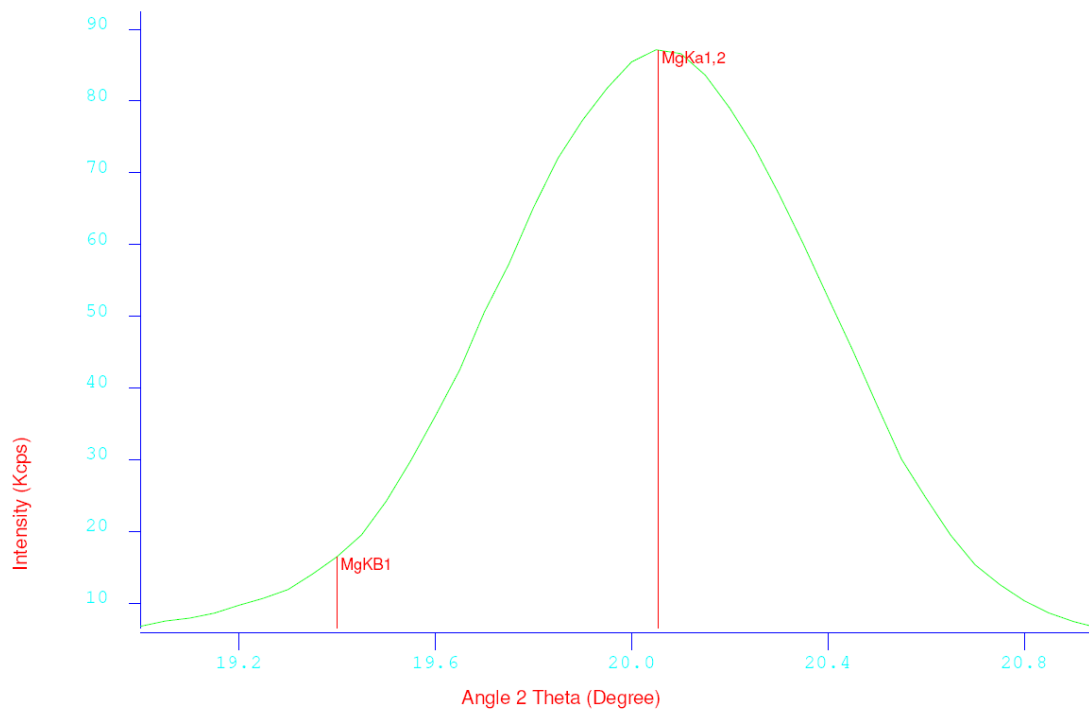
Sy/x =	0.752
b =	4.029
m =	5
n =	7
y0 =	260.720
x0 =	54.45
yavg =	263.483
b ² =	16.233
Σ(xi - xavg) ²	337.792

$$U_{reg} = Sy/x/b \sqrt{1/m + 1/n + (y_0 - y_{avg})^2 / b^2 \sum (xi - x_{avg})^2}$$

b ² Σ(xi - xavg) ² =	5483.325
(y0 - yavg) ² =	7.526
(y0 - yavg) ² / b ² Σ(xi - xavg) ² =	0.001 {1}
1/m + 1/n =	0.343 {2}
{1} + {2} =	0.344
sqrt{1 + 2} =	0.587 {3}
Sy/x/b =	0.187 {4}
(Ur) = {3} x {4}	0.110 (%)

Mg wavelength scan

Scan 1: MGOX (MG SLAG), from: MGOX, XRF Gonio: 1, 40 steps



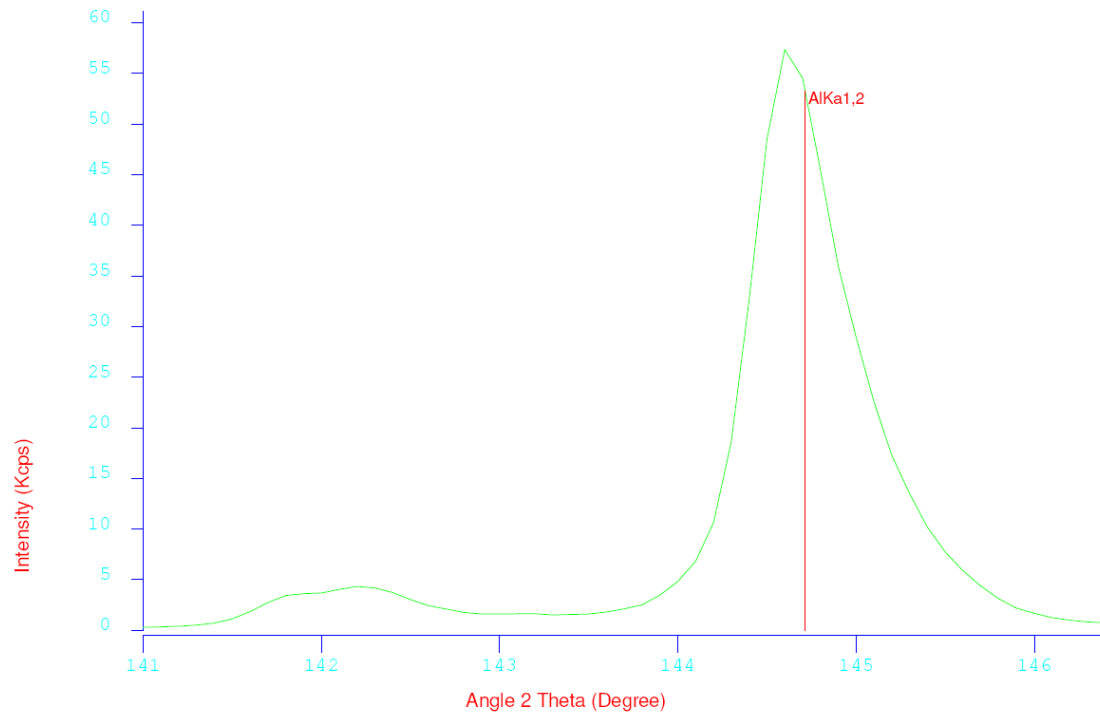
Identification Report:

Scan 1
 Sample Identifier: M3SLAG
 Sample Number: M37815
 XRF9800051
 Goniometer: XRF 1
 Crystal: AX06
 Detector: FPC
 Collimator: 0.60
 kV/mA: 50/50

Line	Intensity (Kcps)			Angle (deg)
	Scan 1	Scan 2	Scan 3	
MgKB1	16.4599			19.3992
MgKa1,2	87.1035			20.0549

Al wavelength scan

Scan 1: ALOX (M3SLAG), from: ALOX, XRF Gonio: 1, 55 steps —



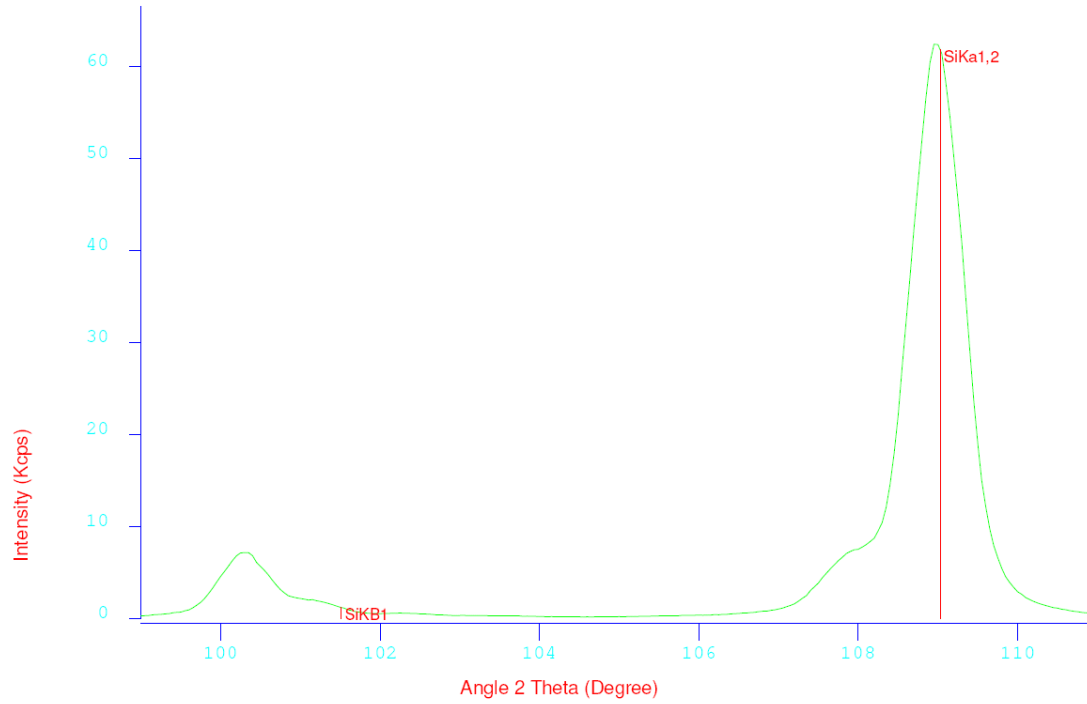
Identification Report:

Scan 1
 Sample Identifier: SLAG
 Sample Number: M37815
 XRF9800051
 Goniometer: XRF 1
 Crystal: PET
 Detector: FPC
 Collimator: 0.25
 kV/mA: 50/50

Line	Intensity (Kcps)			Angle (deg)
	Scan 1	Scan 2	Scan 3	
AlKa1,2	53.2996			144.7133

Si wavelength scan

Scan 1: SIOX (SI SLAG), from: SIOX, XRF Gonio: 1, 240 steps



Identification Report:

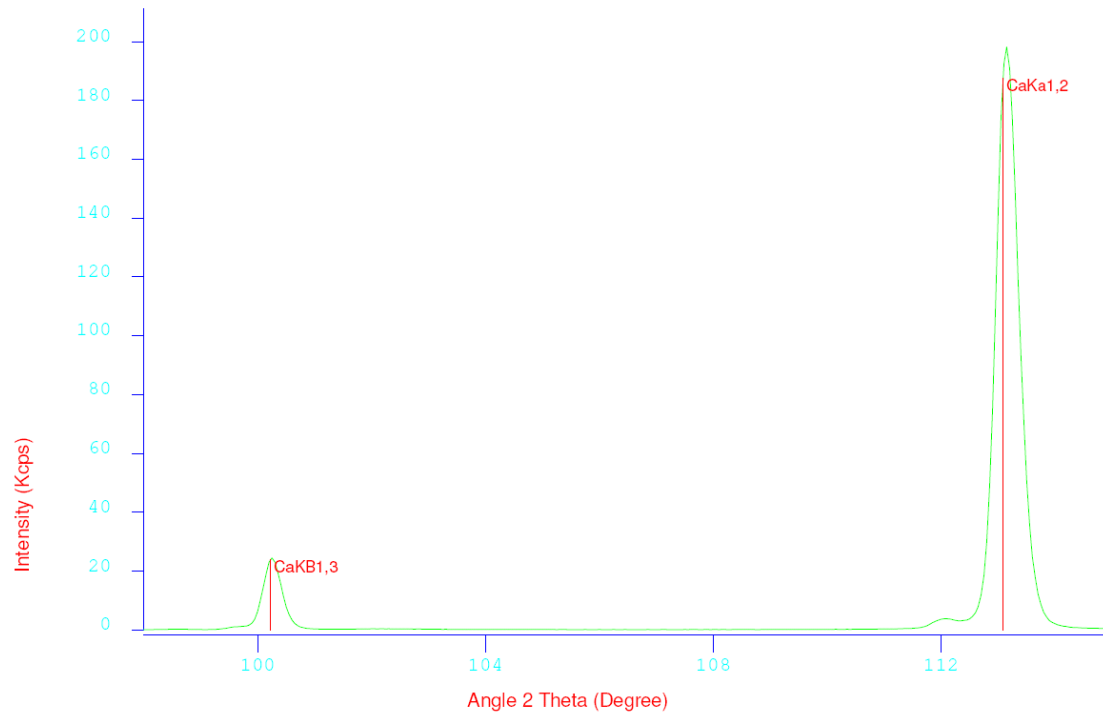
Scan 1
 Sample Identifier: M3SLAG
 Sample Number: M37815
 XRF9800051
 Goniometer: XRF 1
 Crystal: PET
 Detector: FPC
 Collimator: 0.60
 kV/mA: 50/50

Line	Intensity (Kcps)			Angle (deg)
	Scan 1	Scan 2	Scan 3	
SiKB1	1.1980			101.5139
SiKa1,2	61.8035			109.0285

APPENDIX I

Ca wavelength scan

Scan 1: CAOX (M3SLAG), from: CAOX, XRF Gonio: 1, 340 steps



Identification Report:

Scan 1
Sample Identifier: M3SLAG
Sample Number: M37815
XRF9800051
Goniometer: XRF 1
Crystal: LiF200
Detector: FPC
Collimator: 0.25
kV/mA: 50/50

Line	Intensity (Kcps)			Angle (deg)
	Scan 1	Scan 2	Scan 3	
CaKB1,3	23.7469			100.2247
CaKa1,2	187.4360			113.0862

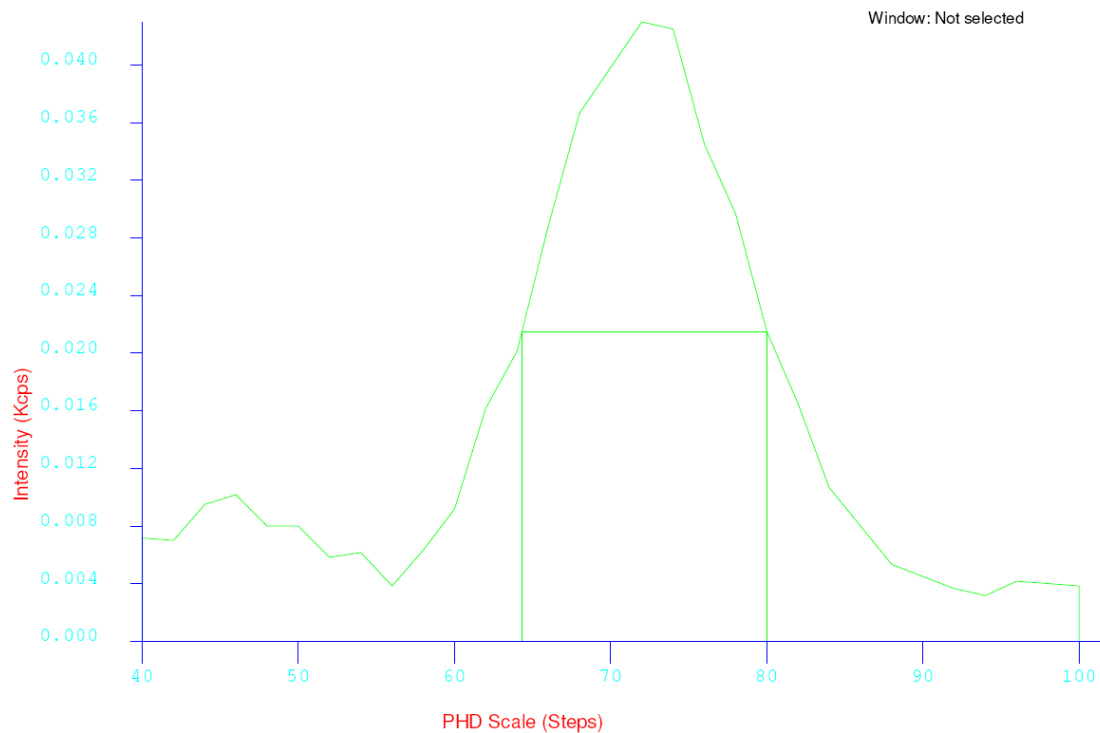
MgK α Energy Profile

Count Rate: 0.8975 kcps

PHD Scale Steps: 72.06 V

Results: MG200A (Mg EP) Monochromator: MnKa_m

Count Rate: 0.8975 Kcps Detector Resolution: 21.79 %



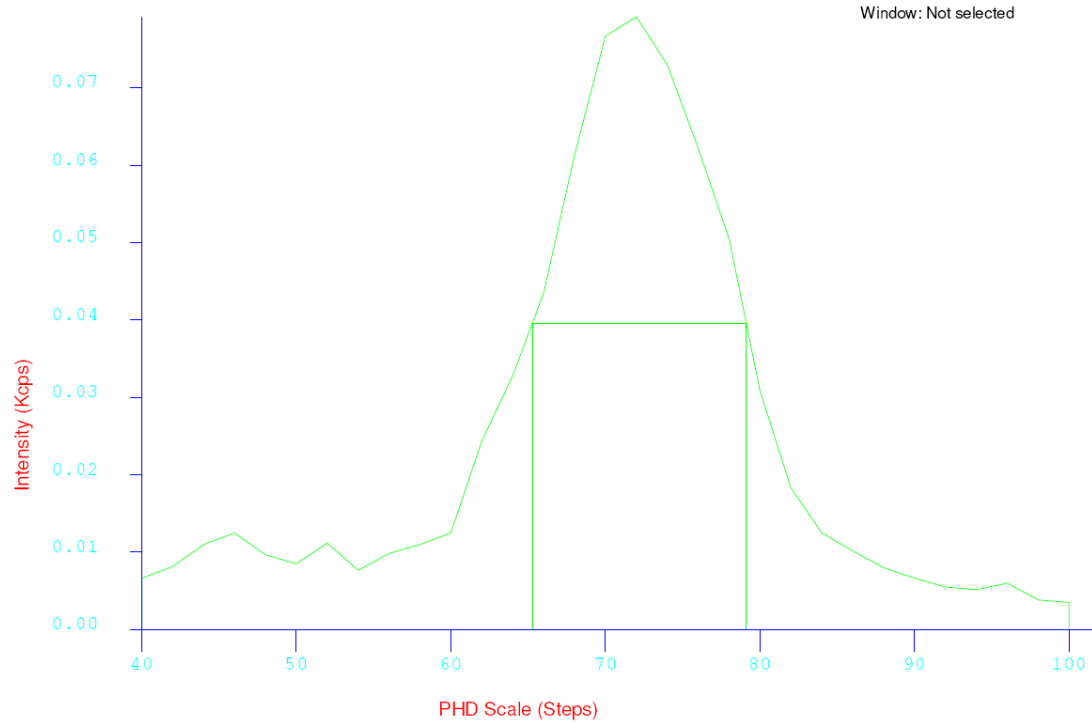
Parameters

Channel Type:	Monochromator
Element Line:	MnKa_m
kV/mA:	50/50
Monochromator Filter:	Off
Automatic Gain Control (AGC):	Off
PHD limits low/high:	40/100
Increment:	2
Integration time:	2
Counting Time/Window:	2

AlK α Energy Profile

Count Rate: 1.4305 kcps
 PHD Scale Steps: 71.98 V

Results: AL200B (AlEP) Monochromator: MnKa_m
 Count Rate: 1.4305 Kcps Detector Resolution: 19.23 %



Parameters

Channel Type:	Monochromator
Element Line:	MnKa_m
kV/mA:	50/50
Monochromator Filter:	Off
Automatic Gain Control (AGC):	Off
PHD limits low/high:	40/100
Increment:	2
Integration time:	2
Counting Time/Window:	2

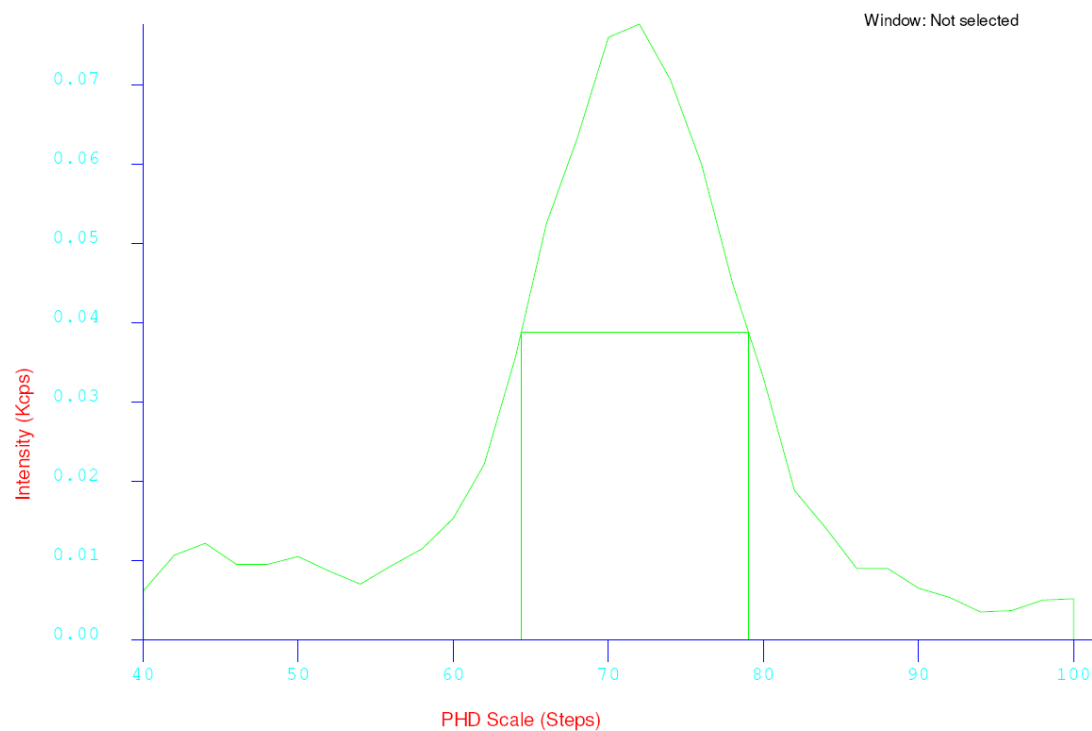
CaK α Energy Profile

Count Rate: 1.4215 kcps

PHD Scale Steps: 71.98 V

Results: CA200B (Ca EP) Monochromator: MnKa_m

Count Rate: 1.4215 Kcps Detector Resolution: 20.35 %



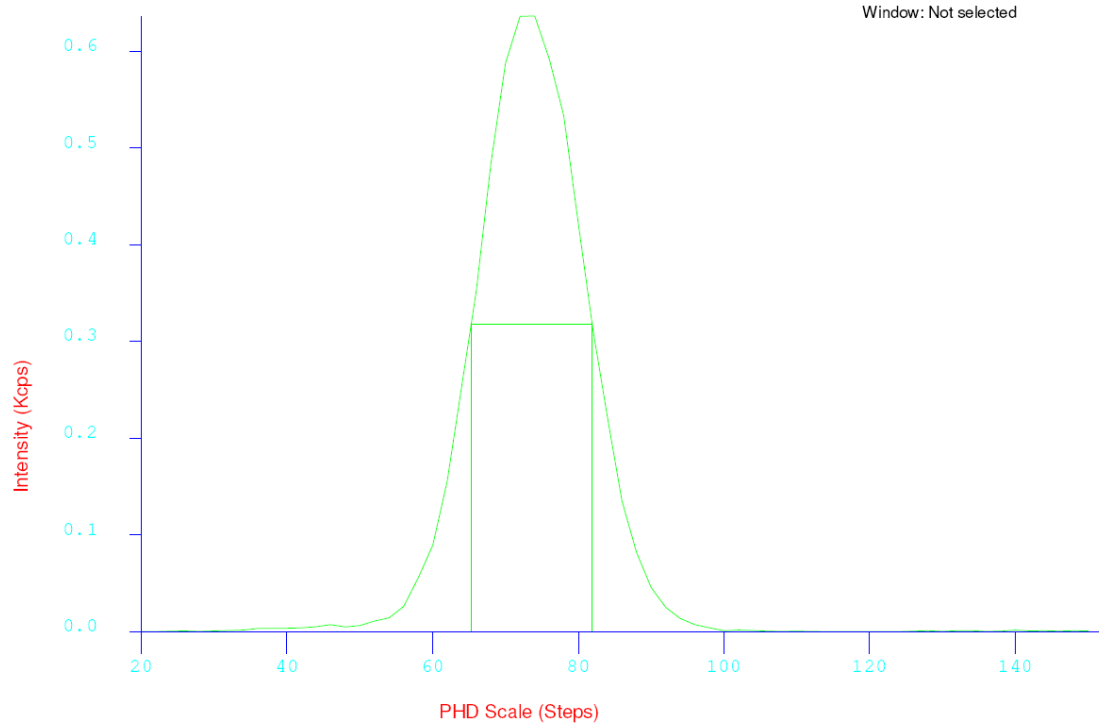
Parameters

Channel Type:	Monochromator
Element Line:	MnKa_m
kV/mA:	50/50
Monochromator Filter:	Off
Automatic Gain Control (AGC):	Off
PHD limits low/high:	40/100
Increment:	2
Integration time:	2
Counting Time/Window:	2

TiK α Energy Profile

Count Rate: 11.7220 kcps
 PHD Scale Steps: 72.95 V

Results: TI200C (TI EP) Monochromator: TiKa_m
 Count Rate: 11.7220 Kcps Detector Resolution: 22.46 %



Parameters

Channel Type:	Monochromator
Element Line:	TiKa_m
kV/mA:	15/15
Monochromator Filter:	Off
Automatic Gain Control (AGC):	Off
PHD limits low/high:	20/150
Increment:	2
Integration time:	2
Counting Time/Window:	2

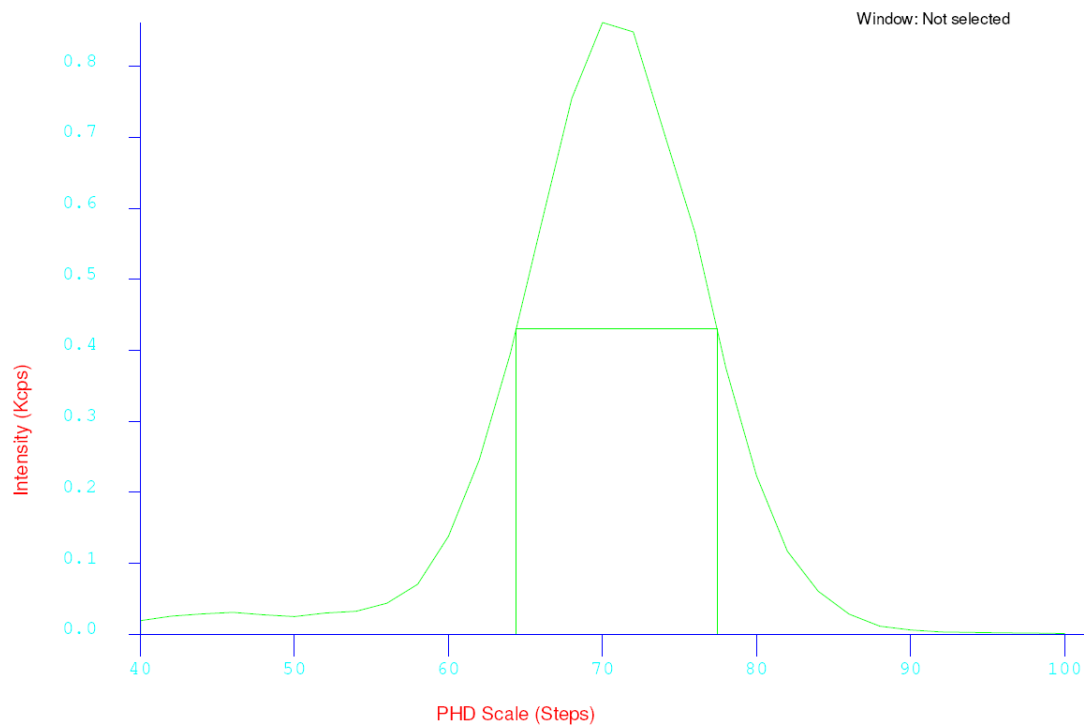
MnK α Energy Profile

Count Rate: 12.5750 kcps

PHD Scale Steps: 70.13 V

Results: MN204 (Mn EP) Monochromator: MnKa_m

Count Rate: 12.5750 Kcps Detector Resolution: 18.61 %



Parameters

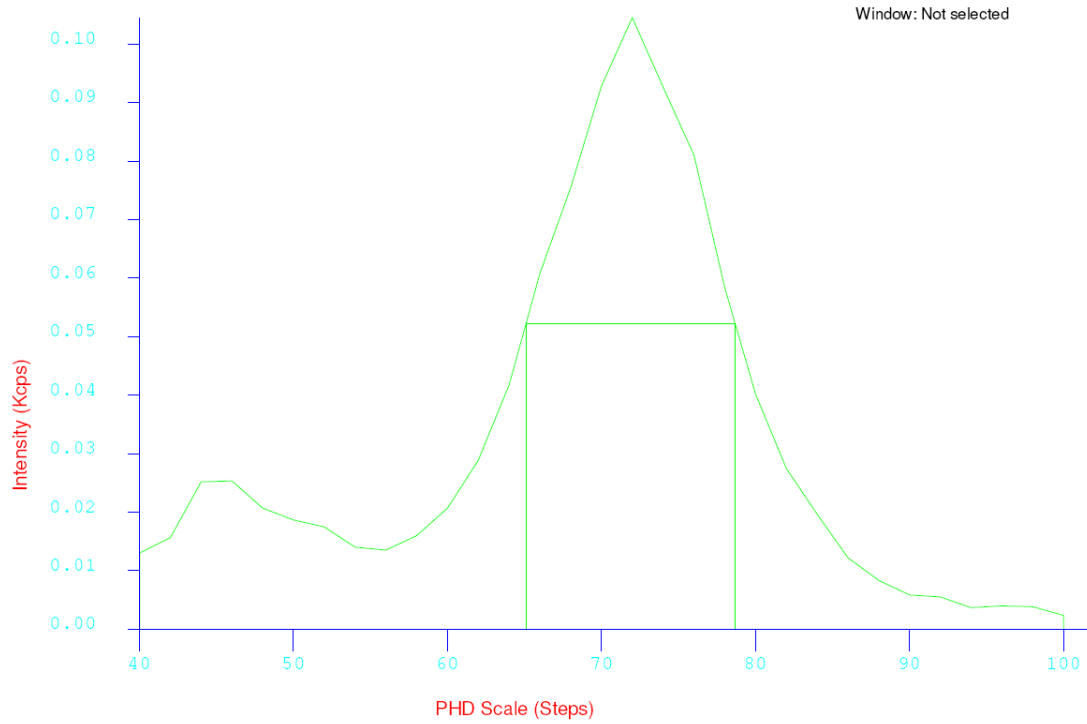
Channel Type:	Monochromator
Element Line:	MnKa_m
kV/mA:	50/30
Monochromator Filter:	Off
Automatic Gain Control (AGC):	Off
PHD limits low/high:	40/100
Increment:	2
Integration time:	2
Counting Time/Window:	2

APPENDIX O

FeK α Energy Profile

Count Rate: 1.8330 kcps
PHD Scale Steps: 72.06 V

Results: FE200C (Fe EP) Monochromator: MnKa_m
Count Rate: 1.8330 Kcps Detector Resolution: 18.85 %



Parameters

Channel Type:	Monochromator
Element Line:	MnKa_m
kV/mA:	50/50
Monochromator Filter:	Off
Automatic Gain Control (AGC):	Off
PHD limits low/high:	40/100
Increment:	2
Integration time:	2
Counting Time/Window:	2

12 REFERENCES

- Abu El- Haija, A.J., Al-Saleh, K.A. *et al.* Quantitative Analysis of Stainless Steel Using Nuclear Techniques, *Materials Science and Engineering*, vol. 95, 1987.
- Agarwal, B.K. and MacAdam, D.L. ed. (1979). *X-ray Spectroscopy: An Introduction*. Springer Series in optical Sciences, vol 15. Springer-Verlag, Berlin, Heidelberg, New York.
- Al-Merey, R., Karajou, J., Issa, H. X-ray fluorescence analysis of geological samples: exploring the effect of sample thickness on the accuracy of results, *Applied Radiation and Isotopes*, vol. 62, 2005.
- Anzelmo, J., Seyfarth, A., Arias, L. Approaching a universal sample preparation method for XRF analysis of powder materials, *Advances in X-ray Analysis*, vol. 44, 2001.
- Bonnelle, C. and Mande, C. (editors) (1982). *Advances in X-ray Spectroscopy*. Pergamon Press.
- Bremser, W. and Hässelbarth, W. Controlling uncertainty in calibration, *Analytica Chimica Acta*, vol. 348, 1997.
- Brown, R.J.C. and Milton, M.J.T. Analytical techniques for trace element analysis; an overview, *Trends in Analytical Chemistry*, vol. 24, 2005.
- Calvert, S.E., Cousens, B.L., Soon, M.Y.S. An X-ray fluorescence spectrometric method for major and minor elements in ferromanganese nodules, *Chemical Geology*, vol 51, 1985.
- De Beer, W.H.J., (2006). *Statistical Method Validation for Test Laboratories*. Training Manual. Technikon Pretoria, Department of Chemistry and Physics.

François, N., Govaerts, B. and Boulanger, B. Optimal designs for inverse prediction in univariate nonlinear calibration models, *Chemometrics and Intelligent Laboratory Systems*, vol. 74, issue 2, 2004.

Garfield, F.M., Klesta, E., Hirsch, J. (2000). *Quality Assurance principles for Analytical Laboratories*. AOAC International.

General requirements for the competence of testing and calibration laboratories. SANS 17025:2005, ISO/IEC 17025:2005 Edition 2.

Han, X.Y., Zhuo, S.J. *et al.* Comparison of the quantitative results corrected by fundamental parameter method and difference calibration specimens in X-ray fluorescence spectrometry, *Journal of Quantitative Spectroscopy & Radiative transfer*, vol. 97, 2006.

Harada, M. and Sakurai, K. K-line X-ray fluorescence analysis of high-Z elements, *Spectrochimica Acta*, Part B vol. 54, 1999.

Hollas, J.M. (1990). *Modern Spectroscopy*. John Wiley and Sons.

Hosogaya, S., Ota, M. *et al.* Method of Estimating Uncertainty of Measurement Values in Case of Measurement Methods Involving Non-Linear Calibration, *Japanese Journal of Clinical Chemistry*, vol. 37(3), 2008.

Howarth, O. (1973). *Theory of Spectroscopy: An Elementary Introduction*. T. Nelson, London.

Jenkins, R. and De Vries, J.L. (1967). *Practical X-ray Spectrometry*. Philips N.V. Gloeilampenfabrieken, Eindhoven, The Netherlands.

Liptrot, G.F. (1992). *Modern Inorganic Chemistry*. 4th Edition. CollinsEducational, London.

Martens, H. and Næs, T. (1989). *Multivariate Calibration*. John Wiley and Sons.

Martin, J., Martin, A. *et al.* The line overlap correction by theoretical intensity, *Advances in X-ray Analysis*, vol.45 , 2002.

Miller, J.N. and Miller, J.C. (2005). *Statistics and Chemometrics for Analytical Chemistry*. Pearson.

Misra, N.L. and Mudher, K.D.S. Total reflection X-ray fluorescence: A technique for trace element analysis in materials, *Progress in Crystal Growth and Characterization of Materials*, 2002.

Sieber, J.R. Matrix-independent XRF methods for certification of standard reference materials, *Advances in X-ray analysis*, vol. 45, 2002.

Skoog, D.A. and Leary, J.J. (1992). *Principles of Instrumental Analysis*. 4th Edition. Saunders College Publishing.

Tellinghuisen, J. Simple algorithms for nonlinear calibration by the classical and standard additions method, *Analyst*, vol. 130, Jan 2005.

White, E.W. and Johnson, G.G. (1970). *X-ray and Absorption Wavelengths and Two-Theta Tables*. American Society for Testing and Materials. Philadelphia, Pa.

Willis, J.P. (2008). *Course on Theory and Practice of XRF Spectrometry*. University of Cape Town. Department of Geological Sciences.

http://www.bruker-axs.de/fileadmin/user_upload/xrfintro/sec1_8.html

XRF Analysis–Theory, Experiment and regression,

http://www.icdd.com/resources/axa/vol40/v40_286.pdf